Final Report for Period: 09/2010 - 08/2011
Submitted on: 08/24/2011
Principal Investigator: Akyildiz, Ian F.
Award ID: 0721580
Organization: Georgia Tech Research Corp
Submitted By:
Akyildiz, Ian - Principal Investigator
Title:
NeTS-WN: COGNET: Cognitive Radio Networks based on OFDM

Project Participants

Senior Personnel

Name: Akyildiz, Ian
Worked for more than 160 Hours: Yes
Contribution to Project:

Name: Laskar, Joy
Worked for more than 160 Hours: Yes
Contribution to Project:

Name: Li, Ye (Geoffrey)
Worked for more than 160 Hours: Yes
Contribution to Project:

Post-doc

Graduate Student

Name: Lee, Won Yeol
Worked for more than 160 Hours: Yes
Contribution to Project:
Spectrum management function for infra-structure-based networks

Name: Chowdhury, Kaushik
Worked for more than 160 Hours: Yes
Contribution to Project:
Spectrum management function for wireless mesh networks

Name: Ma, Jun
Worked for more than 160 Hours: Yes
Contribution to Project:
Soft combination for cooperative spectrum sensing and probability-based spectrum sensing scheme

Name: Zhou, Xiangwei
Worked for more than 160 Hours: Yes
Contribution to Project:
Probability-based spectrum sensing scheme

Name: Narang, Ajit
Worked for more than 160 Hours: Yes
Contribution to Project:
Implementation of the cognitive radio testbed

Name: Saeed, Usman

Worked for more than 160 Hours: Yes

Contribution to Project:
Implementation of the cognitive radio testbed

Name: Tirunelveli Kanthi, Saravanan

Worked for more than 160 Hours: Yes

Contribution to Project:
Implementation of the cognitive radio testbed

Undergraduate Student

Technician, Programmer

Other Participant

Research Experience for Undergraduates

Organizational Partners

Other Collaborators or Contacts

Activities and Findings

Research and Education Activities:

During the reporting period, the PIs and their graduate students have primarily investigated physical layer techniques and spectrum management schemes for cognitive radio networks. A thorough investigation of intrinsic characteristics and unique problems of cognitive radio networks are presented along with a comprehensive survey of existing and possible solutions for seamless communications in cognitive radio networks. Specifically, the physical layer techniques focus on spectrum sensing, resource allocation, and cooperative communications. Furthermore, a spectrum management framework that operates at the higher layers of the protocol stack above the physical layer has been developed. Finally, a cognitive radio testbed is developed to support the testing and the evaluation of the proposed framework and communication protocols, and to measure the performance of multi-resolution spectrum sensing at the device level.

The key results of this work have been published in or submitted to IEEE/ACM Transactions on Networking, IEEE Transactions on Mobile Computing, IEEE Transactions on Communications, IEEE Transactions on Wireless Communications, IEEE Transactions on Broadcasting, IEEE Journal of Selected Topics in Signal Processing, IEEE Journal of Selected Areas in Communications, IEEE Journal of Solid-State Circuits, Proceedings of the IEEE, and IEEE Communications Magazine. For conference publications, the work also appears in the proceedings of IEEE WCNC 2011, IEEE GLOBECOM 2011/2009/2008, IEEE PIMRC 2010, IEEE CCNC 2010, IEEE ICASSP 2010, IEEE ICC 2008/2009, IEEE VTC2009-Spring, IEEE DySPAN 2008, IEEE ISSCC 2008, IEEE RFIC Symposium 2008, IEEE APMC 2008, CrownCom 2008, and European Radar Conference (EuRAD) 2008.

Findings:

For physical layer techniques, advanced spectrum sensing schemes are developed for cognitive radios to sense the spectrum, detect the presence of primary users, and mitigate the interference. For efficient coexistence with primary networks, cooperative communication schemes with directional and relay-assisted transmission are proposed. To enhance the sensing accuracy while satisfying the interference constraints, the statistical characteristics of primary user activity have been investigated for probability-based sensing schemes with resource allocation. Moreover, spectrum shaping schemes that limit the out-of-band interference from CR users have been studied for OFDM-based cognitive radios. Furthermore, spectrum management framework that operates at the higher layers of the protocol stack has been proposed, which addresses the key issues of spectrum sharing and spectrum mobility for reliable mobile communications in infrastructure networks. In addition, a novel primary user activity model has been developed along with a QoS-aware spectrum decision scheme for available spectrum

characterization and decision. To take into account PU activity fluctuations and heterogeneous QoS requirements, an adaptive QoS-based spectrum sharing system and algorithm are developed. Extensive simulations have been performed to show that the developed schemes significantly outperform existing schemes both in performance and functionality. Finally, cognitive radio testbed has been developed to comprehensively evaluate the developed schemes and demonstrate the effectiveness of physical layer techniques. The fully integrated UHF receiver with MRSS functionality has been designed and fabricated using a 0.18 micron CMOS technology.

Training and Development:

Seven graduate students have been funded as part of the project. The students have gained significant amount of knowledge in the general area of cognitive radio networks, and in the specific domain of spectrum sensing, spectrum management, and RF IC design for cognitive radio networks. The PIs have also incorporated findings of the project in the instruction and curriculum of three graduate and three undergraduate level classes the PIs have taught over the last year.

Outreach Activities:

Findings of the project have been presented in the form of journal publications in IEEE/ACM Transactions on Networking, IEEE Transactions on Mobile Computing, IEEE Transactions on Communications, IEEE Transactions on Wireless Communications, IEEE Transactions on Broadcasting, IEEE Journal of Selected Topics in Signal Processing, IEEE Journal of Selected Areas in Communications, IEEE Journal of Solid-State Circuits, Proceedings of the IEEE, and IEEE Communications Magazine. For conference publications, the work also appears in the proceedings of IEEE WCNC 2011, IEEE GLOBECOM 2011/2009/2008, IEEE PIMRC 2010, IEEE CCNC 2010, IEEE ICASSP 2010, IEEE ICC 2008/2009, IEEE VTC2009-Spring, IEEE DySPAN 2008, IEEE ISSCC 2008, IEEE RFIC Symposium 2008, IEEE APMC 2008, CrownCom 2008, and European Radar Conference (EuRAD) 2008. Parts of the findings have also been approved in IEEE 802.22 Standardization.

Journal Publications

I.F. Akyildiz,W.-Y. Lee, M.C. Vuran, and S. Mohanty, "A Survey on Spectrum Management in Cognitive Radio Networks", IEEE Communications Magazine, p. 40, vol. 46, (2008). Published, 10.1109/MCOM.2008.4481339

W.-Y. Lee, and I. F. Akyildiz, "Optimal Spectrum Sensing Framework for Cognitive Radio Networks", IEEE Transactions on Wireless Communication, p. 3845, vol. 7, (2008). Published, 10.1109/T-WC.2008.070391

K. R. Chowdhury, and I. F. Akyildiz, "Cognitive Wireless Mesh Networks with Dynamic Spectrum Access", IEEE Journal on Selected Areas in Communications, p. 168, vol. 26, (2008). Published, 10.1109/JSAC.2008.080115

G. Ganesan, Y. (G.) Li, B. Bing, and S.-Q. Li, "Spatiotemporal Sensing in Cognitive Radio Networks", IEEE Journal on Selected Areas in Communications, p. 5, vol. 26, (2008). Published, 10.1109/JSAC.2008.080102

J. Ma, G. Zhao, and Y. (G.) Li, "Soft Combination and Detection for Cooperative Spectrum Sensing in Cognitive Radio Networks", IEEE Transactions on Wireless Communications, p. 4502, vol. 11, (2008). Published, 10.1109/T-WC.2008.070941

J. Ma, G. Y. Li, and B. H. Juang, "Signal Processing in Cognitive Radio", Proceedings of the IEEE, p. 805, vol. 97, (2009). Published, 10.1109/JPROC.2009.2015707

W.-Y. Lee and I. F. Akyildiz, "Dynamic Resource Allocation for Spectrum Sharing in Infrastructure-Based Cognitive Radio Networks", IEEE Transactions on Mobile Computing, p. , vol. , (2009). Submitted,

W.-Y. Lee and I. F. Akyildiz, "Spectrum-aware mobility management in cognitive radio cellular networks", IEEE Transactions on Mobile Computing, p. , vol. , (2011). Accepted, 10.1109/TMC.2011.69

B. Canberk, I. F. Akyildiz, and S. Oktug, "An Adaptive QoS-based Spectrum Sharing Scheme for CR Networks", IEEE Transactions on Networking, p. , vol. , (2010). Submitted,

J. Ma, X. Zhou, and G. Y. Li,, "Probability-based periodic spectrum sensing during secondary communication", IEEE Transactions on Communications, p. 1291, vol. 58, (2010). Published, 10.1109/TCOMM.2010.04.080327

X. Zhou, J. Ma, G. Y. Li, Y. H. Kwon, and A. Soong, "Probability-based optimization of inter-sensing duration and power control in cognitive radio", IEEE Transactions on Wireless Communications, p. 4922, vol. 8, (2009). Published, 10.1109/TWC.2009.081061

X. Zhou, J. Ma, G. Y. Li, Y. H. Kwon, and A. Soong,, "Probability-based combination for cooperative spectrum sensing", IEEE Transactions on Communications, p. 463, vol. 58, (2010). Published, 10.1109/TCOMM.2010.02.080154

G. Zhao, J. Ma, G. Y. Li, T. Wu, Y. H. Kwon, A. Soong, and C. Yang,, "Spatial spectrum holes for cognitive radio with relay-assisted directional transmission", IEEE Transactions on Wireless Communications, p. 5270, vol. 8, (2009). Published, 10.1109/TWC.2009.081541

J. Park, T. Song, J. Hur, S. M. Lee, J. Choi, K. Kim, K. Lim, C.-H. Lee, H. Kim, and J. Laskar, "A fully integrated UHF-band CMOS receiver with multi-resolution spectrum sensing (MRSS) functionality for IEEE 802.22 cognitive radio applications", IEEE Journal of Solid-State Circuits, p. 258, vol. 44, (2009). Published, 10.1109/JSSC.2008.2007435

W. Y. Lee and I. F. Akyildiz, "A Spectrum Decision Framework for Cognitive Radio Networks", IEEE Transactions on Mobile Computing, p. 161, vol. 10, (2011). Published, 10.1109/TMC.2010.147

B. Canberk, I. F. Akyildiz, and S. Oktug, "Primary user activity modeling using first-difference filter clustering and correlation in cognitive radio networks", IEEE Transactions on Networking, p. 170, vol. 19, (2011). Published, 10.1109/TNET.2010.2065031

L. Li, X. Zhou, H. Xu, G. Y. Li, D. Wang, and A. C. K. Soong, "Energy-efficient transmission for protection of incumbent users", IEEE Transactions on Broadcasting, p. , vol. , (2011). Accepted, 10.1109/TBC.2011.2128230

L. Li, X. Zhou, H. Xu, G. Y. Li, D. Wang, and A. C. K. Soong,, "Simplified relay selection and power allocation in cooperative cognitive radio systems", IEEE Transactions on Wireless Communications, p. 33, vol. 10, (2011). Published, 10.1109/TWC.2010.101810.100311

G. Zhao, C. Yang, G. Y. Li, D. Li, and A. Soong, "Power and channel allocation for cooperative relay in cognitive radio networks", IEEE Journal of Selected Topics in Signal Processing, p. 151, vol. 5, (2011). Published, 10.1109/JSTSP.2010.2052784

X. Zhou, G. Y. Li, D. Li, D.Wang, and A. C. K. Soong, "Probabilistic resource allocation for opportunistic spectrum access", IEEE Transactions on Wireless Communications, p. 2870, vol. 9, (2010). Published, 10.1109/TWC.2010.070610.091511

X. Zhou, G. Y. Li, and G. Sun, "Low-complexity spectral precoding for OFDM-based cognitive radio systems", IEEE Transactions on Wireless Communications, p. , vol. , (2011). Submitted,

Books or Other One-time Publications

J. Park, K.-W. Kim, T. Song, S. M. Lee, J. Hur, K. Lim, and J. Laskar, "A Fully Integrated UHF Receiver with Multi-Resolution Spectrum Sensing (MRSS) Functionality for IEEE 802.22 Cognitive Radio Applications", (2008). Conference Proceedings, Published
Bibliography: Proc. of IEEE International Solid-State Circuits Conference

J. Park, K.-W. Kim, T. Song, S. M. Lee, J. Hur, K. Lim, and J. Laskar, "A Cross-layer Cognitive Radio Testbed for the Evaluation of Spectrum Sensing Receiver and Interference Analysis", (2008). Conference Proceedings, Published
Bibliography: Proc. 3rd
International Conference on Cognitive Radio Oriented Wireless Networks and Communications (CrownCom) 2008

J. Ma and Y. (G.) Li, "A Probability-based Spectrum Sensing Scheme for Cognitive Radio", (2008). Conference Proceedings, Published
Bibliography: Proc. IEEE ICC 2008

X.-W. Zhou, Y. (G.) Li, Y.-H. Kwon, and A. Soong, "Detection Timing and Channel Selection for Periodic Spectrum Sensing in Cognitive Radio", (2008). Conference Proceedings, Published
Bibliography: Proc. IEEE GLOBECOM 2008

G. Zhao, J. Ma, G. Y. Li, A. Soong, and C. Yang,, "Spatial spectrum holes in cognitive radio with relay transmission", (2009). Conference Proceedings, Published
Bibliography: Proc. IEEE VTC2009-Spring

K. Lim, J. Park, J. Laskar, H. Kim, C. H. Lee, "Text on Multi-Resolution Spectrum Sensing", (2007). Standard contribution, Published
Bibliography: IEEE
Standard Meeting, Big Island, Hawaii, IEEE 802.22 Doc. No. 22-07-0451-01-0001, Sept. 2007

W. Y. Lee, and I. F. Akyildiz, "Joint spectrum and power allocation for inter-cell spectrum sharing in cognitive radio networks", (2008). Conference Proceedings, Published
Bibliography: Proc. IEEE Symposia on New Frontiers in Dynamic Spectrum Access Networks (DySPAN) 2008

X. Zhou, G. Y. Li, Y. H. Kwon, A. Soong, and G. Zhao, "Probability-based transmit power control for dynamic spectrum access", (2008). Conference Proceedings, Published
Bibliography: Proc. IEEE DySPAN 2008

X. Zhou, J. Ma, G. Y. Li, Y. H. Kwon, and A. Soong, "Probability-based combination for cooperative spectrum sensing in cognitive radio networks", (2009). Conference proceedings, Published
Bibliography: Proc. IEEE ICC 2009

S. Byun, K.-W. Kim, D.-H. Lee, J. Laskar, and C. S. Kim, "A self-calibrated LC quadrature VCO in a current-limited region", (2008). Conference Proceedings, Published
Bibliography: Proc. IEEE Radio Frequency Integrated Circuits (RFIC) Symposium

S. M. Lee, T. Song, J. Park, K. Lim, and J. Laskar, "Analog pulse compressor for radar system", (2008). Conference Proceedings, Published
Bibliography: Proc. of European Radar Conference (EuRAD) 2008

T. Song, S. M. Lee, J. Park, K. Lim, and J. Laskar, "A Fully-integrated arbitrary waveform generator for analog matched filter", (2008). Conference Proceedings, Published
Bibliography: Proc. of IEEE Asia-Pacific Microwave Conference (APMC) 2008

B. Canberk, I. F. Akyildiz, and S. Oktug, "A QoS-Aware Framework for Available Spectrum Characterization and Decision in Cognitive Radio Networks", (2010). Conference Proceedings, Published
Bibliography: Proc. of IEEE PIMRC 2010

L. Li, X. Zhou, H. Xu, G. Y. Li, D.Wang, and A. C. K. Soong, "Energy-efficient transmission in cognitive radio networks", (2010). Conference Proceedings, Published
Bibliography: Proc. of IEEE CCNC 2010

G. Zhao, C. Yang, G. Y. Li, D. Li, and A. C. K. Soong, "Channel allocation for cooperative relays in cognitive radio networks", (2010). Conference Proceedings, Published
Bibliography: Proc. of IEEE ICASSP 2010

X. Zhou, G. Y. Li, D. Li, D. Wang, and A. C. K. Soong, "Probability-based resource allocation in cognitive radio networks", (2009). Conference Proceedings, Published
Bibliography: Proc. IEEE GLOBECOM 2009

X. Zhou, G. Y. Li, D. Li, D.Wang, and A. C. K. Soong, "Bandwidth efficient combination for cooperative spectrum sensing in cognitive radio networks", (2010). Conference Proceedings, Published
Bibliography: Proc. IEEE ICASSP 2010

X. Zhou, G. Y. Li, D. Li, D. Wang, and A. C. K. Soong, "Bandwidth-efficient cooperative spectrum sensing", (2011). Book, Accepted
Editor(s): H. Venkataraman and G.-M. Muntean
Bibliography: Cognitive Radio for Wireless Cellular and Vehicular Networks

X. Zhou, G. Y. Li, and G. Sun, "Multiuser spectral precoding for OFDM-based cognitive radios", (2011). Conference Proceedings, Accepted
Bibliography: Proc. IEEE GLOBECOM 2011

X. Zhou, G. Y. Li, and G. Sun, "Low-complexity spectrum shaping for OFDM-based cognitive radios", (2011). Conference Proceedings, Published
Bibliography: Proc. of IEEE WCNC

Web/Internet Site

URL(s):
http://www.ece.gatech.edu/research/labs/bwn/CR/
Description:

Other Specific Products

Contributions

Contributions within Discipline:

Contributions to Other Disciplines:

Contributions to Human Resource Development:

Contributions to Resources for Research and Education:

Contributions Beyond Science and Engineering:

Conference Proceedings

Categories for which nothing is reported:

Organizational Partners
Any Product
Contributions: To Any within Discipline
Contributions: To Any Other Disciplines
Contributions: To Any Human Resource Development
Contributions: To Any Resources for Research and Education
Contributions: To Any Beyond Science and Engineering
Any Conference

NeTS: COGNET: Cognitive Radio Networks Based on OFDM

Award Number: CNS-0721580

Final Report

September 1, 2010 – August 31, 2011

Ian F. Akyildiz

Geoffrey Ye Li

School of Electrical & Computer Engineering
Georgia Institute of Technology, Atlanta, GA 30332
Tel: (404) 894-5141; Fax: (404) 894-7883
Email: {ian, liye}@ece.gatech.edu

Contents

Summary

The spectrum under-utilization problem in licensed bands necessitate a new communication paradigm to opportunistically exploit the spectrum availability and improve the spectrum efficiency. This new paradigm, known as cognitive radio networks, brings the promises to the deployment of new wireless services via dynamic spectrum access in heterogeneous wireless architectures. However, cognitive radio networks impose unique challenges in the system design due to the fluctuating nature of the available spectrum as well as diverse quality-of-service (QoS) requirements. For spectrum efficiency and network performance, the heterogeneities in wireless environments must be captured and handled dynamically as mobile terminals roam between wireless architectures and along the wireless spectrum. In this project, a spectrum-aware COGnitive radio NETwork design (COGNET) based on orthogonal frequency division multiplexing (OFDM) technology is proposed to address the above challenges for the realization of this new network paradigm. As the key enabling technology in COGNET, cognitive radio provides the capability of dynamically sharing the licensed spectrum with licensed devices, known as primary users, while limiting the interference with primary users to an unharmful level. In addition, cognitive radio users need to vacate the band and switch to an available band once the primary user is detected. To realize this concept, joint designs of physical layer techniques, spectrum management schemes, and radio-frequency (RF) frontend are developed. Our work spans the entire wireless protocol stack with the implementation of cognitive radio testbed with a fully-integrated multi-resolution spectrum sensing (MRSS) receiver IC.

Specifically, physical layer techniques are developed for cognitive radios to sense the spectrum, detect the presence of primary users, and mitigate the interference. For efficient coexistence with primary networks, cooperative communication schemes with directional and relay-assisted transmission are proposed. To enhance the sensing accuracy while satisfying the interference constraints, the statistical characteristics of primary user activity have been investigated for probability-based sensing schemes with resource allocation. Moreover, spectrum shaping schemes that limit the out-of-band interference from CR users have been studied for OFDM-based cognitive radios. Furthermore, spectrum management framework that operates at the higher layers of the protocol stack has been proposed, which addresses the key issues of spectrum sharing and spectrum mobility for reliable mobile communications in infrastructure networks. In addition, a novel primary user activity model has been developed along with a QoS-aware spectrum decision scheme for available spectrum characterization and decision. To take into account PU activity fluctuations and heterogeneous QoS requirements, an adaptive QoS-based spectrum sharing system and algorithm are developed. Extensive simulations have been performed to show that the developed schemes significantly outperform existing schemes both in performance and functionality. Finally, cognitive radio testbed has been developed to comprehensively evaluate the developed schemes and demonstrate the effectiveness of physical layer techniques. The fully integrated UHF receiver with MRSS functionality has been designed and fabricated using a $0.18\,\mu\mathrm{m}$ CMOS technology.

Findings of the project have been published in prestigious IEEE journals and IEEE conference proceedings. They are also incorporated in the instruction and curriculum of graduate and undergraduate classes.

1 Introduction

Today's wireless networks are regulated by a fixed spectrum assignment policy. Wireless spectrum is regulated by governmental agencies and is assigned to license holders or services on a long-term basis over vast geographical regions. Recent research has shown that a large portion of the assigned spectrum is used sporadically leading to under-utilization and wastage of valuable frequency resources. To address this critical problem, FCC has recently approved the access of unlicensed devices in licensed bands. When the licensed devices, known as primary users (PUs), are not present in the licensed bands, these unlicensed devices, called cognitive radio (CR) users, can opportunistically use the available spectrum. When PU returns to the licensed band, CR users need to vacate the band and switch to another available band by dynamic spectrum access (DSA). Consequently, this new area of research foresees the development of CR networks to improve spectrum efficiency and solve the spectrum under-utilization problem. Due to the fluctuations in spectrum availability as well as diverse quality-of-service (QoS) requirements, CR networks, however, impose unique challenges in the design of CR systems [1,2]. These challenges necessitate novel spectrum-aware design techniques that simultaneously address a wide range of communication problems from RF design to network management.

In this project, we propose a spectrum-aware COGnitive radio NETwork (COGNET) design based on orthogonal frequency division multiplexing (OFDM) technology for the realization of this new network paradigm. As the key enabling technology in COGNET, cognitive radio [1,2] provides the capability of dynamically sharing the wireless spectrum with primary users while limiting the interference with primary users to an unharmful level. This capability can be realized by joint design of physical layer techniques, spectrum management, and radio-frequency (RF) frontend. Specifically, energy and bandwidth efficient spectrum sensing techniques with the consideration of resource allocation, cooperation, and spectrum shaping are devised for PU detection in physical layer. Moreover, spectrum management frameworks including spectrum sharing, spectrum decision, and spectrum mobility are proposed for infrastructure networks to address the key concern of cooperative resource sharing in an efficient manner. In order to continuously monitor spectrum and detect the presence of primary users, the RF front-end in a CR needs to be reconfigured anytime according to the demands and requirements of the higher layers. Hence, the RF frontend should be carefully designed to support the proposed frameworks in the upper layers. Therefore, our work spans the entire wireless protocol stack with the implementation of a physical layer testbed.

In Section 2, physical layer techniques for CR networks are investigated with the focus on spectrum sensing. First, to optimize the performance of CR systems, spectrum sensing algorithms have been developed for both synchronous and asynchronous cases in which multiple nodes located in different spatial regions cooperate to perform sensing. Given a target sensing accuracy and classical assumptions of the signal distribution, the individual readings may be combined in a way that improves performance at an acceptable cost of complexity and overhead. Furthermore, we have investigated the utilization of such statistical information and propose a probability-based spectrum sensing technique where the weight for each sensed sample is based on the probability of the presence of the primary user at the corresponding sampling point. These algorithms operate chiefly at the physical layer with bit-level manipulations to provide a fast and acceptable cooperative detection capability. In addition, unlike classical spectrum sensing schemes, a spectrum reuse scheme has been developed

based on the directional antennas and relay techniques, which allows CR users to access the spectrum bands with the presence of a primary user signal. Furthermore, to enhance the sensing accuracy while satisfying the interference constraints, the statistical characteristics of the licensed band occupancy have been investigated for resource allocation. Spectrum shaping schemes that limit the out-of-band interference from CR users have also been studied for OFDM-based CRs.

In Section 3, spectrum management frameworks are proposed to perform spectrum sharing, spectrum decision, and spectrum mobility functionalities. First, an inter-cell spectrum sharing framework is implemented to allocate the limited spectrum resource efficiently to each CR cell. This is enabled by joint spectrum and power allocation where each cell determines its resource by either (i) opportunistically negotiating additional spectrum, or (ii) having a share of reserved spectrum based on current spectrum utilization, geographical characteristics of PU activity, and cell locations. In addition, in order to maintain reliable and seamless communication channels in CR cellular networks, a spectrum-aware mobility management scheme is proposed for CR cellular networks. This scheme mitigates the heterogeneous spectrum availability as well as enhances cell capacity by determining handoff strategies adaptively dependent on current spectrum utilization and switching cost. Furthermore, in order to accurately track the changing PU activity, a novel real-time based PU activity model for CR networks has been devised. Based on this model, a QoS-aware framework is proposed, which characterizes available spectrums, and accordingly decides on the best spectrum according to diverse user requirements while maintaining the heterogeneous QoS of CR users through a novel admission control and an adaptive spectrum sharing mechanism. Our proposed algorithms and schemes have been extensively tested and results reveal the benefits of using our spectrum management framework in terms of spectrum utilization, throughput, and fairness over classical approaches.

In Section 4, the fully integrated UHF receiver with multi-resolution spectrum-sensing (MRSS) functionality is presented. It is fabricated using a $0.18\,\mu\mathrm{m}$ CMOS technology. The MRSS receiver works like a simple spectrum analyzer with low complexity and power consumption thanks to the proposed digitally assisted analog signal processing technology. The detection time and sensing threshold can be controlled by selecting appropriate windowing signal. When $100\,\mathrm{kHz}$ cos4 window is used, a detectable sensitivity of $-74\,\mathrm{dBm}$ with a $32\,\mathrm{dB}$ dynamic range was obtained. The MRSS receiver has a scalable architecture in terms of area and power consumption as it is possible to be easily migrated into deep sub-micron technology. The MRSS functionality can be adopted in an RF frontend for the spectrum sensing of the future CR wireless communication systems.

The key results of this work have been published in or submitted to *IEEE/ACM Transactions on Networking*, *IEEE Transactions on Mobile Computing*, *IEEE Transactions on Communications*, *IEEE Transactions on Wireless Communications*, *IEEE Transactions on Broadcasting*, *IEEE Journal of Selected Topics in Signal Processing*, *IEEE Journal of Selected Areas in Communications*, *IEEE Journal of Solid-State Circuits*, *Proceedings of the IEEE*, and *IEEE Communications Magazine*. For conference publications, the work also appears in the proceedings of IEEE WCNC 2011, IEEE GLOBECOM 2011/2009/2008, IEEE PIMRC 2010, IEEE CCNC 2010, IEEE ICASSP 2010, IEEE ICC 2008/2009, IEEE VTC2009-Spring, IEEE DySPAN 2008, IEEE ISSCC 2008, IEEE RFIC Symposium 2008, IEEE APMC 2008, CrownCom 2008, and European Radar Conference (EuRAD) 2008.

2 Physical Layer Techniques for Cognitive Radio

As unlicensed (secondary) operators, CR users are allowed to utilize a licensed band only when they do not cause interference to the licensed (primary) users. Since spectrum sensing aims at monitoring the usage and characteristics of the covered spectrum bands, it is required by CR users both before and during the use of licensed spectrum bands. In this project, advanced cooperative spectrum sensing techniques [30, 48, 50] are proposed. To exploit prior statistical information of primary user activity, the probability-based spectrum sensing and resource allocation schemes [31,49,54–59] are proposed. Furthermore, CR promises high spectrum efficiency by means of accessing the spectrum band that primary users are not using at a specific time and location. Such spectrum opportunity is called spectrum holes (SHs) and is the basic resource for CR. To ensure efficient utilization of SHs, coexistence and channel allocation techniques for cooperative communications with relays [28, 29, 44–47] are proposed. Meanwhile, to enhance the bandwidth efficiency of CR and limit the possible interference, spectrum shaping schemes based on spectral precoding [51–53] are proposed.

2.1 Advanced Cooperative Spectrum Sensing

The fundamental characteristics of wireless channels such as multipath fading and shadowing present a major challenge on spectrum sensing. If the primary signal is deeply faded or blocked by large obstacles in the environment, the power of the received primary signal will be too weak to be detected. Fortunately, the impact of multipath fading and shadowing can be mitigated by exploiting spatial diversity in multiuser CR networks. It has been shown that the detection capability of the CR network can be improved by letting multiple CR users take turns to sense the channel instead of designating a fixed CR user for spectrum sensing. Since multipath fading varies significantly on the scale of half-wavelength and shadowing varies significantly on the scale of 20–500 m depending on the environment, the probability that multiple CR users are experiencing deep fading or are blocked by obstacles simultaneously is rather low. Therefore, cooperation among CR users will effectively improve the performance of spectrum sensing. It has been demonstrated that cooperation can improve the detection performance, relax the sensitivity requirements, and decrease the required detection time. To improve the performance of spectrum sensing in practical radio environments, we develop various cooperative spectrum sensing techniques to obtain the spatial diversity in multiuser CR networks [30, 48, 50].

2.1.1 Two-Bit Hard Combination Scheme

Cooperative spectrum sensing in a centralized CR network consists of a base station or access point and a number of CR users. In this network, each CR user sends its sensing information to the base station via common control channels while the base station combines the sensing information and makes a decision on the presence or absence of the primary signal. Generally, the techniques of combining sensing information at the base station can be categorized as soft combination and hard combination. In soft combination, CR users send their original sensing data to the base station without quantization. Although it can achieves excellent detection performance, soft combination requires large overhead to feedback the sensing data and thus reducing

spectral efficiency. On the other hand, hard combination schemes have recently been proposed to achieve a tradeoff between performance and complexity. In hard combination schemes, the CR users send quantized sensing information to the base station. While local hard decision at the CR users causes information loss and performance degradation, it greatly reduces the amount of feedback information.

In the conventional one-bit counting scheme, there is only one threshold dividing the observed energy into two regions with equivalent weights. As a result, all of the CR users above this threshold are allocated the same weight regardless of the possible significant differences in their observed energies. Intuitively, a better detection performance can be achieved if we divide the observed energy into more regions, allocating larger weights to the upper regions and smaller weights to the lower regions. Based on the above heuristic, we propose a new two-bit hard combination scheme [30]. In this scheme, three thresholds divide the observed energy into four regions with different weights. Therefore, each CR user needs to feedback two-bit information to indicate the region of its observed energy. Different from the one-bit counting scheme, the two-bit hard combination scheme calculates a weighted summation of the numbers of CR users falling in different regions. The optimal partition of the regions and weight allocation for the two-bit hard combination scheme have been investigated. It has been demonstrated that, compared to the soft combination scheme, the two-bit hard combination scheme exhibits comparable performance with much less complexity and overhead.

Figure 1 shows the contrastive detection probability curves of the optimal soft combination (OC), the equal gain soft combination (EGC), the softened two-bit hard combination, and the conventional one-bit hard combination schemes. In our simulation, each CR user utilizes 6 samples for energy detection and the sensing data from 4 independent CR users is combined to make a decision on the presence or absence of the primary user. Different CR users are assumed to experience i.i.d. Rayleigh fading channels and the given overall false alarm probability of the 4-user cooperative CR network is 10^{-2}. For the conventional one-bit hard combination scheme, the *OR rule* is applied, i.e., the primary user will be declared present if any one of the 4 CR users detects locally the presence of the primary signal. It verifies that the proposed OC scheme does has the best detection performance since it utilizes the instantaneous channel state information of CR users. The EGC scheme does not require any channel state information of CR users, but still exhibits much better performance than the conventional one-bit hard combination scheme. Simulation results verify that compared to the conventional hard combination, soft combination effectively improves the detection performance. Furthermore, it also indicates that the proposed softened two-bit hard combination scheme exhibits much better performance than the conventional one-bit scheme at the expense of only one more bit of overhead for each CR user. In fact, the two-bit hard combination scheme exhibits even comparable performance with the EGC soft combination scheme despite that it has much less complexity and overhead. Therefore, it achieves a good tradeoff between detection performance and complexity.

2.1.2 Bandwidth-Efficient Reporting

In cooperative spectrum sensing, CR users report individual sensing information to a combining node, which makes a decision on the presence or absence of the licensed user signal. It is usually assumed in the literature that a common control channel is available and used for sending local sensing data. In the initial setup phase that

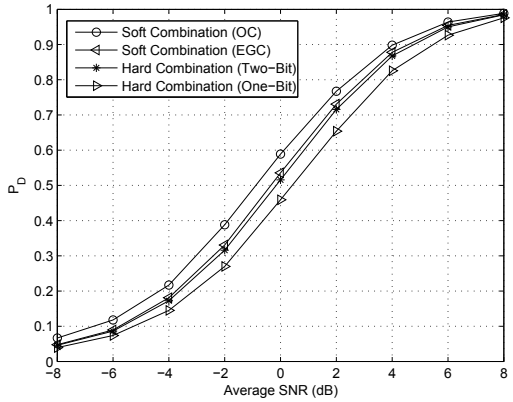

Figure 1: Contrastive detection probability curves of different combination schemes

CR users are conducting spectrum sensing, idle communication channels in licensed spectrum have not been identified so the bandwidth resource for the common control channel is quite limited. It is implied in existing schemes that local sensing data from different users are transmitted through orthogonal channels, i.e., separated in different time slots, frequency bands, or codes. As the number of cooperative users increases, the bandwidth required for reporting also increases as implied and the stringent bandwidth constraint of the common control channel during spectrum sensing may not be satisfied. Therefore, bandwidth-efficient design with the required reporting bandwidth being independent of the number of cooperative users is desired. To satisfy the stringent bandwidth constraint of the common control channel, we propose a general approach that CR users are allowed to simultaneously send local sensing data to a combining node through the same narrowband channel [48, 50]. We develop both local processing at the CR users and final decision rule at the combining node under Bayesian criterion. Through proper preprocessing at individual users, the proposed approach requires fixed bandwidth regardless of the number of cooperative users while maintaining reasonable performance.

Figure 2 gives a general schematic representation for combination of sensing data in cooperative spectrum sensing. As shown in this figure, among the K cooperative CR users, the kth CR user, $1 \leq k \leq K$, independently obtains the signal vector, $\mathbf{r}_k$, and sends the processed sensing data, q_k, to the combining node through the common control channel. Upon receiving the combined sensing data, z, from all the CR users, the combining node makes a decision, d, on the absence or presence of the licensed user signal. We focus on the approach that CR users simultaneously report the processed sensing data through the common control channel so that the combining node receives the superposition of all the data. Although such an approach is not preferred in general wireless communications, it intuitively works in cooperative spectrum sensing since the data from all the CR users are related to the same phenomenon, i.e., on the absence or presence of the licensed user signal. Under this approach, the received sensing data at the combining node is

$$z = \sum_{k=1}^{K} h_k q_k + w, \tag{1}$$

where h_k is the reporting channel gain between the kth CR user and the combining node as shown in Figure 2,

and w_k is the corresponding zero-mean AWGN at the combining node while reporting q_k.

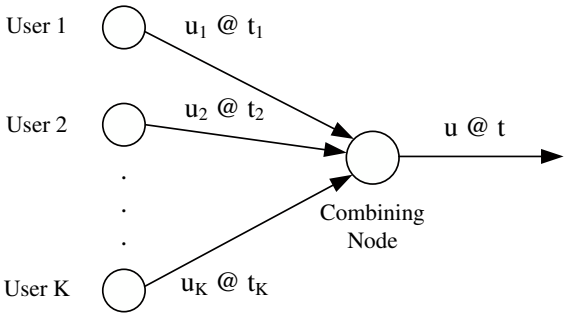

Figure 2: System model: cooperative spectrum sensing

When the reporting channel is Gaussian, we design the local processing function as

$$q_k = Q_k(\mathbf{r}_k) = \log \frac{f(\mathbf{r}_k|\mathcal{H}_1)}{f(\mathbf{r}_k|\mathcal{H}_0)}, \tag{2}$$

where $\mathcal{H}_0$ and $\mathcal{H}_1$ denote the hypotheses corresponding to the absence and presence of the licensed user signal, respectively, and the global decision rule as

$$d = \begin{cases} \mathcal{H}_0, & z < \log \frac{P(\mathcal{H}_0)C_f}{P(\mathcal{H}_1)C_m}, \\ \mathcal{H}_1, & z \geq \log \frac{P(\mathcal{H}_0)C_f}{P(\mathcal{H}_1)C_m}, \end{cases} \tag{3}$$

where $P(\mathcal{H}_0)$ and $P(\mathcal{H}_1)$ denote the prior probabilities of the absence and presence of the licensed user signal, respectively; C_f and C_m are the costs for false alarm (deciding $\mathcal{H}_1$ while the licensed user signal is absent) and mis-detection (deciding $\mathcal{H}_0$ while the licensed user signal is present), respectively.

When the reporting channel between the kth CR user and the combining node experiences fading, we design the local processing function as a quantizer with the following form:

$$q_k = Q_k(\mathbf{r}_k) = \begin{cases} A_0, & l_k < T_{k,1}, \\ A_1, & T_{k,1} \leq l_k < T_{k,2}, \\ \vdots & \\ A_{M-1}, & l_k \geq T_{k,M-1}, \end{cases} \tag{4}$$

where

$$l_k = \frac{f(y_k|\mathcal{H}_1)}{f(y_k|\mathcal{H}_0)} \tag{5}$$

with y_k denoting the observed energy of the kth CR user and q_k takes one of M possible values with the quantization regions divided by $M-1$ thresholds, $T_{k,1}$, $T_{k,2}$, ..., and $T_{k,M-1}$, which can be further determined to achieve the optimal performance. Because of the one-to-one correspondence between the local likelihood ration l_k and the observed energy y_k, the quantization region for A_i can be transformed to $\{y_k : y_k \in R_{k,A_i}\}$. It is proper in this case to make the final decision based on the received power of z in (1). Therefore, the following

threshold test is applied at the combining node:

$$d = \begin{cases} \mathcal{H}_0, & |z|^2 < \varsigma, \\ \mathcal{H}_1, & |z|^2 \geq \varsigma, \end{cases} \tag{6}$$

where the threshold ς can be further determined to achieve the optimal performance.

In our simulation, we assume independent observations across the CR users and let $C_f = 1$, $C_m = 2$, $N = 10$, $\sigma_k^2 = 1$ for $1 \leq k \leq K$, and $P(\mathcal{H}_0) = P(\mathcal{H}_1) = \frac{1}{2}$. Bayesian costs with respect to different relative reporting *signal-to-noise ratios* (SNRs), defined as K/σ^2, where σ^2 is the noise variance at the combining node, with the reporting scheme under Gaussian reporting channel are shown in Figure 3(a), in which the latency between any individual observation and the final combination is uniformly distributed within [0 0.1] sec. The test threshold for making the final decision can be determined as $\frac{1}{2}$. Bayesian costs with respect to different relative reporting SNRs at the combining node when the reporting channel experiences fading are shown in Figure 3(b), in which each CR user uses 4 quantization levels: $A_0 = 0$, $A_1 = 0.1$, $A_2 = 1$, and $A_3 = 10$ while the latency between any individual observation and the final combination is 0. Simulation results demonstrate the effectiveness of the proposed approach.

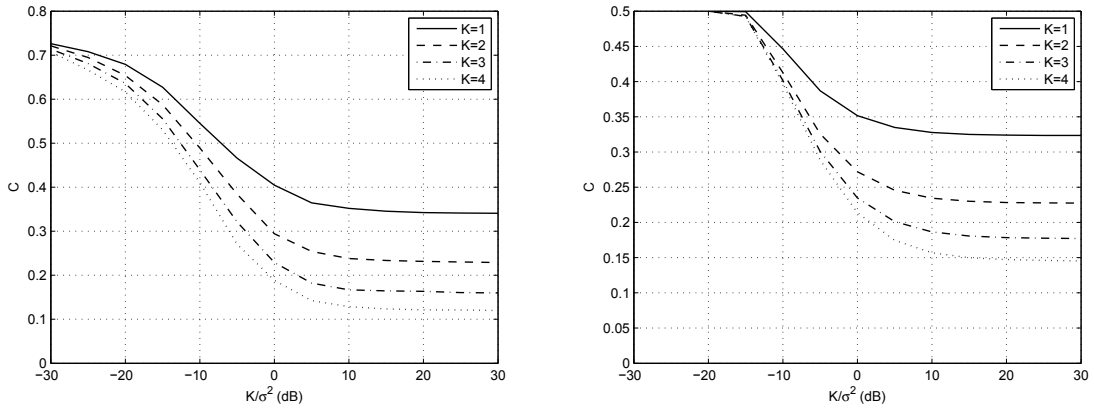

Figure 3: Bayesian costs under (a) Gaussian and (b) fading reporting channels with relative reporting SNRs

2.2 Probability-based Spectrum Sensing and Resource Allocation

Although some of the existing spectrum sensing techniques exploits the primary signal characteristic, none of them exploits the prior statistical information about the presence and absence of the primary signals. This prior information, if available, can be utilized to effectively improve the performance of spectrum sensing and resource allocation. Thus, we investigate the utilization of such statistical information and propose a probability-based spectrum sensing, scheduling, and resource allocation techniques [31, 54–59].

2.2.1 Probability-based Periodic Spectrum Sensing

Under the assumption that the arrival of primary users follows Poisson distribution, a probability model regarding the appearance of the primary user at each sampling point of a CR frame during secondary communication is set up. Based on the Neyman-Pearson criterion, we obtain an optimal spectrum sensing scheme under this probability model that maximizes the detection probability for a given false alarm probability. Although this optimal sensing scheme has huge complexity, it provides a meaningful performance benchmark. While the conventional spectrum sensing scheme always allocates the same weight to each sample, we exploit the probability model of primary user appearance and further develop a probability-based energy detection scheme, in which the weight for each sample is based on the probability of the presence of the primary user at the corresponding sampling point. Since this probability-based scheme has low complexity and nearly optimal detection performance, it is an attractive option in practice. Focusing on periodic spectrum sensing in multiple consecutive frames, we further investigate how the probability model of primary user appearance varies from frame to frame, and show that both the conventional and probability-based energy detection schemes will converge to their respective stable average detection probability [31].

Figure 4 shows the contrastive average detection probability curves of the optimal sensing scheme, the probability-based energy detection scheme, and the conventional energy detection scheme. In our simulation, we assume that the interval between the primary user arrivals, namely the idle duration of the licensed channel, is exponentially distributed with an average of 100 sampling points. Furthermore, 6 samples are utilized in each sensing block at the CR user for periodic spectrum sensing and the given false alarm probability is 10^{-1}. It verifies that the probability-based energy detection scheme exhibits much better performance than the conventional one. This is reasonable since the probability-based scheme utilizes the prior statistical information on the appearance of the primary user within the sensing block while the conventional one does not. Furthermore, it also indicates that the probability-based energy detection scheme has almost the same performance as the optimal sensing scheme especially under low SNR region. Since the probability-based energy detection scheme has much lower complexity than the optimal sensing scheme and, in the meantime, has nearly optimal performance, it is an attractive spectrum sensing scheme in practice.

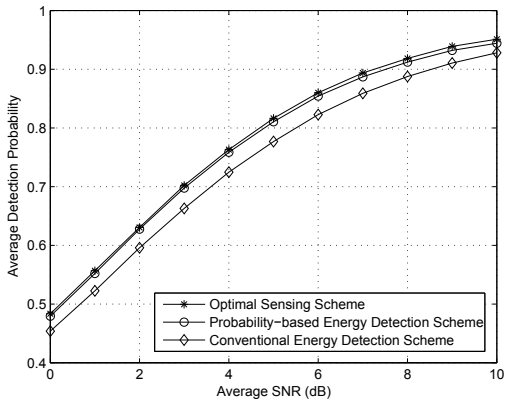

Figure 4: Contrastive average detection probability curves of different spectrum sensing schemes

2.2.2 probability-based Asynchronous Combination

In cooperative spectrum sensing, it is usually assumed in the literature that all users obtain and send the sensing information at the same time, i.e., the decision at the combining node is based on synchronous local observations. In practice, different CR users may have different sensing schedules and initiate spectrum sensing at different moments. In this case, the existing combination methods assuming synchronous sensing would incur a performance loss. To address this problem, we propose a probability-based combination scheme for cooperative spectrum sensing [54, 55]. Taking the time offsets among local sensing observations into account, our scheme enables combination of both synchronous and asynchronous sensing information from different CR users by utilizing the statistics of licensed band occupancy.

Figure 5 gives a general schematic representation for combination of sensing information in cooperative spectrum sensing. As shown in this figure, there are K cooperative users in the CR network and the kth ($k = 1, 2, ..., K$) CR user sends its sensing information u_k obtained at t_k to the combining node. After receiving the sensing information from individual CR users, the combining node makes the decision u on the absence or presence of the licensed signal at t. Note that $t > t_k$ for $k = 1, 2, ..., K$. The sensing information from the kth CR user, u_k, is either one-bit hard decision on the absence or presence of the licensed signal, or multi-bit quantized data on its observation. Specifically, User k divides the whole range of its measurement, such as the received signal energy within a predetermined interval, into L_k regions and reports to the combining node which region its observation falls in. Therefore, L_k is the number of distinct quantized sensing results from User k. Note that L_k's for different CR users are not necessarily the same. When $L_k = 1$, the sensing information from the kth user reduces to one-bit hard decision on the absence or presence of the licensed signal; when L_k goes to infinity, the sensing information of User k becomes its original measurement. Without loss of generality, we denote the L_k possible quantized sensing results of User k observed at t_k as $u_k(t_k) = l$ for $l = 0, 1, ..., L_k - 1$.

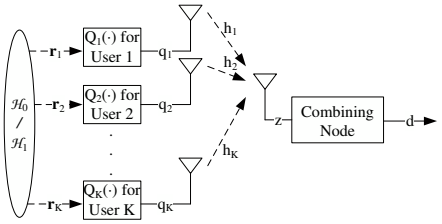

Figure 5: General combining model in cooperative spectrum sensing

For optimal combination of local sensing information, here we apply the Bayesian decision rule since it minimizes the average cost of false alarm and mis-detection. Consequently, the optimum decision is based on the following likelihood ratio,

$$Y = \frac{P(u_1, u_2, ..., u_K|\mathcal{H}_1)}{P(u_1, u_2, ..., u_K|\mathcal{H}_0)}, \tag{7}$$

where $\mathcal{H}_1$ and $\mathcal{H}_0$ denote the hypotheses corresponding to the presence and absence of the licensed signal at t,

respectively. Define the average cost as

$$R = C_F \Pr\{u = \mathcal{H}_1 | \mathcal{H}_0\} P_0 + C_M \Pr\{u = \mathcal{H}_0 | \mathcal{H}_1\} P_1, \tag{8}$$

where P_1 and P_0 denote the prior probabilities of the presence and absence of the licensed signal, which can be substituted with the stationary probabilities; C_F and C_M are the costs for false alarm (the decision is H_1 while the licensed signal is absent at t) and mis-detection (the decision is H_0 while the licensed signal is present at t), respectively. In practice, C_M is usually larger than C_F because, in the mis-detection case, the CR users are allowed to utilize the licensed band and may generate interference to licensed users, which is more severe than possible loss of spectrum opportunities in the false alarm case. To minimize the average cost, the optimum decision rule is given as

$$Y \underset{\mathcal{H}_0}{\overset{\mathcal{H}_1}{\gtrless}} \frac{P_0 C_F}{P_1 C_M}. \tag{9}$$

Since individual CR users are at different locations, we assume that their observations are statistically independent and therefore,

$$P(u_1, u_2, ..., u_K | \mathcal{H}_i) = \prod_{k=1}^{K} P(u_k | \mathcal{H}_i). \tag{10}$$

According to the Bayes' theorem,

$$P(u_k | \mathcal{H}_i) = P(u_k | B_k) P(B_k | \mathcal{H}_i) + P(u_k | I_k) P(I_k | \mathcal{H}_i), \tag{11}$$

where B_k and I_k denote that the licensed signal is present and absent at t_k, respectively. $P(u_k|B_k)$ and $P(u_k|I_k)$ are parameters reflecting the detection performance of the kth user. With the help of age distribution of a renewal process, we can obtain $P(I_k|\mathcal{H}_0)$, $P(I_k|\mathcal{H}_1)$, $P(B_k|\mathcal{H}_1)$, and $P(B_k|\mathcal{H}_0)$.

We compare our scheme under the hard decision case with the conventional scheme that always assumes synchronous local observations as well as a simplified sliding-window scheme that maintains the sensing information within 1 sec before the final decision is made. We let 10 CR users take turns to perform spectrum sensing and the time offsets between adjacent observations are the same. In our simulation, $C_F = 1$, $C_M = 2$. The performance of the schemes with respect to different maximum offsets between the first observation and the final decision is shown in Figure 6. We also compare them under both faultless reporting channel and a binary symmetric channel (BSC) channel with crossover probability 0.1. It is obvious that our scheme has lower average cost than both the conventional and the sliding-window schemes. The performance gap between them turns more and more obvious as the maximum offset between the first observation and the final decision increases, which demonstrates the effectiveness of our scheme in combining asynchronous sensing information. When there are reporting errors for the local information, our scheme remains superior.

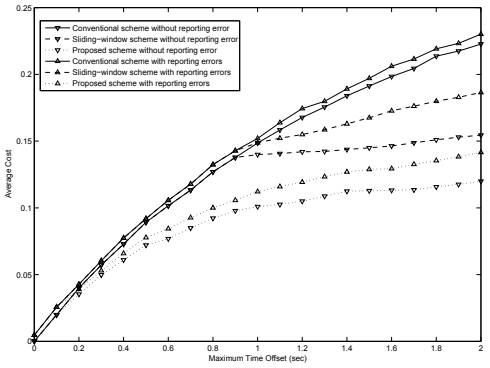

Figure 6: Contrastive average cost curves of different combination schemes

2.2.3 Probability-based Sensing Scheduling

The efficiency of opportunistic spectrum sharing relies not only on the spectrum sensing techniques applied but also on the scheduling of sensing activities. On one hand, if sensing activities are scheduled too often, CR users may waste too much time on sensing. On the other hand, if sensing activities are seldom scheduled, spectrum usage status may not be quickly discovered. In a periodic spectrum sensing framework where each frame consists of a sensing block and an inter-sensing block, the ratio of the sensing block length to the inter-sensing block length represents how frequently sensing activities are scheduled, and therefore is a key parameter in spectrum sensing scheduling. Probability-based strategies are proposed to determine the optimal inter-sensing duration for CR [57, 58]. With utilization of the statistics of licensed band occupancy, appropriate inter-sensing duration is determined to capture the recurrence of spectrum opportunity in time when the licensed signal is detected, or to provide CR system with the maximum spectrum efficiency under a certain level of interference with licensed communication when the licensed signal is declared absent.

The licensed band is modeled as an alternating renewal source between busy and idle states, where busy and idle denote that the band is occupied and unoccupied by the licensed users, respectively. The busy and idle periods are random variables with *probability density functions* (PDFs) $f_B(t)$ and $f_I(t)$, respectively, which can be assumed exponentially distributed with $f_B(t) = \alpha e^{-\alpha t}$ and $f_I(t) = \beta e^{-\beta t}$, where α is the transition rate from busy to idle state, and β is the transition rate from idle to busy state, both of which can be estimated with statistical methods. Accordingly, the average busy and idle periods are $1/\alpha$ and $1/\beta$, and the stationary probabilities for the band to be busy and idle are $\bar{P}_B = \frac{\beta}{\alpha+\beta}$ and $\bar{P}_I = \frac{\alpha}{\alpha+\beta}$. Denote the probability density functions of the remaining time that the band stays in the current busy and idle states as $f_{BR}(t)$ and $f_{IR}(t)$, respectively, which are the same as $f_B(t)$ and $f_I(t)$ due to the memoryless property of the exponential distribution.

In our model, the activity of the CR user is periodic. In each frame, the CR user first monitors the band in the sensing block for M samples. Depending on whether the band is identified as busy or idle, the CR user will either keep silent or start transmitting or receiving in the inter-sensing (silent or data) block for L samples. Since the band may be reoccupied or released by the licensed users in the future, the CR user should restart a new frame beginning with the sensing block again following the previous inter-sensing block. We assume

that the CR user adopts a predetermined length of the sensing block for certain detection performance. In other words, M is fixed. According to our model, if the band is busy at the end of a sensing block, the conditional probability that it is still busy at the lth sample of the upcoming inter-sensing block is

$$P_{B_l|B} = \int_{l\tau}^{\infty} f_{BR}(t)dt = e^{-\alpha l\tau}, \tag{12}$$

where t is the remaining time in the current state from the last sample of the sensing block, and τ denotes the sampling interval. The conditional probability that it is idle at the lth sample of the upcoming inter-sensing block is $P_{I_l|B} = 1 - P_{B_l|B}$. Similarly, if the band is idle at the end of the sensing block, the conditional idle and busy probabilities at the lth sample of the upcoming inter-sensing block are

$$P_{I_l|I} = \int_{l\tau}^{\infty} f_{IR}(t)dt = e^{-\beta l\tau} \tag{13}$$

and $P_{B_l|I} = 1 - P_{I_l|I}$, respectively.

If a CR user detects the band as busy within the sensing block, it will keep silent in the upcoming inter-sensing block of the current frame and initiate detection in the sensing block of the next frame. If the length of the silent block is larger, spectrum sensing actions will be taken less frequently, which saves energy. However, the spectrum opportunity may not be quickly recognized and the latency of the CR user's packet may be increased. It is obvious that there is a tradeoff between energy efficiency and bandwidth efficiency when selecting the length of the silent block. To that end, we introduce the concept of *average spectrum opportunity loss*, which is defined as the expected number of idle samples within the upcoming inter-sensing block if the band is detected as busy in the sensing block. From the definition, it can be expressed as

$$T_{I_L|\hat{B}} = \sum_{l=1}^{L} P_{I_l|\hat{B}}, \tag{14}$$

where $P_{I_l|\hat{B}}$ is the conditional idle probability at the lth sample of the upcoming inter-sensing block if the band is detected as busy in the sensing block. With such a concept, we are able to estimate the throughput loss within the block, which is the product of the average spectrum opportunity loss and average transmission rate of the CR user for a given average transmit power.

There are two cases that the CR user may keep silent in the inter-sensing block: i) the sensing decision is busy while the band is really busy at the end of the sensing block (correct detection), and ii) the sensing decision is busy while the band is actually idle at the end of the sensing block (false alarm). Since $P_B + P_I = 1$, we have

$$P_{I_l|\hat{B}} = P_{I_l|B}P_{B|\hat{B}} + P_{I_l|I}P_{I|\hat{B}}, \tag{15}$$

where $P_{I_l|B}$ and $P_{I_l|I}$ are the conditional idle probabilities with perfect sensing as we have introduced in Section II; $P_{B|\hat{B}}$ and $P_{I|\hat{B}}$ are the conditional busy and idle probabilities at the end of the sensing block if the band is

detected as busy in the sensing block, respectively. According to the Bayes' theorem, we have

$$P_{B|\hat{B}} = \frac{P_{\hat{B}|B}P_B}{P_{\hat{B}|B}P_B + P_{\hat{B}|I}P_I} \tag{16}$$

and

$$P_{I|\hat{B}} = \frac{P_{\hat{B}|I}P_I}{P_{\hat{B}|B}P_B + P_{\hat{B}|I}P_I}, \tag{17}$$

where $P_{\hat{B}|B}$ or $P_{\hat{B}|I}$ is the conditional probability that the band is detected as busy if the band is busy or idle at the end of the sensing block, which can be set equal to the average detection probability, P_D, or false alarm probability, P_F; P_B or P_I is the busy or idle probability at the end of the sensing block, which can be substituted with the stationary probability $\bar{P}_B$ or $\bar{P}_I$.

Accordingly, we find the relationship between the length of the silent block and the average spectrum opportunity loss for the case with exponentially distributed busy and idle states as

$$T_{I_L|\hat{B}} = (L - \frac{1-e^{-\alpha\tau L}}{1-e^{-\alpha\tau}}e^{-\alpha\tau})P_{B|\hat{B}} + \frac{1-e^{-\beta\tau L}}{1-e^{-\beta\tau}}e^{-\beta\tau}P_{I|\hat{B}}. \tag{18}$$

To identify the spectrum opportunity quickly, it is usually required that L is small such that $\alpha\tau L$ and $\beta\tau L$ are close to 0. Therefore, the spectrum opportunity loss can be well approximated with partial Taylor polynomials as

$$T_{I_L|\hat{B}} = \frac{\alpha\tau L^2}{2}P_{B|\hat{B}} + (L - \frac{\beta\tau L^2}{2})P_{I|\hat{B}}. \tag{19}$$

By taking the partial derivative with L, we find that it is an increasing function of L. So if it requires that the spectrum opportunity loss to be no larger than a predefined value, T_λ, which is set according to the speed requirement for emptying the queue of the CR user divided by its average transmission rate, the optimal length of the silent block is

$$L_{opt} = \left\lfloor \frac{\sqrt{P_{I|\hat{B}}^2 + 2(P_{B|\hat{B}}\alpha\tau - P_{I|\hat{B}}\beta\tau)T_\lambda} - P_{I|\hat{B}}}{P_{B|\hat{B}}\alpha\tau - P_{I|\hat{B}}\beta\tau} \right\rfloor. \tag{20}$$

Figure 7(a) shows the relationship between the average spectrum opportunity loss, $T_{I_L|\hat{B}}$ and the length of the silent block, L. In this figure, $\tau = 0.0001$ sec, $M = 50$, $\alpha = \beta = 0.4$ sec^{-1}, $P_D = 0.95$, and $P_F = 0.1$. It verifies that the average spectrum opportunity loss is an increasing function of the silent block length. In this figure, we also show that the corresponding optimal length of the silent block is around 800 samples given $T_\lambda = 100$. And it can be observed that the optimal inter-sensing duration always exists. However, for different channel usage settings, i.e., different combinations of channel state transition rates α and β, optimal inter-sensing durations are different. Here, the optimal inter-sensing duration is $0.195(sec)$ when $\alpha = 1(1/sec)$ and $\beta = 0.5(1/sec)$, and, the optimal inter-sensing duration is $0.125(sec)$ when $\alpha = 0.5(1/sec)$ and $\beta = 1(1/sec)$. If our optimization scheme is not used and the inter-sensing duration is deviated from the optimal one, either channel efficiency is lowered or interference threshold is violated.

If a CR user detects the band as idle within the sensing block, it will start transmitting or receiving data in the

band within the upcoming inter-sensing (data) block. Intuitively, if the data block is too long, the licensed user is with high possibility to reoccupy the band so that they may interfere with each other. If it is too short, the CR communication may be interrupted too frequently for spectrum sensing and the CR user may lose the remaining spectrum opportunity within the idle band, which results in low bandwidth efficiency. Therefore, there exist better strategies to determine the length of the data block, for the overall benefits of the licensed user and the CR user. In this section, we will first study how to choosing the optimal length of the data block. Here we use two metrics to characterize the system performance including average transmission rate and average interference power. *Average transmission rate*, η, is defined as the expected average rate of the CR communication within the whole frame. Mathematically,

$$\eta = \frac{\sum_{l=1}^{L} P_{I_l|\hat{I}} R_l}{M+L}, \tag{21}$$

where $P_{I_l|\hat{I}}$ is the conditional idle probability at the lth sample of the upcoming inter-sensing block if the band is detected as idle in the sensing block, and R_l is the transmission rate of the CR user at the lth sample of the upcoming inter-sensing block, which is related to the transmit power S_l at the lth sample by

$$R_l = \log_2(1 + \frac{S_l G}{N_0}), \tag{22}$$

where G is the power gain from the CR transmitter to receiver and N_0 is the noise variance at the CR receiver. G and N_0 are both assumed to be constant during one data block, which can be obtained by channel and noise estimation methods. Similarly, *average interference power*, ε, is defined as the expected average interference power at the licensed receiver from CR communication within the whole frame. Mathematically,

$$\varepsilon = \frac{\sum_{l=1}^{L} P_{B_l|\hat{I}} S_l G'}{M+L}, \tag{23}$$

where $P_{B_l|\hat{I}}$ is the conditional busy probability at the lth sample of the upcoming inter-sensing block if the band is detected as idle in the sensing block, which is equal to $1 - P_{I_l|\hat{I}}$, and G' is the power gain from the CR transmitter to the licensed receiver. G' is also assumed to be constant during each data block. If the channel between the CR transmitter and the licensed receiver is reciprocal and the licensed communication is bi-directional, G' can be estimated through measuring the licensed signal strength at the CR transmitter during spectrum sensing when the licensed receiver is transmitting.

The data block length optimization can be formulated as selecting the length of the data block so that

1. the average interference power in (23) is no more than a predefined threshold, and
2. the average transmission rate in (21) is maximized.

Similar to the discussion in the previous section, denote $P_{B|\hat{I}}$ and $P_{I|\hat{I}}$ as the conditional busy and idle probabilities at the end of the sensing block if the band is detected as idle in the sensing block, which can be represented as

$$P_{B|\hat{I}} = \frac{(1-P_D)\bar{P}_B}{(1-P_D)\bar{P}_B + (1-P_F)\bar{P}_I} \tag{24}$$

and

$$P_{I|\hat{I}} = \frac{(1-P_F)\bar{P}_I}{(1-P_D)\bar{P}_B + (1-P_F)\bar{P}_I}, \tag{25}$$

respectively, and set the transmit power of the CR user at each sample of the upcoming data block to be equal to S, we find the relationship between the length of the data block and the average transmission rate as

$$\eta = R\frac{\frac{\alpha\tau L^2}{2}P_{B|\hat{I}} + (L - \frac{\beta\tau L^2}{2})P_{I|\hat{I}}}{M+L} \tag{26}$$

and

$$\varepsilon = SG'\frac{(L - \frac{\alpha\tau L^2}{2})P_{B|\hat{I}} + \frac{\beta\tau L^2}{2}P_{I|\hat{I}}}{M+L}. \tag{27}$$

By taking the partial derivative with L, we find that the average transmission rate is initially increasing and then decreasing as the length of the data block increases, and the average interference power is an increasing function of the data block length. The maximum value of η is achieved at

$$L = L_{opt}^{(1)} = \left\lfloor \sqrt{M^2 + \frac{2P_{I|\hat{I}}M}{P_{I|\hat{I}}\beta\tau - P_{B|\hat{I}}\alpha\tau}} - M \right\rfloor. \tag{28}$$

To ensure $\frac{\varepsilon}{SG'} \leq \Gamma$, where Γ is the predefined threshold, we need

$$L \leq L_{opt}^{(2)} = \left\lfloor \frac{\sqrt{(P_{B|\hat{I}} - \Gamma)^2 + 2(P_{I|\hat{I}}\beta\tau - p_{B|\hat{I}}\alpha\tau)\Gamma L} - P_{B|\hat{I}} + \Gamma}{P_{I|\hat{I}}\beta\tau - P_{B|\hat{I}}\alpha\tau} \right\rfloor. \tag{29}$$

Therefore, the optimal length of the data block is

$$L_{opt} = \min(L_{opt}^{(1)}, L_{opt}^{(2)}). \tag{30}$$

Figure 7(b) shows the normalized average transmission rate, η/R, and interference power, ε/SG', with respect to the length of the data block, L, given the same parameters as in the previous example and $\alpha = \beta = 0.4$ sec^{-1}. It verifies that the average transmission rate is initially increasing and later decreasing with increased length of the data block while the average interference power is an increasing function of the data block length. In this figure, we also show how to find the corresponding optimal length of the data block given $\Gamma = 0.08SG'$. We find the maximum normalized average transmission rate and the corresponding length of the data block, $L_{opt}^{(1)}$, and find the interference power constraint and the corresponding length of the data block, $L_{opt}^{(2)}$. Then we select the optimal length of the data block, $L_{opt} = \min(L_{opt}^{(1)}, L_{opt}^{(2)})$.

2.2.4 Probability-based Transmit Power Control

According to our previous discussion, statistical information obtained from spectrum sensing is unique for CR, which should be used to assist the resource allocation in CR networks. We propose to vary transmit power of

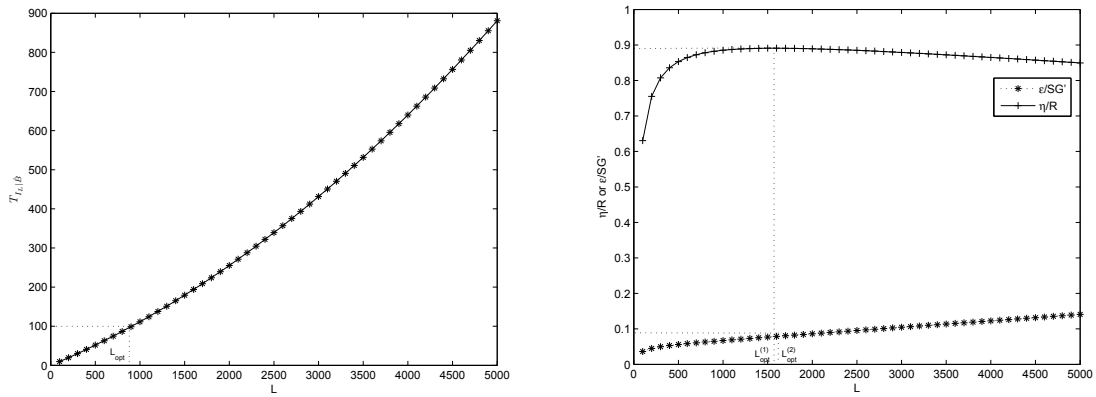

(a) (b)

Figure 7: (a) Average spectrum opportunity loss versus silent block length and (b) normalized average transmission rate and interference power versus data block length.

the CR user dynamically according to the non-interfering probability at each sample in a data block so as to increase the transmission rate and decrease the interference power [58, 59].

Our objective is to maximize the average transmission rate of the CR user in (21) under its average transmit power constraint, $\bar{S}$, that is, to maximize

$$\eta = \frac{\sum_{l=1}^{L} P_{I_l|\hat{I}} \log_2(1 + S_l G/N_0)}{M + L}, \tag{31}$$

subject to

$$\frac{1}{L}\sum_{l=1}^{L} S_l \leq \bar{S}. \tag{32}$$

This optimization problem can be solved via the Lagrangian methods. Consider the Lagrangian

$$\mathcal{L}(\lambda, S_1, S_2, ..., S_L) = \sum_{l=1}^{L} P_{I_l|\hat{I}} \log_2(1 + S_l G/N_0) - \lambda \sum_{l=1}^{L} S_l, \tag{33}$$

where λ is the Lagrange multiplier. The power allocation

$$S_l = \left(\frac{P_{I_l|\hat{I}}}{\mu} - \frac{N_0}{G}\right)^+ \tag{34}$$

satisfies is therefore optimal, where $(x)^+ = \max(x, 0)$ and μ is a parameter chosen such that the power constraint is met, that is,

$$\frac{1}{L}\sum_{l=1}^{L} \left(\frac{P_{I_l|\hat{I}}}{\mu} - \frac{N_0}{G}\right)^+ = \bar{S}. \tag{35}$$

If N_0/G is very small, which corresponds to the case of large signal to noise ratio at the CR receiver side, the transmit power is directly proportional to the conditional idle probability at each sample that $S_l = \frac{P_{I_l|\hat{I}}}{\bar{P}_{I_l|\hat{I}}}\bar{S}$ where $\bar{P}_{I_l|\hat{I}} = \frac{1}{L}\sum_{l=1}^{L} P_{I_l|\hat{I}}$. Note that the channel and noise information is not needed for implementation in this case.

With probability-based transmit power control, the relative transmission rate increment, $\Delta\eta/\eta_0$, and interference power decrease, $-\Delta\varepsilon/\varepsilon_0$, for different values of the average receive SNR, γ, and the data block length, L, are shown in Figure 8(a) and 8(b). Here the sensing block length is set to be 50, and the average busy and idle durations of the licensed user are both 2.5 sec. Note that our scheme exhibits greater performance gain at smaller average receive SNR. As the average receive SNR gets larger, our power control scheme is closer to the constant power allocation, which is similar to the trend of power allocation among parallel subchannels of *orthogonal frequency-division multiplexing* (OFDM) systems.

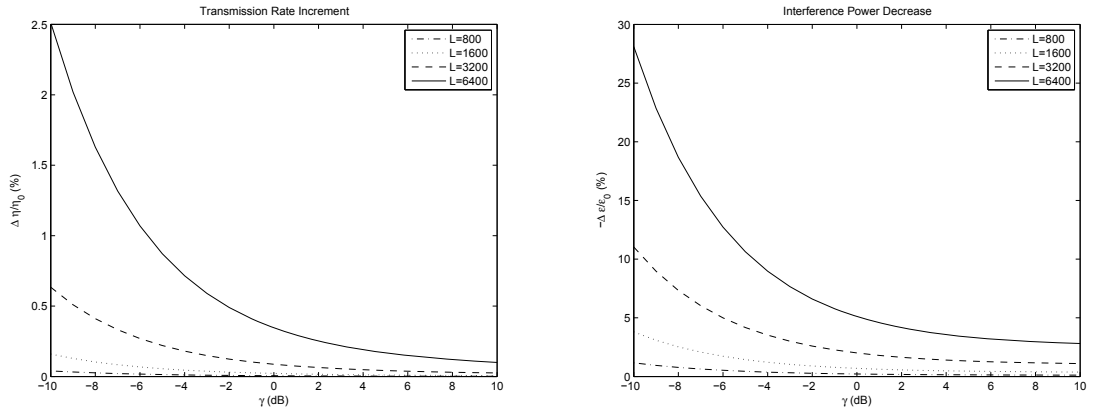

(a) (b)

Figure 8: (a) Transmission rate increment and (b) interference power decrease vs. average receive SNR

2.2.5 Probabilistic Resource Allocation

Due to the existence of licensed users and possible mutual interference between two classes of users, the problem of resource allocation for *opportunistic spectrum access* (OSA) in CR networks is no longer the same as that in traditional wireless networks. After determining the availability of licensed spectrum, CR users adjust their transmission parameters through resource allocation to achieve certain performance requirements and realize effective interference management. In a multi-channel environment where the licensed spectrum is divided into several non-overlapping frequency channels, resource allocation usually includes channel and power allocation among CR users. Most of the existing work on resource allocation in CR networks makes use of the hard decisions on the availability of licensed channels so that channel and power allocation is carried out only among the decided available channels and is then similar to that in *orthogonal frequency division multiple access* (OFDMA) systems. Since decision errors from spectrum sensing are inevitable in practice, these resource allocation algorithms inherit the imprecise information in the hard decisions, which may introduce

unacceptable interference to licensed users and lose the flexibility of OSA. Therefore, we propose a probabilistic resource allocation approach to further exploit the flexibility of OSA [49, 56]. Based on the probabilities of channel availability obtained from spectrum sensing, the proposed approach optimizes channel and power allocation in a multi-channel environment. The given algorithm maximizes the overall utility of a CR network and ensures sufficient protection of licensed users from unacceptable interference, which also supports diverse *quality-of-service* (QoS) requirements and enables a distributed implementation in multi-user networks.

We consider a CR network with K active users exploiting communication opportunities over a portion of licensed spectrum. Each CR user consists of a transmitter and an intended receiver. The total bandwidth of interest is equally divided into N non-overlapping channels, each with a bandwidth of B. OSA is realized by assigning different licensed channels to CR users and allocating transmit powers accordingly. Each channel is exclusively assigned to at most one CR user at a time, so there will be no mutual interference among different users. The proposed resource allocation approach considers average utility and interference for given sensing information. The average utility within Channel n for CR User k is defined as

$$\bar{U}_{k,n} = \mathbf{E}[U_{k,n}], \tag{36}$$

where $U_{k,n}$ is the utility of User k accessing Channel n, and the expectation is taken under the conditional distribution of the utility related to the absence or presence of the licensed signal at the CR receiver given the current sensing information. Even though other utility measures may be applied, we will focus on using the achievable data rate. Consequently,

$$U_{k,n} = \begin{cases} r_{k,n}, & \text{no licensed signal at the CR receiver,} \\ 0, & \text{otherwise,} \end{cases} \tag{37}$$

where $r_{k,n}$ is the maximum data rate of the user over Channel n if the licensed signal is absent at the receiver of User k. Here we assume that if the licensed signal is present at the CR receiver, the transmission of the CR user will fail. Therefore, the average data rate will be

$$\bar{r}_{k,n} = q^{(I)}_{R_k,n} r_{k,n}, \tag{38}$$

where $q^{(I)}_{R_k,n}$ is the conditional probability that the licensed signal is absent in Channel n at the receiver of CR User k given the current sensing information. Similarly, average interference to the licensed user must be considered when performing resource allocation. The average interference in Channel n from the transmitter of CR User k can be expressed as

$$\bar{I}_{k,n} = q^{(B)}_{T_k,n} I_{k,n}, \tag{39}$$

where $q^{(B)}_{T_k,n}$ is the conditional probability that the licensed signal is present in Channel n at the transmitter of CR User k given the current sensing information, $I_{k,n}$ is the interference power the transmitter of User k will generate to the licensed receiver if a certain licensed user is simultaneously using Channel n.

The approach to compute the probabilities of licensed channel availability from spectrum sensing is given. Resource allocation in a CR network maximizes the overall system utility, which is the weighted sum data rate

of the CR network. To protect licensed communication, we also post an allowable average interference level at the licensed receiver over each channel. Furthermore, each CR user should guarantee a minimum average data rate. It can be formulated as an optimization problem and solved with dual decomposition approach [43].

In our simulation, we consider 8 CR users utilizing 16 licensed channels each with a bandwidth of 100 KHz. The maximum transmit power for the CR user is 10 mW and the interference constraint for each channel is 0.6 mW, which are normalized to zero path loss. The channels between the CR transmitters and receivers, and between the CR transmitters and licensed receivers are independent realizations of Rayleigh fading with unit power. Each CR user combines spectrum sensing information from 4 nearby cooperative CR nodes providing local hard decisions on licensed channel availability and the probability of incorrect local decision is 0.1. Meanwhile, the stable probability of presence of licensed signal in each channel is 0.5. The weights for the data rates of the CR users are all set to be 1, and the minimum data rate requirements are 100 Kbps. Given spectrum sensing information, the probabilistic resource allocation approach is compared with both decision-based aggressive, in which resource is allocated within all determined available channels assuming spectrum sensing decision is perfect, and conservative resource allocation, in which resource is allocated within all decided available channels while possible interference is not allowed to exceed the interference constraint. The weighted sum data rates, which turn into sum data rates, under different noise powers with different resource allocation approaches are shown in Figure 9, which implies that it is preferable to use the proposed probabilistic approach in multi-user CR networks. The proposed probabilistic approach achieves the best throughput performance, especially when it is compared with decision-based conservative resource allocation. Meanwhile, the interference of decision-based aggressive resource allocation with the licensed receivers does not always satisfy the interference constraint.

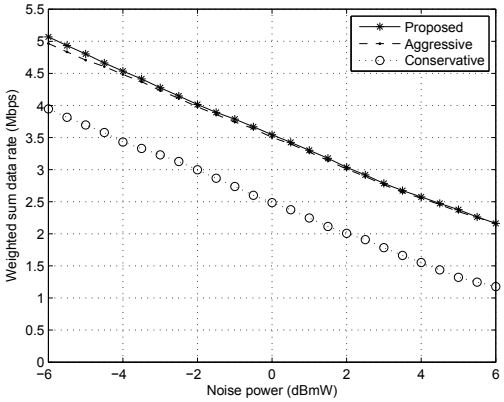

Figure 9: Weighted sum data rates with respect to different noise powers with 8 CR users

2.3 Cooperative Relay

Spectrum hole (SH) is a spectrum band that can be utilized by unlicensed users in CR networks. To exploit the new spectrum opportunity in spatial domain and maximize the achievable end-to-end throughput, we propose

a cooperative communication scheme with directional relays [44, 46] and investigate the channel allocation problem for cooperative relays [45, 47]. In addition, we consider the issue of joint relay selection and power allocation for relay-assisted transmission [28] and energy efficiency [27, 29] in cooperative CR networks.

2.3.1 Directional and Relay-assisted Transmission

Most of existing contributions propose to detect SHs by determining whether a primary signal is present or absent so that the CR and primary users utilize the spectrum band(s) either at different time slots or in different geographic regions. We propose a novel scheme with directional relays for CR users to exploit new spectrum opportunity, called spatial SHs [44, 46]. It provides higher spectrum efficiency with the coexistence of primary and CR users at the same time, region, and spectrum band. We analyze the successful communication probabilities (SCP) of CR users and demonstrate that the spectrum efficiency can be considerably improved.

Conventionally, SHs can be roughly divided into two categories: temporal spectrum holes and geographic spectrum holes. For the former one, a CR user accesses a spectrum band when PUs are not using it temporarily, which means that both the CR and PUs can be deployed in the same spectrum band and area but at different time slots, and the secondary transmission is realized by utilizing the silent time slots of PUs. While for the latter one, a CR user can access a spectrum band when the CR and PUs are in different geographic areas since pathloss and shadowing of wireless channels separate them and make it possible for both to work at the same time without interfering each other.

Usually, it is hard for the CR and primary users to work at the same time and location. However, as shown in Figure 10(a), if CR users are with directional transmission ability, which can be implemented by directional antennas or by transmit antenna arrays with beamforming, they will be able to coexist with PUs. Therefore, such secondary communication opportunities at the same time and geographic area with the PUs are called spatial spectrum holes (SSHs) since they are using different spatial domains where primary and CR links are.

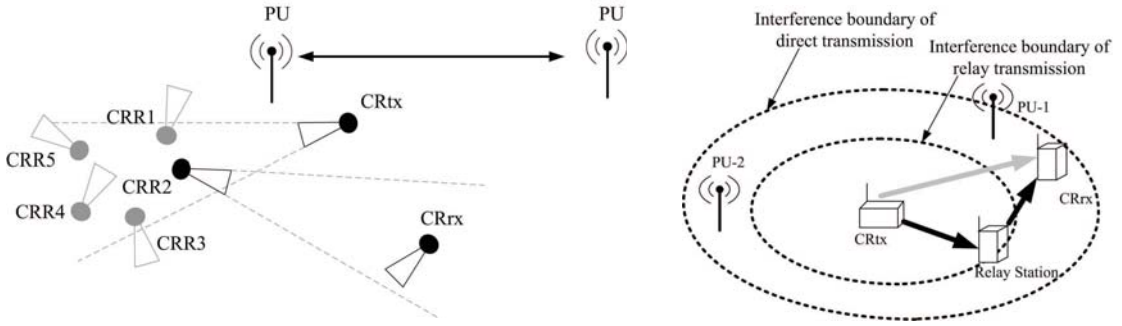

(a) (b)

Figure 10: Spatial spectrum holes with (a) directional transmission (b) CR relays.

We also propose a concept of SSHs that are generated by relay transmissions, and investigate a relay-assisted scheme when directional antennas with beamforming are not available for CR users [46]. With the

help of relay techniques, CR users are able to achieve more communication opportunities even when direct transmissions are not available.

Figure 10(b) shows a schematic representation of the coexistence of the primary and secondary systems in this scenario when relay technique is available. As shown in the figure, if a CR user sends data directly to its receiver, it has a large interference boundary and a large area inside the boundary that needs to be cleared, which means that the CR user can only communicate through the spectrum band if there are no PUs within the interference boundary. Otherwise, the CR user may generate harmful interference to PUs when it works. However, if the CR user lowers its transmit power and uses other CR users as relay stations to forward data to its destination, it can still access the spectrum band without interfering with PUs since smaller interference boundary can be obtained in this way.

As shown in Figure 10(b), a CR transmitter (CRtx) intends to send data to its CR receiver (CRrx) through a licensed spectrum band. Thus the CRtx will perform spectrum sensing to detect whether such a CR transmission in the spectrum band will cause interference to PUs or not. If the PU is close to the CRrx, such as PU-1 in the figure, it is hard for CRrx to communicate with the CRtx without causing interference to the PU. On the other hand, if the PU is far away from the CRrx, such as PU-2 in the figure, the CRtx may communicate with the CRrx with the help of relays. In this case, the CRtx lowers its transmit power and shortens the radius of the interference region, and as a result, the CRtx may still transmit without causing interference to PU-2. Furthermore, with the help of relay stations, the data will be conveyed from the CRtx to the CRrx successfully on a non-interfering basis.

Assume that a CRtx intends to communicate with a CRrx, where the distance between them is d. The area inside a circle with radius d and center CRtx is considered. There is a PU within it and the probabilities that the PU appears in each positions are the same, and N CR users are uniformly distributed in it at the same time. Figure 11 shows the average SCP versus the number of CR users and we also plot the SCP bound for comparison. From the figure, the average SCP dramatically increases as the number of CR users goes up, which represents the density of CR users. There is over 50% chance that the CR user is able to successfully send data to its receiver if there are more than 20 CR users in the considered area.

2.3.2 Power and Channel Allocation for Cooperative Relay

Recent studies on spectrum sensing have shown that the available spectrum bands may vary with different CR users. It happens when the transmission range of CR users is larger than or similar to that of PUs. Then different CR users may obtain different sensing results since they are at different locations and have different impacts on PU systems. For example, an available spectrum band at a CR transmitter may not be available at its intended CR receiver and vice versa. Nevertheless, secondary communication can only be established through common available bands between a pair of CR users. If there are no available bands in common, then no direct link can be established.

In order to solve the problem, cooperative relay has been introduced into CR networks. With the assistance of a CR user as a relay that has rich available spectrum bands, some of non-common spectrum bands between

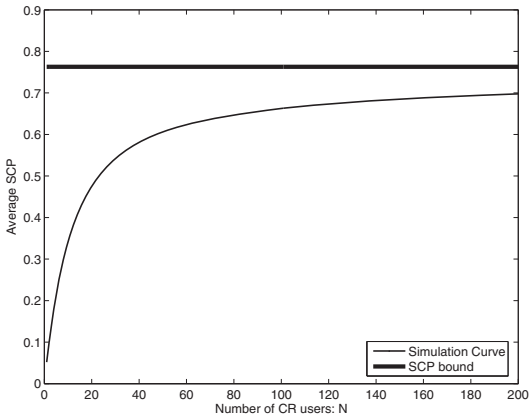

Figure 11: Average SPC performance

the CR source and the CR destination can be bridged to exploit more spectrum opportunities. We investigate power and channel allocation for cooperative relay in a three-node CR network [45, 47], which consists of a source, a relay, and a destination and can operate in multiple spectrum bands. In the context, *CR relay channels* (CRRC) can be divided into three categories as shown in Figure 12(a). If a spectrum band is available at all three CR nodes, it is called a *relay channel* since it can provide end-to-end communication using cooperative relay protocols. If a spectrum band is available at both the source and the destination but not at the relay, it is called a *direct channel* for it can provide end-to-end communication directly. If one spectrum band is available at the source and the relay, and another one is available at the relay and the destination, it is called a *dual-hop channel* since end-to-end communication can be established via the relay. Each kind of the above channels has been studied. Dual-hop channels may increase throughput, extend coverage, and reduce interference. Relay channels improve the performance through spatial diversity by using additional paths between source and destination. However, in CRRC, if CR nodes are with rich available bands, some of the bands can be used as a relay, a direct, or a dual-hop channel, and different combinations may result in different performance. Allocating each available band to one of the three kinds of channels will bring us new degrees of freedom, which has not been discussed in CR. Instead of addressing the transmission for each kind of channels separatively, we design transmission schemes to exploit all channels jointly to optimize overall system performance. In general, a dual-hop channel has a bottleneck in throughput whereas a relay channel loses half of its throughput due to its half duplex constraint in practice. We propose to assign the spectrum band of the relay channel to assist the transmission in dual-hop or direct channels. This not only compensates for the bottleneck of the dual-hop channel but also enables the spectrum band of the relay channel to work in full-duplex mode. As a result, the overall end-to-end throughput can be significantly improved. Furthermore, we apply power allocation for CRRC so that the maximum overall end-to-end throughput can be achieved.

In CRRC, some available spectrum bands can be used in different ways, which will result in different overall end-to-end throughput. Here, Band 3 (BD3) that is available to all three CR nodes can be used in the four different modes in Figure 12(b):

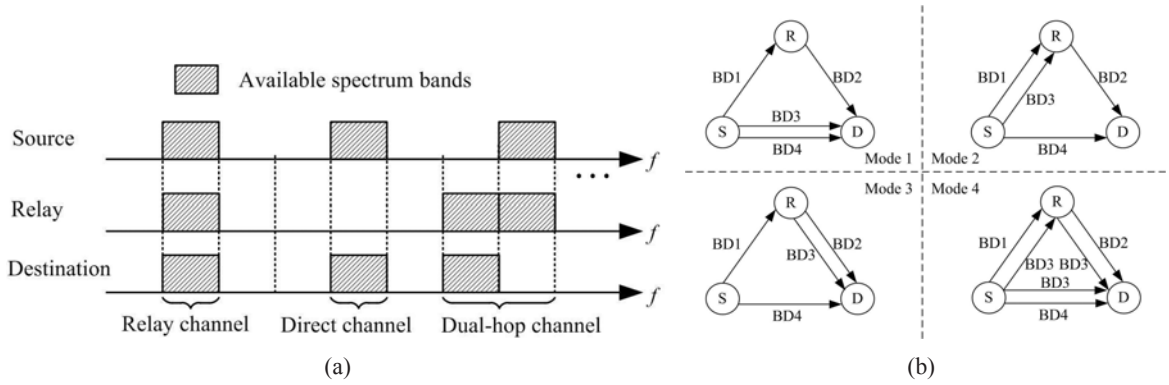

Figure 12: (a) CRRC in CR networks and (b) different modes of channel allocation.

- *Mode 1:* Direct transmission from the source to the destination.
- *Mode 2:* Dual-hop transmission from the source to the relay.
- *Mode 3:* Dual-hop transmission from the relay to the destination.
- *Mode 4:* Relay diversity transmission by using all three links with cooperative relay protocols.

If one of the first three modes is used, i.e., Modes 1, 2, and 3, the overall end-to-end throughput consists of the throughput of the direct and the dual-hop transmission with enhanced SD, SR, and RD links and can be expressed as (40).

$$R_{all}(\mathbf{p}^S, \mathbf{p}^R) = R_{direct} + R_{dual} = \begin{cases} \left(C(p_4^S g_4) + C(p_3^S g_3^{sd})\right) + \min\left\{C(p_1^S g_1), C(p_2^R g_2)\right\} & \text{: Mode 1} \\ C(p_4^S g_4) + \min\left\{C(p_1^S g_1) + C(p_3^S g_3^{sr}), C(p_2^R g_2)\right\} & \text{: Mode 2} \\ C(p_4^S g_4) + \min\left\{C(p_1^S g_1), C(p_2^R g_2) + C(p_3^R g_3^{rd})\right\} & \text{: Mode 3} \end{cases} \quad (40)$$

If the last mode is used, the overall end-to-end throughput can be obtained by

$$R_{all}(\mathbf{p}^S, \mathbf{p}^R) = R_{direct} + R_{dual} + R_{relay}. \quad (41)$$

The channel allocation is to select a proper mode to maximize the overall end-to-end throughput. From (41) and (40), the throughput in each mode is also determined by power allocation. To achieve the maximum overall end-to-end throughput, the throughput in each mode should be maximized by power allocation. Afterwards, we can pick the mode with the highest throughput to perform cooperative transmission in CRRC. The power allocation is performed by water-filling. In this section, we first present numerical results to illustrate the performance of our power and channel allocation in the typical case with four spectrum bands. Based on the observation from the results, we will find a low complexity method and show its performance in the case with an arbitrary number of spectrum bands.

In our simulation, we assume that three CR nodes are with equal distance[1] and they experience independent Rayleigh fading channels. We further assume that each spectrum band has 1 MHz bandwidth, the noise power

[1]For simplicity, we consider the scenario with equal distance among three CR nodes.

at each CR node is -126 dBW, and the path loss between two CR nodes is 126 dB. Furthermore, all curves are averaged over 200 channel realizations and the per band power constraint is set to 3 W, i.e., $P_{\max} = 3$ W, which represents the maximum allowable transmit power on each spectrum band. In the following, we will present the overall end-to-end throughput, R_{all}, for different power and channel allocation schemes. Legends "PA+CA", "PA only", "CA only", and "No PA No CA" represent the scheme with both power and channel allocation, the scheme that only works in Mode 4 with power allocation, the scheme that performs channel allocation with equal power allocation, and the scheme that only works in Mode 4 with equal power allocation, respectively.

Figure 13 compares the overall end-to-end throughput of the low complexity approach and those schemes with and without power and channel allocation in different sum power constraints. Here, N spectrum bands is available. We assume that the spectrum availability of N spectrum bands is independent and each of them may be one of the four typical spectrum bands in CRRC with equal probability. Then there are $L = \frac{N}{4}$ relay channels on average. We further assume that the source and the relay have the same sum power constraint. We compare the performance curves of difference schemes when the sum power constraints are 10 W. It is shown from the figure that the low complexity approach outperforms the scheme without power and channel allocation, and has the similar performance to the power and channel allocation scheme with all four modes. In particular, the throughput improvement of the low complexity approach increases as the number of spectrum bands grows. This is because the more available spectrum bands there are, the more relay channels may appear, and the more benefits from power and channel allocation can be obtained. Similar results are observed when the sum power constraints are 5 W.

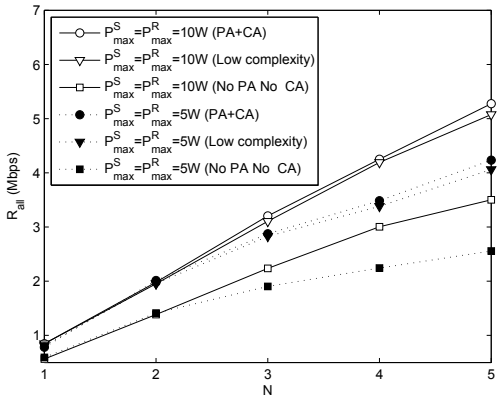

Figure 13: Performance of the low complexity approach in the case with N spectrum bands

We also investigate simplified relay selection and power allocation for relay-assisted transmission in co-operative CR networks [28]. An optimal scheme for joint relay selection and resource allocation is obtained to achieve the maximum system throughput with limited interference to primary users. A low-complexity suboptimal approach for relay selection is also proposed.

2.3.3 Energy-efficient Transmission

Even though there is a lot of work on spectrum efficiency, energy efficiency is seldom considered, which is especially important for battery operated mobile devices. In conventional networks, we can control transmit data to achieve energy efficiency without considering the transmission duration. In CR networks, transmission duration should be considered since it is a main factor to introduce interference to primary users. If the transmission duration is long, CR users may cause severe interfere if primary user reuse the spectrum during CR users' transmission. However, if it is short, it may waste the idle spectrum. Therefore, we propose energy-efficient power allocation and transmission duration design in CR networks [27, 29].

We assume licensed spectrum is divided into orthogonal channels, each with equal bandwidth, and primary users randomly choose among these channels. Usage of each channel is modeled as an *independent and identically distributed* (i.i.d.) renewal process with active and idle states. The duration of each active or idle period is assumed to be exponentially distributed with means of α_1 or α_0, respectively. A CR user operates on a frame-by-frame basis. Each frame is divided into a sensing slot with duration of τ_S and a data transmission or silent slot depending on the sensing outcome with duration of τ_T. Consequently, the length of one slot is $T = \tau_S + \tau_T$. We assume that the sensing duration is predetermined and then we optimize the transmission duration and power allocation to maximize the energy efficiency. We take sensing errors, which include mis-detection and false alarm, into consideration. Mis-detection happens when the sensing outcome shows a channel is idle while it is used by a primary user. It will cause interference to the primary user if the CR user transmits data over this channel. False alarm happens when the sensing outcome shows that a channel is busy while it is actually idle. It will waste the spectrum resource. The power may be consumed by the circuit or data transmission. The circuit power, P_C, is the average power consumption by device electronics and is almost fixed. The power consumed in data transmission, P_T, depends on the transmission data rate and channel quality. We consider channels with Rayleigh fading and additive white Gaussian noise (AWGN). Assume the AWGN is with zero mean and variance σ^2. Denote the channel gain from the CR transmitter to its receiver over Channel k to be h_k. We assume it is constant during one frame. Therefore, the maximum data transmission rate over each unit bandwidth of Channel k is

$$r_k = \log_2\left(1 + \frac{|h_k|^2 P_k}{\sigma^2}\right), \tag{42}$$

where P_k is the transmission power allocated to Channel k. Interference with primary users appears when a primary user reoccupies the channel during the CR user's data transmission or when mis-detection happens. The probability that the primary user reoccupies the channel during the CR user's transmission is

$$q_I^s(\tau_T) = \int_0^{\tau_T} p_I(t)dt = 1 - \exp\left(-\frac{\tau_T}{\alpha_0}\right), \tag{43}$$

where $p_I(t)$ is the probability density function of the exponential distributed idle period of the licensed channel. The interference with the primary user caused by the reoccupation of the primary user can be measured by the

ratio of the average interference duration to the average active duration of the primary user and expressed as

$$q_I^p(\tau_T) = \frac{\left(\frac{\tau_T}{\tau_S+\tau_T}\right)\left\{\tau_T - \alpha_0\left[1-\exp\left(-\frac{\tau_T}{\alpha_0}\right)\right]\right\}}{\alpha_1}. \tag{44}$$

Denote q_{md} and q_{fa} as the probabilities of mis-detection and false alarm, respectively. Then, the interference probability for the CR user is

$$Q_I^s(\tau_T) = (1-q_{fa})q(H_0)q_I^s(\tau_T) + q_{md}q(H_1) \tag{45}$$

and the interference probability for the primary network is

$$Q_I^p(\tau_T) = (1-q_{fa})q(H_0)q_I^p(\tau_T) + q_{md}q(H_1), \tag{46}$$

where $q(H_0)$ and $q(H_1)$ are the probabilities that the licensed channel is idle and active, respectively. In our analysis, we assume that the transmitted data will be lost if interference is generated during the transmission slot, and the data will be successfully transmitted if there is no interference. Denote the power allocation vector as $\mathbf{P} = [P_1, P_2, ..., P_K]^T$. Energy efficiency is defined as the successfully transmitted data bits per unit of energy consumption in a frame. Therefore, the energy-efficient optimization problem can be formulated as to find $\mathbf{P}$ and τ_T so as to maximize

$$J(\mathbf{P}, \tau_T) = \arg\max_{\mathbf{P},\tau_T} \frac{\left(1-Q_I^s(\tau_T)\right)\tau_T \sum_{k=1}^{K} r_k}{P_C\left(\tau_S+\tau_T\right) + \tau_T \sum_{k=1}^{K} P_k} \tag{47a}$$

subject to

$$Q_I^p(\tau_T) \le \alpha_q, \ \sum_{k=1}^{K} P_k \le P, \tag{47b}$$

and

$$P_k \left|\tilde{h}_k\right|^2 \le \theta_k \ \text{ for } k = 1, ..., K. \tag{47c}$$

In (47), α_q denotes the threshold for the interference probability, $\tilde{h}_k$ is the channel gain from the CR transmitter to the primary user, θ_k denotes the maximum allowable interference power to the primary user, P is the overall transmission power budget. We develop two schemes to solve this problem. One is joint optimization of power and transmission duration, the other is a suboptimal scheme with much lower complexity.

In our simulation, the sensing duration is $\tau_S = 1$ msec, and the average active and idle durations of each channel are $\alpha_1 = 352$ msec and $\alpha_0 = 650$ msec, respectively. The circuit power for the CR user is $P_C = 200$ mW. The interference threshold is 0.1 for each channel. We assume that the channels experience independent Rayleigh fading with unit bandwidth. We compare the energy efficiency of the CR user while allocating the optimal, suboptimal, and equal power in each channel. Figure 14 shows the energy efficiency versus the transmission duration with different power allocation schemes and different number of channels. We can see

that the optimal scheme performs best among the three schemes. The suboptimal scheme performs almost as good as the optimal one when the transmission duration is larger than 8 msec, which matches the condition of the suboptimal scheme. We also can see that both the optimal and suboptimal schemes achieve about 29% performance gain over the equal power allocation.

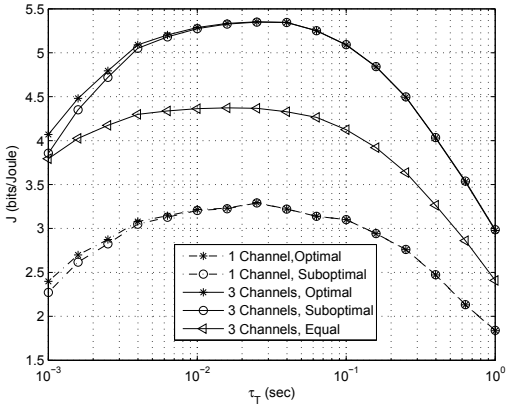

Figure 14: Performance achieved with different numbers of channels while performing different power allocation schemes

2.4 Spectrum Shaping for OFDM-based Cognitive Radios

After identifying the idle spectrum bands, CR users can utilize these bands for secondary communication. OFDM has been proposed as a candidate transmission technique for CR. By dividing a frequency band into orthogonal subcarriers, OFDM has its potential flexibility to fill spectrum gaps. However, OFDM signals exhibit relatively high power spectral sidelobes, which may bring severe out-of-band interference. Therefore, spectrum shaping that suppresses the OFDM signal sidelobes becomes necessary. To enhance the bandwidth efficiency of OFDM-based CR and limit the possible interference, we develop efficient spectrum shaping schemes based on spectral precoding [51–53].

2.4.1 Low-Complexity Spectrum Shaping

We propose a low-complexity scheme that maps antipodal symbol pairs onto adjacent subcarriers at the edges of the utilized subbands, in which sidelobe suppression is achieved at moderate system throughput loss [51,52].

We consider an OFDM-based CR user utilizing a frequency band identified as unoccupied by any licensed user through spectrum sensing. The baseband OFDM signal during one symbol duration can be expressed as

$$s(t) = I(t) \sum_{n \in \mathcal{N}} d_n e^{j2\pi \frac{n}{T_s} t}, \tag{48}$$

where $\mathcal{N}$ is the set of the utilized subcarriers, either continuous or discontinuous in the frequency domain, with

$|\mathcal{N}| = N_u$, d_n is the transmitted symbol over the nth subcarrier, T_s is the effective symbol duration, and $I(t)$ is an indicator function such that

$$I(t) = \begin{cases} 1, & -T_g \leq t \leq T_s, \\ 0, & \text{otherwise} \end{cases} \tag{49}$$

when a guard interval of cyclic prefix with length T_g is inserted. The Fourier transform of $s(t)$ can be expressed as

$$S(f) = \sum_{n \in \mathcal{N}} d_n a_n(f) \tag{50}$$

with

$$a_n(f) = T e^{-j\pi(T_s - T_g)(f - \frac{n}{T_s})} \text{sinc}(\pi T(f - \frac{n}{T_s})), \tag{51}$$

where $T = T_s + T_g$ is the symbol duration and $\text{sinc}(x) = \sin(x)/x$. The PSD of the OFDM signal is therefore

$$P(f) = \frac{1}{T} E\{|S(f)|^2\} = \frac{1}{T} \mathbf{a}^T(f) E\{\mathbf{d}\mathbf{d}^H\} \mathbf{a}^*(f), \tag{52}$$

where $\mathbf{a}(f) = (a_{n_0}(f), a_{n_1}(f), ..., a_{n_{N_u-1}}(f))^T$ and $\mathbf{d} = (d_{n_0}, d_{n_1}, ..., d_{n_{N_u-1}})^T$ with $n_i \in \mathcal{N}$ for $i \in \{0, 1, ..., N_u - 1\}$. The superscripts, T, $*$, and H, denote the transpose, conjugate transpose, and conjugate of a vector or a matrix, respectively.

To protect licensed users, guard bands may be required as shown in Figure 15 by deactivating subcarriers at the edges of the utilized subband. In this way, the PSD of the CR signal will be under acceptable levels in the adjacent frequency bands. To further increase the bandwidth efficiency, a linear operation, which is called spectral precoding, can be applied prior to OFDM modulation instead of directly mapping information symbols onto the utilized subcarriers so that the sidelobes of the OFDM signal will roll off faster and the guard bands can be narrowed. Let $\mathbf{b} = (b_0, b_1, ..., b_{M_u-1})^T$ be a vector containing M_u information symbols that are assumed to be independent with zero mean and unit variance. In other words, $E\{\mathbf{b}\mathbf{b}^H\} = \mathbf{I}_{M_u}$, where $\mathbf{I}_{M_u}$ is an $M_u \times M_u$ identity matrix. Generally, spectral precoding can be expressed as

$$\mathbf{d} = \mathbf{G}\mathbf{b}, \tag{53}$$

where $\mathbf{G}$ denotes an $N_u \times M_u$ precoding matrix consisting of complex-valued precoding coefficients, $g_{n,m}$, $n \in \mathcal{N}$, $m \in \{0, 1, ..., M_u - 1\}$, lying in the nth row and the mth column. To ensure proper decoding, the utilized subcarriers is required to be no fewer than the information symbols, i.e., $N_u \geq M_u$. The coding rate of the spectral precoder is then defined as

$$\lambda_u = \frac{M_u}{N_u}. \tag{54}$$

Then we will have

$$P(f) = \frac{1}{T} \mathbf{a}^T(f) \mathbf{G}\mathbf{G}^H \mathbf{a}^*(f) = \frac{1}{T} ||\mathbf{G}^T \mathbf{a}(f)||_2^2. \tag{55}$$

Note that $a_n(f)$ may be viewed as the interference coefficient from the nth subcarrier to the frequency f. Adjacent subcarriers have similar impact factors on $S(f)$ at any specific frequency f as the values of the

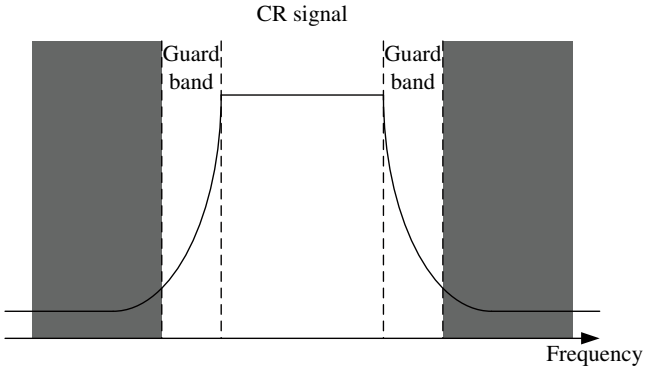

Figure 15: Opportunistic spectrum utilization with guard bands.

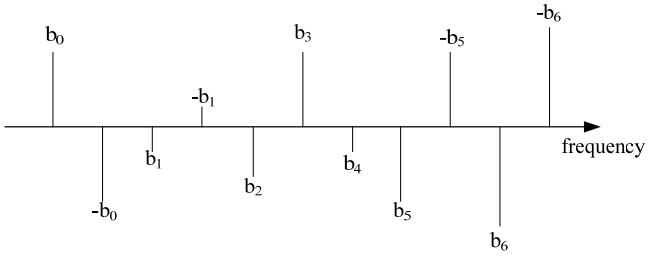

Figure 16: Subcarriers of the OFDM symbol with the proposed spectrum shaping scheme.

interference coefficients are close. We propose to map an antipodal symbol pair onto two adjacent subcarriers so that their contribution to the OOB interference of the OFDM signal will be mostly canceled. Meanwhile, as the subcarriers at the edges have higher impacts on $S(f)$ at the frequencies outside of the utilized subbands, it is preferable to apply such an antipodal coding scheme to the subcarriers at the edges. Figure 16 demonstrates our spectrum shaping scheme when $M_u = 7$ and $N_u = 11$. The proposed spectrum shaping scheme enhances spectral compactness and ensures high bandwidth efficiency. The complexity of the precoder at the transmitter and its decoder at the receiver is very low because of the special structure.

Figure 17 shows the PSD of the OFDM signals with different spectral precoding schemes where $T_s = \frac{1}{15}$ ms, $T_g = \frac{1}{16}T_s$, and $N_u = 512$. All the N_u subcarriers are used in different schemes except that half subcarriers at the edges of the utilized spectrum band are deactivated in the tone nulling scheme [41]. Here, we choose $M_u = \frac{3}{4}N_u$ in the proposed scheme, $L = 5$ in the ν_L-coded OFDM scheme [3], and ± 3999 KHz and ± 4000 KHz are notched in the frequency notching scheme [17]. It is obvious that the uncoded OFDM signal exhibits the slowest power spectral sidelobe decaying, which is not desired. The tone nulling scheme exhibits a similar sidelobe level with the proposed scheme. However, the former does not utilize the subcarriers at the edges at all while the latter uses them to map antipodal symbol pairs and transmit more information symbols. Although the ν_5-coded, 0-continuous, and 1-continuous OFDM signals [18] exhibit lower sidelobe levels, the frequency notching and proposed schemes exhibit the greatest decaying rate near the edges of the utilized spectrum band, whose sidelobe level reaches -30 dBm/Hz the earliest. Therefore, it is suitable to use the proposed scheme to achieve the narrowest guard band under a relatively loose spectral mask requirement when the transmit power

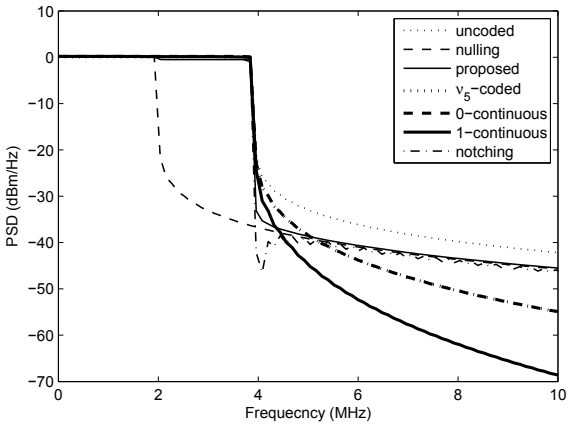

Figure 17: PSD curves of spectral precoded OFDM signals.

level of the CR users is low.

2.4.2 Multiuser Spectral Precoding

We also propose a spectral precoding scheme for multiple OFDM-based CR users to reduce out-of-band emission [53]. By constructing individual precoders to render spectrum nulls, the proposed scheme ensures user independence and provides sufficient OOB radiation suppression with low complexity and no BER performance loss.

we consider K OFDM-based CR users utilizing the set of N_u subcarriers, $\mathcal{N}$, in a frequency band identified as unoccupied by licensed users through spectrum sensing. Let $\mathcal{N}_k$ denote the set of subcarriers, either continuous or discontinuous in frequency, utilized by the kth CR user with $|\mathcal{N}_k| = N_k$ for $0 \leq k \leq K-1$. To minimize inter-user interference, we assume that each subcarrier is used by at most one CR user at the same time, i.e., $\mathcal{N}_{k_1} \bigcap \mathcal{N}_{k_2} = \emptyset$ for $k_1 \neq k_2$ and $\bigcup_{k=0}^{K-1} \mathcal{N}_k = \mathcal{N}$. To remove the interdependency among individual CR users, spectral precoding is realized on a user basis, which can be expressed as

$$\mathbf{d}_k = \mathbf{G}_k \mathbf{b}_k \tag{56}$$

for the kth user, where $\mathbf{b}_k$ is a vector consisting of M_k information symbols and $\mathbf{G}_k$ denotes an $N_k \times M_k$ precoding matrix consisting of complex-valued precoding coefficients. To ensure proper decoding, the number of utilized subcarriers is usually no smaller than that of the information symbols for each user, i.e., $N_k \geq M_k$. The spectral coding rate for the kth user is defined as

$$\lambda_k = \frac{M_k}{N_k}. \tag{57}$$

The information symbols are assumed to be independent with zero mean and unit variance. In other words, $E\{\mathbf{b}_k \mathbf{b}_k^H\} = \mathbf{I}_{M_k}$, where $\mathbf{I}_{M_k}$ is an $M_k \times M_k$ identity matrix. Let $\mathbf{b}_O = \{\mathbf{b}_0^T, \mathbf{b}_1^T, ..., \mathbf{b}_{K-1}^T\}^T$. Then

$E\{\mathbf{b}_O\mathbf{b}_O^H\} = \mathbf{I}_{\sum_{k=0}^{K-1} M_k}$. Meanwhile, let $\mathbf{d}_O = \{\mathbf{d}_0^T, \mathbf{d}_1^T, ..., \mathbf{d}_{K-1}^T\}^T$, which is the reordered $\mathbf{d}$ vector. Then $\mathbf{a}(f)$ in (27) can be reordered as $\mathbf{a}_O(f) = \{\mathbf{a}_0^T, \mathbf{a}_1^T, ..., \mathbf{a}_{K-1}^T\}^T$ accordingly. And we have

$$\begin{aligned} P(f) &= \frac{1}{T}\mathbf{a}_O^T(f)E\{\mathbf{G}_O\mathbf{b}_O(\mathbf{G}_O\mathbf{b}_O)^H\}\mathbf{a}_O^*(f) \\ &= \frac{1}{T}\mathbf{a}_O^T(f)\mathbf{G}_O\mathbf{G}_O^H\mathbf{a}_O^*(f) \\ &= \frac{1}{T}||\mathbf{a}_O^T\mathbf{G}_O(f)||_2^2, \end{aligned} \tag{58}$$

where

$$\mathbf{G}_O = \text{diag}\,(\mathbf{G}_0, \mathbf{G}_1, ..., \mathbf{G}_{K-1}) \tag{59}$$

is a block diagonal matrix.

We force the PSD in (58) to be zero at a few frequencies, f_l, $l = 0, 1, ..., L_f - 1$, selected in the adjacent bands. Then we have

$$\mathbf{A}_O\mathbf{G}_O = \mathbf{0}, \tag{60}$$

where the lth row of the matrix $\mathbf{A}_O$ is $\mathbf{a}_O^T(f_l)$. In this way, the PSD of the CR signal may be entirely under the spectral mask in the adjacent bands. Constructing a matrix $\mathbf{A}_k$ whose columns are the $(\sum_{i=0}^{k-1} N_i)$th, $(\sum_{i=0}^{k-1} N_i + 1)$th, ..., $(\sum_{i=0}^{k} N_i - 1)$th columns of $\mathbf{A}_O$ for the kth user, we further have

$$\mathbf{A}_k\mathbf{G}_k = \mathbf{0} \tag{61}$$

for $k = 0, 1, ..., K - 1$, which indicates that we can design individual precoders independently. The *singular value decomposition* (SVD) of $\mathbf{A}_k$ can be obtained as

$$\mathbf{A}_k = \mathbf{U}_k\mathbf{\Sigma}_k\mathbf{V}_k^H, \tag{62}$$

where $\mathbf{U}_k$ is an $L_f \times L_f$ matrix, $\mathbf{\Sigma}_k$ is an $L_f \times N_k$ matrix, and $\mathbf{V}_k$ is an $N_k \times N_k$ matrix. Note that the last $N_k - L_f$ columns of $\mathbf{V}_k$, denoted by $\mathbf{v}_k^{(L_f)}$, $\mathbf{v}_k^{(L_f+1)}$, ...,$\mathbf{v}_k^{(N_k-1)}$, constitute an orthogonal basis for the null space of $\mathbf{A}_k$. Therefore,

$$\mathbf{G}_k = [\mathbf{v}_k^{(L_f)}\ \mathbf{v}_k^{(L_f+1)}\ ...\ \mathbf{v}_k^{(N_k-1)}] \tag{63}$$

satisfies (61) and can be used as the precoding matrix for the kth user. By choosing notched frequencies appropriately, our scheme ensures that the OOB radiation is under the spectral mask and the licensed users are well protected. Spectral compactness is enhanced and bandwidth efficiency is potentially improved with no or narrower guard bands. Unlike the existing spectral precoding schemes [3, 17, 18], there is no restriction on the number of utilized subcarriers in the proposed scheme. It is always possible for CR users to utilize small spectrum segments with a few subcarriers.

In Figure 18, the PSD curves of the precoded OFDM signals of 4 users utilizing 4 equally divided portions of a frequency band are shown. There are totally 8 notched frequencies on two sides: {-6101,-6099,-4101,-4099,4099,4101,6099,6101} KHz. It can be seen that the resulted PSD curves are well below the spectral

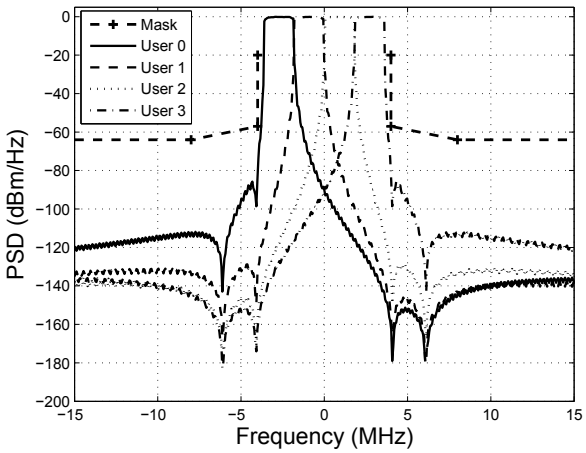

Figure 18: PSD curves of user signals with the proposed spectral precoder.

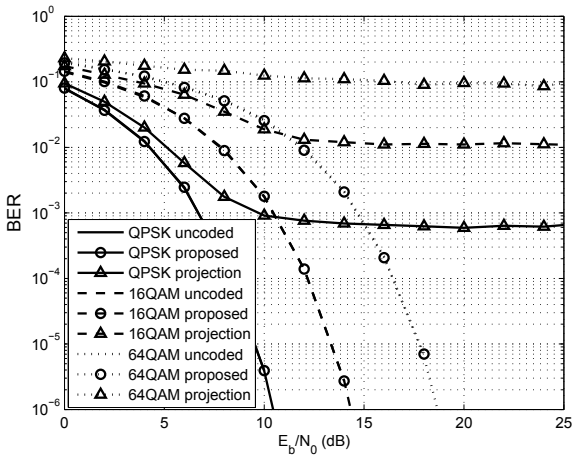

Figure 19: User BER curves under different spectrum shaping schemes.

mask. Therefore, sufficient suppression of OOB radiation is achieved with the proposed scheme. If we apply the projection precoder in [17] to the individual users, the same PSD curves will be generated. Figure 19 illustrates the BER performance of User 0 with different schemes using QPSK, 16QAM, and 64QAM without channel coding under AWGN. It can be noticed that the proposed spectral precoding scheme never introduces any BER performance loss to the OFDM system. But the projection precoder [17] brings significant BER performance loss in such a case, which is undesired.

3 Spectrum Management for Cognitive Radio Networks

In order to provide reliable communications over dynamic spectrum environment, CR networks necessitates effective spectrum management schemes. In this context, spectrum management functions based on the infrastructure-

based networks,are presented especially focusing on spectrum sharing and mobility [22–24]. Furthermore, we develop a new primary user activity model [7], and accordingly propose a QoS aware framework for available spectrum characterization and decision [5]. In addition, we propose a QoS-based spectrum sharing system and algorithm with the adaptive spectrum sharing scheme to take into account PU activity fluctuations and heterogeneous CR QoS requirements [4].

3.1 Join Spectrum and Power Allocation for Inter-Cell Spectrum Sharing

Figure 20 shows the proposed framework for spectrum sharing in infrastructure-based CR networks. An *event monitoring* has two different functionalities: spectrum sensing and QoS monitoring. According to the detected event type, the base-station determines the spectrum sharing strategies. An *intra-cell spectrum sharing* enables the base-station to avoid the interference to the primary networks as well as to maintain the QoS of its CR users by allocating spectrum resource adaptively to the event detected inside its coverage. An *inter-cell spectrum sharing* is comprised of two sub-functionalities: *spectrum allocation* and *power allocation*. When the service quality of the cell is below the guaranteed level, the base-station initiates the inter-cell spectrum sharing and adjusts its spectrum allocation. Based on the spectrum allocation, the base-station determines its transmission power over the allocated spectrum bands [22, 24].

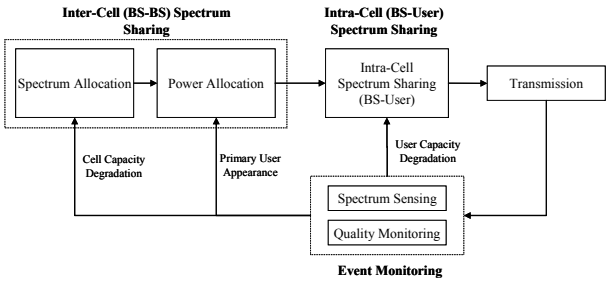

Figure 20: Inter-cell spectrum sharing framework

For the inter-cell spectrum sharing, each base-station needs to exchange the following local cell information with its neighbor base-stations:

- *Spectrum Availability / Utilization:* The base-station needs to announce the availability of all spectrum bands as well as its current spectrum utilization to its neighbor cells.
- *Minimum Busy Interference* $I_i^{\min}(j)$*:* To reduce the communication overhead, we use a single representative information among all sensing results. When the primary user (PU) activity is detected in spectrum i, the base-station j sends the minimum signal strength among all sensing data observed in its users.
- *Maximum Idle Interference* $I_i^{\max}(j)$*:* If no PU activity is detected at spectrum i, the base-station j sends the maximum value among the interference measured during the transmission period.

3.1.1 Spectrum Allocation for an Exclusive Model

Due to the inefficient and unfair spectrum utilization, a classical exclusive approach is not suitable to CR networks. The proposed approach improves the spectrum availability in exclusive allocation by considering the permissible transmission power derived from spatio-temporal characteristics of the PU activity.

Cell Characterization: Even in the same spectrum band, PU activities show different characteristics according to the location. According to the types of cells in the interference range, we classify three different scenarios for exclusive spectrum allocation as shown in Figure 21.

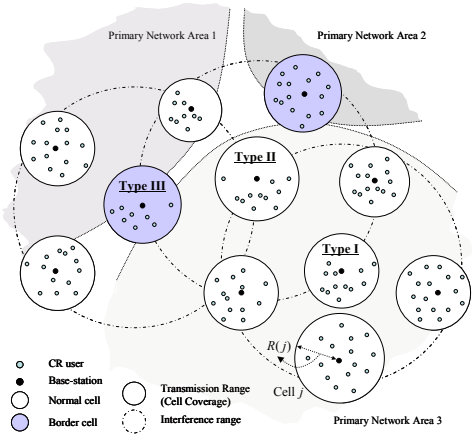

Figure 21: Infrastructure-based CR networks and their cell types

- *Type I. Same PU Activity in the Interference Range:* If no primary user is detected, the base-station can transmit with the maximum power $P_i^{\max}(j)$. Otherwise the transmission power is zero. Thus, the probabilities $Pr(\cdot)$ of both cases can be derived as follows:

$$\begin{aligned} Pr(P_i^{\max}(j)) &= p_i^{\text{off}}(k') \\ Pr(0) &= 1 - p_i^{\text{off}}(k') \end{aligned} \tag{64}$$

  where k' is the PU activity region in the interference range, and $p_i^{\text{off}}(k')$ is the idle probability of spectrum i ar region k'.

- *Type II. Multiple PU Activities in the Interference Range:* The neighbor cells located in different PU activity regions can restrict the transmission power of the current cell even though no PU activity is detected in its transmission range. Let $\mathcal{K}$ be the set of PU activity regions in the interference range, and k' be the region in the transmission range. Here we define the dominant regions $\mathcal{K}_k^*$ as the set of PU activity regions which allow smaller transmission power than the region k when primary users are detected in all regions. Then the probabilities of each permissible transmission power can be determined

as follows:

$$\begin{aligned} Pr(P_i^{\max}(j)) &= \prod_{k\in\mathcal{K}} p_i^{\text{off}}(k) \\ Pr(P_i^{\text{pu}}(j,k)) &= p_i^{\text{off}}(k') \cdot \prod_{k^*\in\mathcal{K}_k^*} p_i^{\text{off}}(k^*)\cdot(1-p_i^{\text{off}}(k)) \quad (k\in\mathcal{K},\ k\neq k') \end{aligned} \tag{65}$$

The probability of zero transmission power is the same as that of Type I.

- *Type III. Multiple PU Activities in the Transmission Range:* The probability of $P_i^{\max}(j)$ is the same as that of Type II. Let the set of primary network regions in its transmission range be $\mathcal{K}'$. Then the probabilities of $P_i^{\text{pu}}(j,k)$ and zero power can be derived as follows:

$$\begin{aligned} Pr(P_i^{\text{pu}}(j,k)) &= \prod_{k'\in\mathcal{K}'} p_i^{\text{off}}(k') \cdot \prod_{k^*\in\mathcal{K}_k^*} p_i^{\text{off}}(k^*)\cdot(1-p_i^{\text{off}}(k))l \quad (k\in\mathcal{K}-\mathcal{K}') \\ Pr(0) &= 1-\prod_{k\in\mathcal{K}'} p_i^{\text{off}}(k') \end{aligned} \tag{66}$$

Permissible Transmission Power: When no PU activity is detected in any neighbors, the cell j can use the maximum power, $P_i^{\max}(j)$, in spectrum i. Let the power propagation function be $\mathcal{F}(.)$. Then $P_i^{\max}(j)$ can be obtained as follows:

$$I_\Delta(j^*) = P_{\text{temp}} W_i - I_i^{\max}(j^*), \quad j^*\in\mathcal{N}(j) \tag{67}$$

$$P_i^{\max}(j) = \min_{j^*\in\mathcal{N}(j)} \mathcal{F}^{-1}(I_\Delta(j^*), D(j,j^*)+R(j^*)) \tag{68}$$

where $I_\Delta(j^*)$ is the available power for CR users at the neighbor cell j^* and $\mathcal{N}(j)$ is the set of neighbors of the cell j.

If some neighbors are located in different PU activity regions, the permissible transmission power can be determined according to their locations. Since $I_i^{\max}(\cdot)$ is not available in neighbor cells currently busy, it can be estimated as $I_i^{\min}(j^*)-\gamma\cdot P_{\text{temp}}\cdot W_i$. In this case, the permissible transmission power can be determined so that the received power at the border of neighbor cell nearest from the base-station, does not exceed $I_\Delta(j^*)$. Thus, the restricted transmission power can be obtained as follows:

$$P_i^{\text{pu}}(j,k) = \min_{j^*\in\mathcal{N}_i(j,k)} \mathcal{F}^{-1}(I_\Delta(j,j^*), D(j,j^*)-R_{j^*}) \tag{69}$$

where $\mathcal{N}_i(j,k)$ is the set of neighbors of the cell j located at region k of spectrum i.

Spectrum Selection: *Opportunistic cell capacity* $C_i(j)$, defined as the capacity of spectrum i at the boundary of cell j, can be derived as follows:
Type I:

$$C_i(j) = W_i \log_2(1+\frac{\mathcal{F}(P^{\max}(j),R(j))}{I_i^{\max}(j)}) p_i^{\text{off}} \tag{70}$$

Type II & III:

$$C_i(j) = W_i[\log_2(1 + \frac{\mathcal{F}(P_i^{\max}(j), R(j))}{I_i^{\max}(j)}) \cdot Pr(P_i^{\max}(j)) + \sum_{k \in \mathcal{K}} \log_2(1 + \frac{\mathcal{F}(P_i^{\mathrm{pu}}(j,k), R(j))}{I_i^{\max}(j)}) \cdot Pr(P_i^{\mathrm{pu}}(j,k)] \tag{71}$$

If the base-station has the multiple available spectrum bands for the exclusive allocation, it selects the one of them with the highest opportunistic capacity.

3.1.2 Spectrum Allocation for Common Use Model

In the common use approach, the cell can share the same spectrum with its neighbor cells, which improves fairness but causes capacity degradation due to the inter-cell interference. To mitigate this effect, the following issues should be considered in the common use approach: 1) The common use approach aims at finding a spectrum to enable the cell capacity to be maximized. 2) To reduce the inter-cell interference, CR networks need to find a spectrum to cause less influence on neighbor cells. 3) the uplink transmission is highly probable to interfere with the PU activity detected in its neighbor cells. To address these issues, we propose a two-step spectrum sharing for the common use model.

Angle-Based Allocation for Uplink Transmission: The best way to reduce interference in uplink transmission is to use the spectrum which does not have any PU activities in neighbor cells. If the base-station cannot find this spectrum, alternatively it can exploit the multiple spectrum bands to allow all directions to be covered with their idle regions, referred to as an *angle-based allocation*.

Interference-Based Spectrum Allocation: For the maximum cell capacity, the cell should find the spectrum with the lowest interference in its transmission range. In addition, the cell needs to select the spectrum with lower interference, which shows less influence on the neighbor cells. Furthermore, it is much advantageous for the cell to choose the spectrum with the widest idle angle range. From these observations, we devise the following selection criterion for the common use approach, called an *interference-based spectrum allocation*:

$$i^* = \arg\max_{i \in \mathcal{S}(j)} \frac{\theta_i^{\max}(j)}{2\pi} \cdot \frac{\min\limits_{j \in \mathcal{N}(j)} I_i^{\max}(j^*)}{I_i^{\max}(j)} \tag{72}$$

where $\theta_i^{\max}(j)$ is the maximum idle angle in spectrum i at cell j. $\mathcal{S}(j)$ is the set of available spectrum bands at base-station j. Here, in order to consider the effect on all neighbors, the lowest $I_i^{\max}(j^*)$ is chosen among the interference measured in neighbors.

3.1.3 Joint Spectrum and Power Allocation for Inter-Cell Spectrum Sharing

Power Allocation: Generally a water filling method is used to optimally allocate the transmission power in the presence of noise. However, unlike the classical water filling, in the inter-cell spectrum sharing, each spectrum has an upper power limit according to the PU activities:

In case of the exclusive allocation, the upper power limit $P_i^{\text{up}}(j)$ can be obtained as explained in Eq. (68). However, $I_i^{\max}(j^*)$ in the common use mode, does not contain the its own signal strength, which needs to be considered in determining available power. In this case, the transmission power of the neighbor cell can be estimated as $\mathcal{F}^{-1}(I_i^{\max}(j), D(j, j^*) - R_j)$. Thus, the available power at the farthest border of the cell j^* from the base-station j can be obtained as follows:

$$I_\Delta(j^*) = P_{\text{temp}} \cdot W_i - [I_i^{\max}(j^*) + \mathcal{F}(\mathcal{F}^{-1}(I_i^{\max}(j), D(j, j^*) - R_j), R_{j^*})] \tag{73}$$

Then $P_i^{\text{up}}(j)$ can be derived using Eq. (69).

Spectrum Sharing Procedures: In order to reduce this unnecessary influence on the entire networks, we classify the spectrum as the *assigned* and *unassigned* spectrum bands. The assigned spectrum bands are allowed to be accessed by the current cell. The assigned spectrum can be released to the unassigned one only when it is currently idle and is requested by the the neighbor cells for their exclusive allocation.

Based on this spectrum classification, the inter-cell spectrum sharing can be performed as follows: If the spectrum sharing event is detected, the base-station initiates the spectrum sharing procedure. If the detected event is related only to the PU activities, the base-station reduces or turns off its transmission power on that spectrum. If the event is a resource shortage for uplink transmission, it selects the spectrum having the proper idle angle through the angle-based allocation. If the base-station detects the quality degradation, it performs the exclusive allocation for the assigned spectrum and then for the unassigned spectrum if necessary. If it cannot find the proper spectrum bands, it turns to the common use sharing and performs the interference-based allocation. Once spectrum is allocated, each base-station allocates the proper transmission power over the assigned spectrum bands.

3.1.4 Results

In order to evaluate the performance of the proposed sharing method, we implement the network simulator to support the network topology consisting of multiple cells in 10km x 10km area. Here we assume 20 cells which have different number of users from 20 to 40. The transmission range of each cell is uniformly distributed from 1 to 1.5km. The interference range is set to twice larger than the transmission range. Furthermore, we consider 20 10MHz licensed spectrum bands with different PU activities, α_i and β_i, which are uniformly distributed in $[0.1, 0.5]$. Each spectrum band has 2-5 PU activity regions. For the simplicity, each PU activity region on spectrum i is assumed to have the same α_i and β_i.

In this simulation, we use the free space power attenuation model where the channel gain is set to -31.54dB, the reference distance is 1m, and the path loss coefficient is 3.5. The base-station has 3000mwatt transmission power in total and can allocate up to 600mwatt to each spectrum. The transmission power of the CR user is set to 125mwatt. Noise power in the receiver is -174dBm/Hz. For the protection of primary networks, we set the interference temperature to 6dB greater than the noise power. The CR network uses the TDD with the same length of uplink and down link time slots. While base-stations can use the multiple spectrum bands at the same

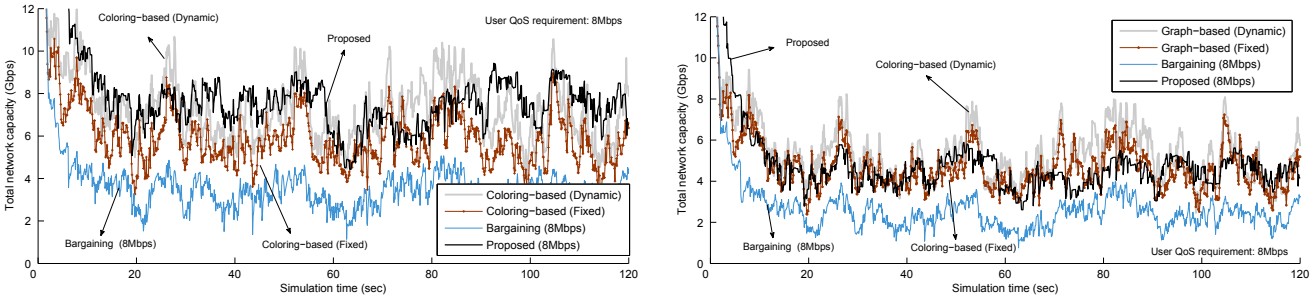

(a) (b)

Figure 22: Performance comparison in total capacity: (a) downlink, and (b) uplink.

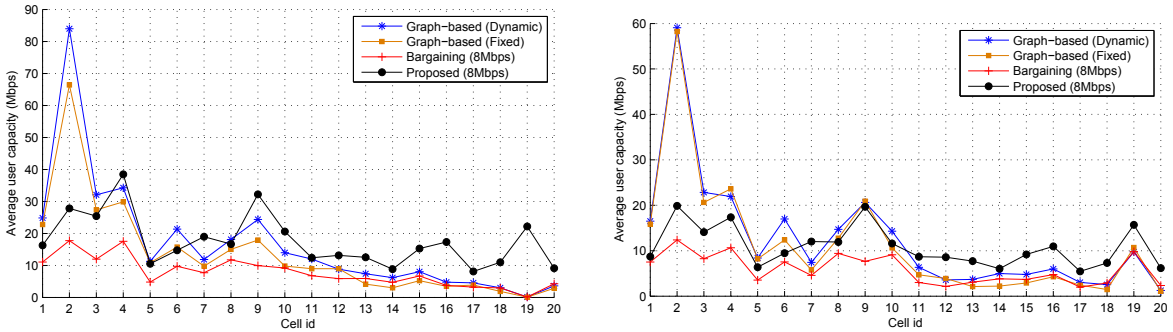

(a) (b)

Figure 23: Performance comparison in capacity fairness: (a) downlink, and (b) uplink.

time, CR users can use only one spectrum for uplink and down link transmissions, respectively. For the intra-spectrum sharing, we use the proportional fairness principle, i.e., once users are assigned to the spectrum, each user is assumed to share the time slot fairly with other assigned users. Here the minimum QoS requirement for each user is set to 8Mbps.

To evaluate the proposed method, we use three different existing spectrum sharing methods as follows:

- *Fixed spectrum allocation:* Spectrum allocation can be obtained by the coloring method with a maximum proportional fairness criterion [37]. Here, each cell is assigned to the pre-determined spectrum bands and does not change them regardless of time-varying spectrum availability. Instead, this method considers the number of neighbor cells and PU activities.

- *Dynamic spectrum allocation:* This method is also based on the same coloring method used in the fixed allocation. However, in this method, spectrum allocation is dynamically updated over the entire network whenever spectrum availability changes, which leads to optimal performance in spectrum sharing.

- *Local bargaining:* In this method, each cell can negotiate with its neighbor to obtain spectrum bands when its capacity is below a threshold [8].

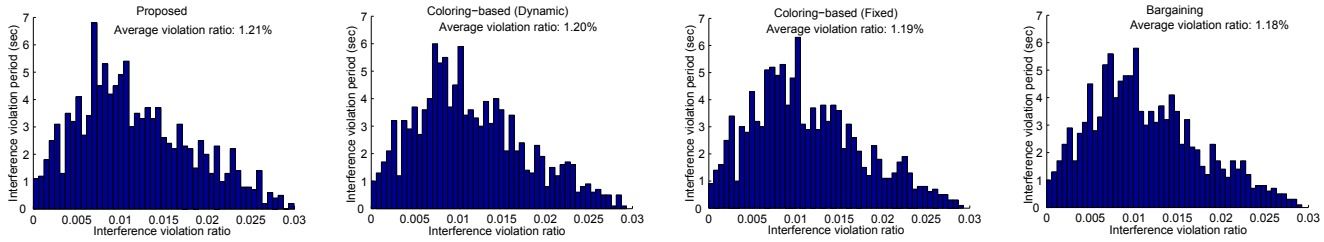

Figure 24: Histogram for interference violation ratio: (a) proposed method, (b) dynamic allocation, (c) fixed allocation, and (d) local bargaining.

First we compare the proposed method with three existing methods. Figure 22 shows total network capacity for both uplink and downlink transmissions. The dynamic allocation uses the graph-based optimization with global topology knowledge which leads to the highest capacity. While the fixed allocation does not require frequent optimization, it shows lower total capacity due to the lack of the channel adaptation. In the bargaining method, each cell takes the spectrum band from other neighbor cells if it cannot satisfy the QoS. However, since each cell cannot perform the spectrum allocation if its neighbors are currently involving in other bargaining process, the spectrum utilization becomes lowest than the others. Since the proposed method exploits the exclusive and common use model adaptively dependent on the network environments, it achieves a higher downlink capacity than the fixed allocation and bargaining schemes, and the same or slightly lower capacity compared to the dynamic (optimal) spectrum allocation while requiring less computational overhead as shown in Figure 22. One the contrary, the proposed method achieves the same total capacity as the uplink to the fixed allocation scheme due to the interference constraints.

Next, we investigate the capacity fairness, which is also an important objective in inter-cell spectrum sharing. As shown in Figure 23, existing methods show high fluctuation in their capacity, especially cells #12-#20 achieve significantly lower capacities than the other cells. However, the proposed method maintains better fairness in capacity over all cells than the other methods.

Another important issue in CR networks is the interference avoidance with primary networks which has not been addressed in previous methods. Figure 24 shows the interference ratio under different sharing schemes, which is defined as the ratio of the area violating the interference temperature limit to total area occupied by primary networks. As shown in Figure 24, our proposed method shows similar interference ratio to other existing methods. In order to protect the primary networks, previous methods are assumed to adopt the same strategy used to avoid the inter-cell interference, i.e., CR cells cannot use the spectrum band on which some of their neighbor cells detect the PU activities, leading to inefficient spectrum utilization. However, since the proposed method determines the transmission power not to exceed the interference temperature, it achieves both higher capacity and better fairness while maintaining similar interference avoidance performance to other previous methods.

3.2 Spectrum-Aware Mobility Management

Spectrum mobility imposes unique characteristics in mobility management for CR cellular networks. Mobility management, especially a handoff scheme is one of the most important functions in the classical cellular networks. The main difference between classical wireless networks and CR networks lies in the primary user (PU) activities, which introduces the following challenges to design mobility management in CR networks:

- *Dynamic Spectrum Availability:* According to the PU activities, the spectrum availability varies over time and space in the CR network.
- *Broad range of available spectrum:* Unlike the classical wireless networks, CR networks have discontiguous available spectrums distributed over a wide frequency range. Thus, when CR users switch their spectrum, they need to reconfigure the operating frequency so as to tune to a new spectrum band, leading to higher switching delays than that in classical wireless networks.
- *Heterogeneous Mobility Events:* CR networks have two types of handoff schemes: classical inter-cell handoff due to *user mobility* and *spectrum handoff* due to spectrum mobility.

To address the challenges mentioned above, we propose a novel CR cellular network architecture based on the spectrum pooling concept. Based on this architecture, both spectrum and user mobility management frameworks are developed so as to exploit heterogeneous handoff schemes adaptively to dynamic radio environments [23].

3.2.1 System Model

To solve the switching latency problem, we introduce the spectrum pooling concept [41]. A *spectrum pool* is defined as a set of contiguous licensed spectrum bands each of which consists of multiple channels. Spectrum pools are assigned to each cell exclusively with its neighbor cells. The spectrum pool consists of multiple *basic spectrum* bands which support only the basic area (BA), and a single *extended spectrum* providing both the basic and the extended areas (EA). While the basic area is not overlapped with the coverage of its neighbor cells, the extended area has much larger coverage extended to the basic area of its neighbors. The basic spectrum is assumed to support $N_i^{\max}(j)$ for users in the basic area.

Although a large coverage improves the mobility support in CR networks, the users in the extended area require more spectrum resource than those in the basic area, leading to degradation of cell capacity. Assume that the extended spectrum band j at the spectrum pool i can support $\rho N_i^{\max}(j)$ channels for the users in the basic area. Then it supports the $N_i^{\max}(j)$ channels for the users in the extended area due to the longer distant from the BS where ρ is greater than unity and can be determined dependent on the transmission power and the minimum signal strength for decoding. Furthermore, due to the extended spectrum, the current cell has another type of neighbors, referred to as *extended neighbors*. The extended neighbors are the cells which have the same spectrum pool within the interference range of the extended spectrum. In this architecture, unlike the basic

spectrum, the extended spectrum in the current cell cannot be used in its extended neighbors so as to avoid inter-cell interference.

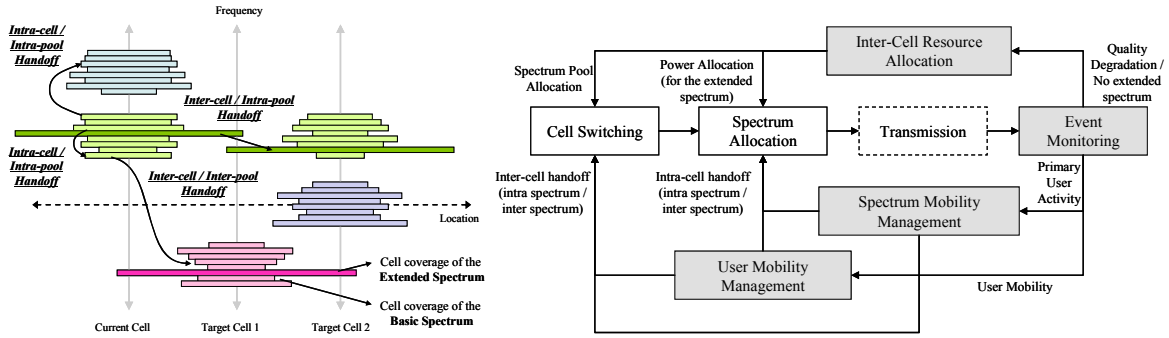

Figure 25: (a) Different handoff types in CR networks and (b) the proposed mobility management framework.

By taking into account both user and spectrum mobilities based on the proposed architecture, we define the following four handoff schemes as shown in Figure 25(a):

- *Intra-cell/intra-pool handoff:* The CR user moves to the spectrum band in the same spectrum pool without switching a serving BS.
- *Inter-cell/intra-pool handoff:* The CR user switches its serving BS to the neighbor BS without changing the spectrum pool.
- *Inter-cell/inter-pool handoff:* The CR user switches its serving BS to the neighbor BS, which has a different spectrum pool.
- *Intra-cell/inter-pool handoff:* CR users change their spectrum bands from one spectrum pool to another within the current cell.

Figure 25(b) shows the proposed mobility framework. Here each base-station monitors the current spectrum availability and the service quality of current transmissions. If the current cell does not have enough spectrum resource, the base-station performs the inter-cell resource allocation so as to get more spectrum pools or allocate the more transmission power for its extended spectrum. If CR users are approaching the cell boundary or detect the PU activity, CR networks need to determine the proper handoff scheme through either user or spectrum mobility management functions. According to the decision, the user needs either to select the target cell (*cell selection*) or to decide on the spectrum resource (*spectrum allocation*).

3.2.2 User and Cell Selections

When the PU activity is detected in the cell, the base-station needs to check its spectrum availability. If the cell has enough spectrum resource, the base-station performs the intra-cell / intra-pool handoff for all users requiring

new spectrum bands. Otherwise, some of current users are forced to move to the neighbor cells through user and cell selections. Since the intra-cell / intra-pool handoff is exactly same as the spectrum decision proposed in [26], we mainly focus on the user and cell selections for the inter-cell / inter-pool handoff scheme in this research.

User Selection: Let $\mathcal{S}_i$ be a set of the currently available spectrum in the cell i. Then, the number of unused channels in the available spectrum bands at the cell i, N_i^{av}, can be expressed as $\sum_{j\in\mathcal{S}_i} N_i^{\max}(j) - (N_i^{\text{b}} + \rho N_i^{\text{e}})$. Here N_i^{b} and N_i^{e} are the numbers of channels used in the basic area and the extended area of cell i, respectively. If the number of the channels required for spectrum switching, N^{req} is less than N_i^{av}, CR users just perform the intra-cell intra-pool handoff. A

If $N_i^{\text{av}} < N^{\text{req}} \leq N_i^{\text{av}} + \rho N_j^{\text{e}}$, current cell is overloaded and forces some of users to be out to its neighbor cells. In this case, CR users using $\lceil \frac{N^{\text{req}} - N_i^{\text{av}}}{\rho} \rceil$ channels in the extended area need to be selected and moved to the neighbor cells. As the users stay in the extended area for a longer time, cell capacity becomes lower. Also these users have a higher probability to be interrupted by the PU activity. Furthermore, a user with more channels reduces the number of users that the current cell can admit. Thus, the BS selects the users in the extended area with the longest expected staying time as well as the highest channel occupancy. As a result, a decision metric can be obtained as $K_m \cdot d_m / v_m$ where d_m is the expected moving distance of the user m to the cell boundary, which is dependent on the user mobility model. v_m is the velocity of the user m, and K_m is the number of channels required by user m. The BS chooses users in the extended area with the largest decision metric, repeatedly until it can avoid the cell overload state.

If $N^{\text{req}} > N_i^{\text{av}} + \rho N_i^{\text{e}}$, it is not enough to select all users in the extended area. To avoid dropping or blocking connections due to the cell overload, the BS hands over some of users in the basic area to its neighbor cells. Unlike the previous case, the BS selects CR users using $N^{\text{req}} - (N_i^{\text{av}} + \rho N_i^{\text{e}})$ channels with the shortest expected staying time in the basic area since they are highly likely to move to the extended area, which will require more spectrum resource. Similar to the previous case, it is more advantageous to kick off the users with more channels. Thus, the BS chooses CR users in the basic area with the smallest decision metric, $d_m/(v_m \cdot K_m)$.

Cell Selection: To observe the signal strength from other base-station, CR users need to reconfigure their RF front-ends, leading to relatively long temporary disconnection of the transmission. Thus, we propose the stochastic connectivity estimation for selecting the cell properly. If the received signal needs to be greater than $P_{0,\text{dB}}$ for decoding data reliably, the connection probability can be obtained as follows [40]:

$$\begin{aligned} P^{\text{c}} &= Pr[P_{\text{t,dB}} - \bar{L}_{0,\text{dB}} - 10\log_{10} E[\chi^2] - 10\xi \log_{10} R - X_{\sigma_{\text{s}}} \geq P_{0,\text{dB}}] \\ &= \frac{1}{2}(1 - \text{erf}[(10\xi \log_{10} R + P_{0,\text{dB}} - P_{\text{t,dB}} - \bar{L}_{0,\text{dB}} - 10\log_{10} E[\chi^2])/\sqrt{2}\sigma_{\text{s}}]) \end{aligned} \tag{74}$$

where $P_{\text{t,dB}}$ is the transmission power, $\bar{L}_{0,\text{dB}}$ is the average path loss at the reference distance, 1 meter, and R is the distance from the base-station. $10\log_{10} E[\chi^2]$ is the average multi-path fading in dB, ξ is the path loss exponent, $X_{\sigma_{\text{s}}}$ is shadowing, χ^2 is multi-path fading, and $\text{erf}[z]$ is the error function defined by $\int_0^z \frac{2}{\sqrt{\pi}} e^- x^2 dx$.

The connectivity of spectrum pool i, P_i^{c}, can be defined as the probability that at least one spectrum band in

the spectrum pool provides the valid connection, which can be expressed as $1-\prod_{j\in\mathcal{S}_i}(1-P_i^{\mathrm{c}}(j))$ where $P_i^{\mathrm{c}}(j)$ is the connection probability of the spectrum j in the pool j. Besides the connectivity, spectrum utilization is also important factor in determining the target cell. Thus, CR users select the target cell i^* with the highest weighted connectivity, P_i^{w}, which can be obtained by considering both connectivity and spectrum utilization as follows:

$$P_i^{\mathrm{w}} = (1 - \prod_{j\in\mathcal{S}_i}(1 - P_i^{\mathrm{c}}(j))) \cdot (1 - \frac{N_i^{\mathrm{b}} + \rho N_i^{\mathrm{e}}}{\sum_{j\in\mathcal{S}_i} N_i^{\max}(j)}) \tag{75}$$

3.2.3 Mobility Management

The user mobility is another main reason to initiate the handoff in CR networks, which happens at the boundary of either the basic area or the extended area. When CR users approach the boundary of the extended area, they try to perform the inter-cell / intra-pool handoff, which is exactly same as the classical handoff. However, when CR users approach the basic cell boundary, they need to determine whether they will stay in the extended area of the current cell. Generally, for mobile users, larger cell coverage is known to be much more advantageous since it reduces the number of handoffs. However, as the cell coverage becomes larger, the PU activity becomes higher as well.

Thus, in this research, we focus on the mobility management in the boundary of basic area. Once a target cell is determined, the base-station determines the handoff type by considering the expected switching costs of the intra-cell / intra-pool handoff and the inter-cell / inter-pool handoff at the boundary of the basic area.

Primary User Activity in the Extended Area: If CR users determine to perform the intra-cell / intra-pool handoff, they can stay in the current cell, which does not require instant switching latency. However, in the extended area, CR users may experience the mobility events, which causes the inter-cell / inter-pool handoff due to the lack of available spectrum for the intra-spectrum / intra-pool handoff.

In order to avoid the inter-cell / inter-pool handoff, neither the PU activity or false alarm should not be detected in the extended area. Based on these observations, we can derive the probability that no primary user can be detected during the expected staying time $T_m = d_m/v_m$ as follows:

$$P_i^{\mathrm{av}}(T_m) = \prod_{i'\in\mathcal{N}_i^{\mathrm{E}}} (1 - P_{i'}^{\mathrm{f}})^{\lceil \frac{T_m}{\Delta t} \rceil} \cdot \prod_{k\in \mathrm{A}_i^{\mathrm{E}}(j)} e^{-\beta(j,k)T_m} \tag{76}$$

where $\beta_i(j,k)$ is the PU activity (idle $\rightarrow$ busy) at the area k of the spectrum band j in the spectrum pool i, and Δt is the sensing period. Then the probability to perform the inter-cell / inter-pool handoff due to the PU activity can be obtained as $1 - P^{\mathrm{av}}(T_m)$.

Capacity Overload in the Basic Area: When the current cell is overloaded, CR users in the extended area may need to perform the inter-cell / inter-pool handoff. In this section, we derive the probability of the cell overload.

First, since each PU activity area in the spectrum has can have 2 states, busy and idle, we can model a

transition matrix $\mathbf{X}(j,k)$ with following transition probabilities:

$$\begin{aligned} x_{1,1}(j,k) &= 1 - e^{-\beta(j,k)\Delta t} \\ x_{1,2}(j,k) &= e^{-\beta(j,k)\Delta t} \\ x_{2,1}(j,k) &= e^{-\alpha(j,k)\Delta t} \\ x_{2,2}(j,k) &= 1 - e^{-\alpha(j,k)\Delta t} \end{aligned} \tag{77}$$

where $x_{1,1}(j,k)$ and $x_{1,2}(j,k)$ are the transition probabilities from idle to idle and from idle to busy, respectively. $x_{2,1}(j,k)$ and $x_{2,2}(j,k)$ represent the transition probabilities from busy to idle and from busy to busy, respectively.

From this, the transition matrix after $r\Delta t$ can be obtained as $[\mathbf{X}(j,k)]^r$. Let $\mathbf{x_0}(j,k) \in \{(1,0),(0,1)\}$ be an initial vector to describe a current spectrum status where $(1,0)$ and $(0,1)$ denote that an area k at spectrumm j is currently idle and busy, respectively. Then the idle probability of area k after $r\Delta t$, $P_i^{\text{idle}}(j,k,r\Delta)$ is the first element of the vector, $x_0[\mathbf{X}(j,k)]^r$, which can be obtained by Eq. (78).

$$P_i^{\text{idle}}(j,k,r\Delta t) = \begin{cases} \dfrac{x_{2,1}(j,k)}{x_{1,2}(j,k)+x_{2,1}(j,k)} + (1-x_{1,2}(j,k)-x_{2,1}(j,k))^r \cdot \dfrac{x_{1,2}(j,k)}{x_{1,2}(j,k)+x_{2,1}(j,k)}, & x_0 = (1,0) \\ \dfrac{x_{2,1}(j,k)}{x_{1,2}(j,k)+x_{2,1}(j,k)} - (1-x_{1,2}(j,k)-x_{2,1}(j,k))^r \cdot \dfrac{x_{2,1}(j,k)}{x_{1,2}(j,k)+x_{2,1}(j,k)}, & x_0 = (0,1) \end{cases} \tag{78}$$

Based on idle probabilities at each PU activity area, we can derive the idle and busy probabilities of spectrum j. Assume that a current cell i has multiple PU activity regions in spectrum j. Then it can use that spectrum only when all of these regions should be idle, and hence the idle and busy probabilities, is expressed as follows:

$$\begin{aligned} P_i^{\text{idle}}(j,r\Delta t) &= \prod_{k \in \mathcal{A}_i^{\text{B}}(j)} P_i^{\text{idle}}(j,k,r\Delta t) \\ P_i^{\text{busy}}(j,r\Delta t) &= 1 - P_i^{\text{idle}}(j,r\Delta t) \end{aligned} \tag{79}$$

where $\mathcal{A}_i^{\text{B}}(j)$ is the set of PU activity regions of the basic area in spectrum j at cell i.

Based on both probabilities of each spectrum in the pool, we derive the expected spectrum availability of cell i as follows: The current cell i has $|S_i|$ assigned spectrum bands in the pool, which are either busy or idle. Since the extended spectrum is not considered as explained earlier, it has $2^{|S_i|-1}$ states according to spectrum availability. Among spectrum states, some of states $n \in \mathcal{L}_{\text{E}}$ cannot satisfy the channel requirements to support current users, and finally result in inter-cell/inter-pool handoff of some of users in the extended area. To resolve cell overload at each state in $\mathcal{L}_{\text{E}}$, current cell needs to obtain additional channels by switching CR users to neighbor cells. The numbers of required channels are different from one state to another. Let $u_{\text{E}}^{\text{req}}(n)$ be the probability that users in the extended area are switched to neighbor cell due to cell overload at state $n \in \mathcal{L}_{\text{E}}$.

To order to maintain the underload state after $r\Delta t$, all spectrum bands in $\mathcal{I}_n, n \in \mathcal{L}_E$ should be idle and the rest of spectrums $j \notin \mathcal{I}_n$ should be busy where $\mathcal{I}_n$ is a set of idle spectrum bands at state n. Furthermore, the cell should not have any cell overload and any PU activities in the extended area before $r\Delta t$. By considering these conditions, we derive the underload probability of cell i, $P_{\mathrm{E},i}^{\mathrm{under}}$, as follows:

$$P_{\mathrm{E},i}^{\mathrm{under}}(\Delta t) = \sum_{n \in \mathcal{L}_{\mathrm{E}}} [\prod_{j \in \mathcal{I}_n} P_i^{\mathrm{idle}}(j, \Delta t) \prod_{j \notin \mathcal{I}_n} P_i^{\mathrm{busy}}(j, \Delta t)] \tag{80}$$

$$P_{\mathrm{E},i}^{\mathrm{under}}(r\Delta t) = P_{\mathrm{E},i}^{\mathrm{under}}((r-1)\Delta t) \cdot \sum_{n \in \mathcal{L}_{\mathrm{E}}} [\prod_{j \in \mathcal{I}_n} P_i^{\mathrm{idle}}(j, r\Delta t) \prod_{j \notin \mathcal{I}_n} P_i^{\mathrm{busy}}(j, r\Delta t)] \quad (r = 2, 3, ...) \tag{81}$$

For cell overload after $r\Delta t$, we should consider the states not in $\mathcal{L}_E$. Furthermore, the cell should not experience any cell overload as well as any PU activity before. Then the cell overload probability can be expressed as follows:

$$P_{\mathrm{E},i}^{\mathrm{over}}(\Delta t) = \sum_{n \notin \mathcal{L}_{\mathrm{E}}} [\prod_{j \in \mathcal{I}_n} P_i^{\mathrm{idle}}(j, \Delta t) \prod_{j \notin \mathcal{I}_n} P_i^{\mathrm{busy}}(j, \Delta t) \cdot u_{\mathrm{E}}^{\mathrm{req}}(n)] \tag{82}$$

$$P_{\mathrm{E},i}^{\mathrm{over}}(r\Delta t) = P_{\mathrm{E},i}^{\mathrm{under}}((r-1)\Delta t) \cdot \sum_{n \notin \mathcal{L}_{\mathrm{E}}} [\prod_{j \in \mathcal{I}_n} P_i^{\mathrm{idle}}(j, r\Delta t) \prod_{j \notin \mathcal{I}_n} P_i^{\mathrm{busy}}(j, r\Delta t) \cdot u_{\mathrm{E}}^{\mathrm{req}}(n)] \quad (r = 2, 3, ...) \tag{83}$$

Based on both overload and underload probabilities, we obtain a probability that a CR user in the extended area initiates inter-cell/inter-pool handoff due to cell overload, P_E^{over}, as follows:

$$P_{\mathrm{E}}^{\mathrm{over}} = \sum_{r=1}^{R} [P_{\mathrm{E},i}^{\mathrm{over}}(r\Delta t) \cdot P_i^{\mathrm{av}}(r\Delta t)] \tag{84}$$

where $R = \lceil T_m/\Delta t \rceil$ where T_m is the expected time of the user m to stay in the extended area. Note that the extended spectrum is assumed to be available in estimating $P_{\mathrm{E}}^{\mathrm{over}}$ as mentioned in the beginning of this section.

Capacity Overload in the Basic Area: If the BS determines to perform the inter-cell/inter-pool handoff (Type 3) at the boundary of the basic area, mobile CR users may experience the capacity overload in the basic area of the target cell, which causes inter-cell/inter-pool handoff. This cell overload probability can be determined with the similar procedures used in deriving $P_{\mathrm{E}}^{\mathrm{over}}$.

First, the spectrum availability states for cell overload in the basic area $\mathcal{L}_{\mathrm{B}}$ can be derived with the similar procedures to the capacity overload in the extended area, and accordingly the probability of inter-cell/inter-pool handoff in the basic area to resolve cell overload, $u_{\mathrm{B}}^{\mathrm{req}}(n)$ is obtained. Then, the probabilities of cell underload and overload in the basic area, $P_{\mathrm{B},i}^{\mathrm{under}}$ and $P_{\mathrm{B},i}^{\mathrm{over}}$, can be obtained by replacing $\mathcal{L}_{\mathrm{E}}$ and $u_{\mathrm{E}}^{\mathrm{req}}(n)$ with $\mathcal{L}_{\mathrm{B}}$ and $u_{\mathrm{B}}^{\mathrm{req}}(n)$, respectively in Eqs. (80), (81), (82) and (83). Accordingly, the probability that the CR users in the

basic area performs inter-cell/inter-poll handoff, $P_{\mathrm{B}}^{\mathrm{over}}$, is estimated as follow.

$$P_{\mathrm{B}}^{\mathrm{over}} = \sum_{r=1}^{R} P_{\mathrm{B},i}^{\mathrm{over}}(r\Delta t) \tag{85}$$

Unlike Eq. (84), we consider all spectrum bands including the extended spectrum in this case. Thus, we do not need to consider the probability of the spectrum availability in the extended area, $P^{\mathrm{av}}(\cdot)$, separately.

Switching cost-based decision: According to the probability on future mobility events, we estimate the switching cost of two possible options in the boundary of the basic area. First, when CR users stay in the current cell by performing intra-cell/intra-pool handoff to the extended area, the expected switching cost T_{EA} can be obtained as follows:

$$T_{\mathrm{EA}} = D_1 + P_{\mathrm{E}}^{\mathrm{over}} \cdot D_2 + (1 - P_{\mathrm{E}}^{\mathrm{over}})(1 - P_i^{\mathrm{av}}(T_m)) \cdot D_4 + P_i^{\mathrm{av}}(T_m)(1 - P_i^{\mathrm{av}}(T_m)) \cdot D_5 \tag{86}$$

where D_1 is a switching delay in intra-cell/intra-pool handoff. D_2, D_3, and D_4 are switching delays in inter-cell/inter-pool handoffs due to PU activity in the basic area, user mobility, and PU activity in the extended area, respectively. D_5 is a delay in inter-cell/intra-pool handoff. The total delay includes the intra-cell/intra-pool handoff when the CR user switches to the extended spectrum, inter-cell/inter-pool handoffs due to the cell overload and and PU activity, and inter-cell/intra-pool handoff when it is successfully handed over to the extended neighbors.

Second, when CR users move to the neighbor cell by performing inter-cell/inter-pool handoff, the expected switching cost can be expressed as the sum of the instant switching delay and the expected switching delay due to the overload in that neighbor cell as follows:

$$T_{\mathrm{BA}} = D_3 + D_1 \frac{T_m}{\overline{T}_{\mathrm{off},i} + D_1} + P_{\mathrm{B}}^{\mathrm{over}} \cdot D_2 \tag{87}$$

The latency in this case includes the inter-cell/inter-pool handoff to a new target cell, intra-cell/intra-pool handoff in the target cell, and inter-cell/inter-pool handoff due to cell overload. Here the average number of intra-cell/intra-pool handoff is obtained as $T_m/(\overline{T}_{\mathrm{off},i} + D_1)$. $\overline{T}_{\mathrm{off},i}$ is the average idle period of the spectrum in cell i, which is expressed as the average of $1/\sum_{k \in \mathcal{A}_i^{\mathrm{B}}(j)} \beta(j,k)$ over all spectrum j. Based on the analysis above, the BS determines the handoff type with the lower expected spectrum cost.

3.2.4 Results

In this simulation, we investigate transmission statistics in mobile users under different network environments to evaluate the performance of both spectrum and mobility management schemes. To do this, we perform 30 one hour-simulations for each case and obtain average values. Here we analyze the performance of mobility management in terms of three factors: user QoS requirement (i.e., how many channels are required for a current communication), current network load (i.e., how many channels are currently occupied by other users), and the

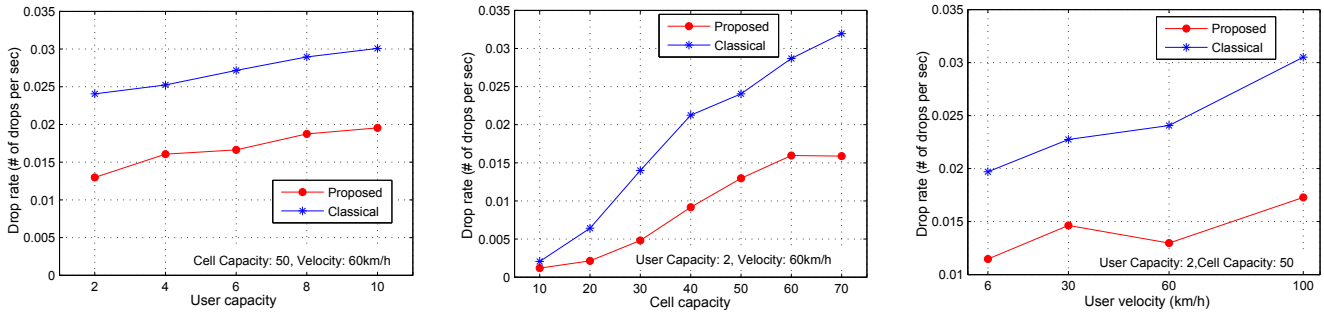

(a) (b) (c)

Figure 26: Drop rate in the proposed method (a) with different user capacity, (b) different cell occupancy, and (c) different user velocity.

velocity of mobile users.

One of the most important statistics in mobility management is the probability of a call drop. The call drop occurs when a mobile user cannot find any available spectrum resource in both serving and target cells, which degrades the service quality of mobile users significantly. Here we do not consider a call blocking probability. Figure 26 shows that the proposed method shows better performance in the drop rate than classical and fixed allocation methods. As shown in Figure 26 (a), although the user QoS requirement increases, the proposed method maintain a certain level of drop rate by exploiting spectrum mobility management. If the network load increases, a drop rate becomes higher due to the lack of available spectrum resource, but is still lower than classical method by exploiting different handoff types adaptively to cell conditions. Furthermore, the proposed method allows mobile users to adaptively use the extended area while reducing the number of inter-cell/inter-pool handoff through a user mobility management scheme. As a result, the proposed method sustains a lower drop rate although a mobile user traverse across wider areas and more cells boundaries with higher velocity, as shown in Figure 26 (c).

Figure 27 shows the link efficiency, which is defined as a real transmission time over an entire simulation time. In this simulation, the classical method shows lower link efficiency over all cases due to quality degradation caused by frequent inter-cell/inter-pool handoffs. Furthermore, when current cell is overloaded. some of mobile users cannot use spectrum resources until spectrum availability changes or they move into a new target cell area, which also reduces the link efficiency. On the contrary, the proposed method shows higher link efficiency by intelligently determine the handoff types so as to reduce the latency as well as a drop rate.

3.3 Primary User Activity Modeling using First-Difference Filter Clustering and Correlation

In recent studies, the PU activity is assumed to follow the Poisson model with exponentially distributed inter-arrivals [10, 25]. However, the Poisson model fails in capturing the bursty and spiky characteristics of the monitored data [36]. As a result, the existing works based on the Poisson model derive the PU activity models that are smooth and burst-free traffic in which short term fluctuations are neglected, which is shown in Figure 28.

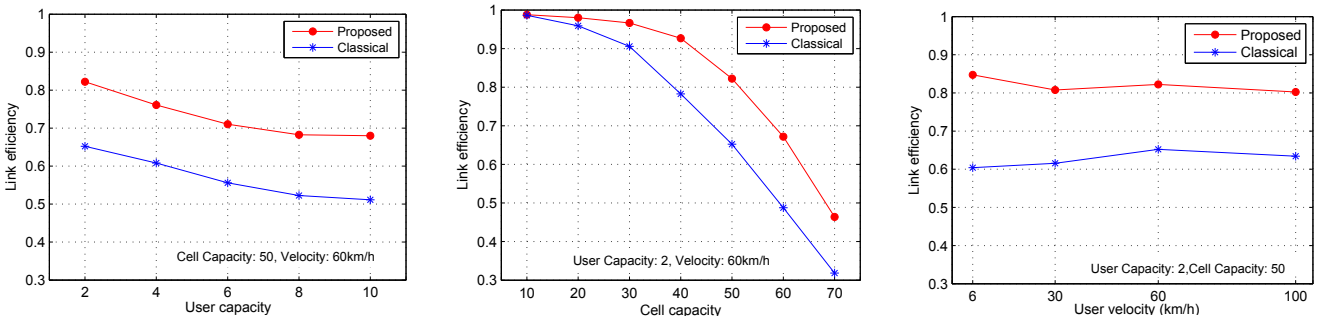

(a) (b) (c)

Figure 27: Link efficiency in the proposed method (a) with different user capacity, (b) different cell occupancy, and (c) different user velocity.

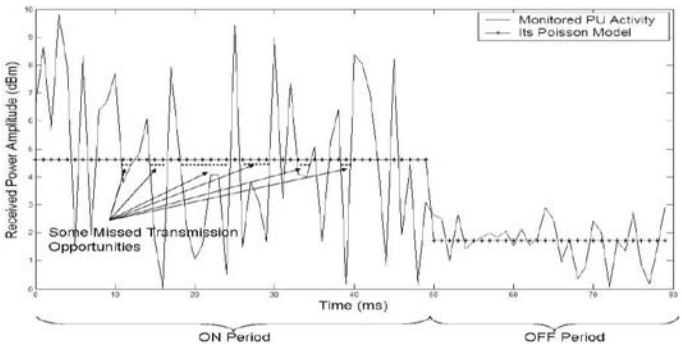

Figure 28: Missed Transmission Opportunities caused by the Poisson Modeling

Here, we observe that the actual PU activity fluctuates around the ON horizontal level, which is not exactly tracked by the Poisson approximation. Some of these fluctuations result in durations, where the PU is actually absent (shown by the dashed lines). These durations, mistakenly classified as an ON period by the Poisson model, serve as missed transmission opportunities for the CR users as the band is not utilized. Since the Poisson model does not consider correlations and similarities within data, it is incapable of identifying such fluctuations. This leads to fewer cases of correct spectrum hole detection, thus causing a degradation in CR network performance. Consequently, it is desired to detect these missed transmission opportunities while achieving less interference simultaneously.

3.3.1 System Model

Our proposed model consists of two main modules: *PU activity monitoring module* and *clustering-modeling module* which are illustrated in Figure 29.

The PU Activity Monitoring Module which is implemented in each CR user, monitors the spectrum band to take p consecutive samples of PU activity. Once the monitoring is finished, this module gives the monitored

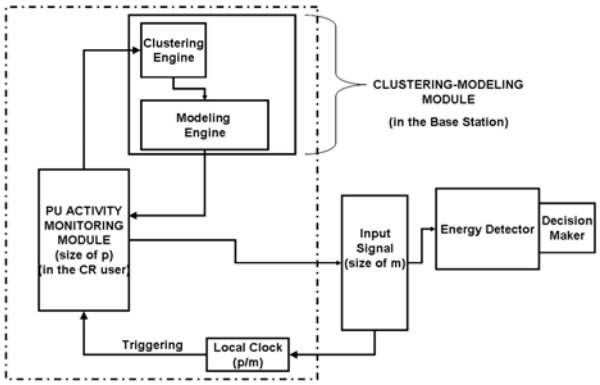

Figure 29: The Block Diagram of the Proposed Model

PU activity vector $\underline{q}$ for modeling and analysis to the *Clustering-Modeling Module* which is implemented in the base station. The *Clustering-Modeling Module* activates its *Clustering Engine* where the monitored PU activity samples are accumulated into *clusters* using a *First-Difference Filtering* procedure enhanced with temporal correlation calculations. As a result, a new clustered PU activity vector with clusters is generated and then input to the *Modeling Engine* as seen in Figure 29. In this engine, a correlation based modeling scheme produces the new modeled PU activity and parameterizes PU activity characteristics, i.e., P_{IDLE}, the probability occupying the spectrum and P_{BUSY}, the probability of PU presence. The newly generated PU activity characteristics and the modeled PU activity vector $\underline{r}$ are input back to the *PU Activity Monitoring Module* in the CR user. Then, the modeled PU activity is input to the energy detector which takes the modeled PU activity vector size of $m << p$, and realizes its energy detection for spectrum sensing. As the energy detector operates in a loop with p/m iterations, the time is controlled by a local clock. Therefore, at the end of an iteration, the energy detector triggers the *PU Activity Monitoring Module* using the local clock for a new analysis. More details on *Clustering-Modeling Module* are in the following subsections.

3.3.2 PU Activity Monitoring

This module which is implemented in each CR user, is responsible for monitoring the PU activity ($\underline{q}$) of size p from the spectrum band. The module receives the modeled PU activity and the new PU activity characteristics (P_{BUSY} and P_{IDLE}) back from the *Clustering-Modeling Module*.

3.3.3 Clustering Modeling

The monitored PU activity is input to the *Clustering-Modeling Module* in the base station. The module has two engines to process the monitored PU activity: the *Clustering Engine* and the *Modeling Engine* which are explained below.

- Clustering Engine: At the beginning of the clustering process, the *Clustering Engine* receives the monitored PU activity vector $\underline{q}$ from the *PU Activity Monitoring Module*. Since the monitored PU activity $\underline{q}$ is

input to the *Clustering Engine Module*, we may assume that the modeled PU activity vector $\underline{r}$ is identical to the monitored PU activity vector $\underline{q}$ at the beginning of the *Clustering Engine*, i.e. $\underline{q} = \underline{r}$. Then, all the consecutive samples (the current sample $r(m)$ and the last sample $r(m-1)$) are passed through the first-difference Finite Impulse Response (FIR) filter. In the next step, the filter output $D(m)$ is checked with δ-test, which is a set of First-Difference Filtering procedures. If the δ-test is successful, the ρ-test is applied. Consequently, the modeled PU activity sample $r(m)$ is placed in the existing cluster $C(k)$ with its predecessor ($r(m-1)$) if both tests are successful, whereas any fail from these two tests leads the sample $r(m)$ to form a new cluster $C(k+1)$. As a result, only the modeled PU activity sample $r(m)$, which is $close$ to its predecessor $r(m-1)$ (successful in δ-test) and highly correlated with the last two samples $r(m-1)$, $r(m-2)$(successful in ρ-test, which is a correlation calculation procedure), is placed in the same cluster with its predecessor $r(m-1)$. Furthermore, by using clusters, groups of first-difference filtered PU activity samples which have different correlation statistics are separated. In other words, spiky and bursty characteristics of the modeled PU activity are more accurately distinguished by cluster exploitation, leading the CR user to detect the PU activity fluctuations more precisely, hence causing less interference.

- Modeling Engine: This engine is used to model the clustered PU activity provided by the *Clustering Engine*. In the $Modeling\ Engine$, the pair $(C(k), C(k+1))$ is decided to be characterized by a decision region after passing by $Correlation\ Slope$ and ρ-test. Consequently, the clusters of the pair, $C(k+1)$ and its predecessor $C(k)$, are decided individually to become either $BUSY$ or $IDLE$ using the specific decision of the region in which the pair is allocated. As the output of the $Modeling\ Engine$, the total number of IDLE clusters r_{IDLE}, the total number of BUSY clusters r_{BUSY}, the modeled PU activity vector $\underline{r}$, PU activity characteristics P_{BUSY} and P_{IDLE}, as well as the calculation of P_f and T are input to the $PU\ Activity\ Monitoring\ Module$ as seen in Figure 29. Using the $Modeling\ Engine$, we analyze each cluster pair $(C(k), C(k+1))$ independently, thus the fluctuations in PU activity are better classified. This leads to more accurate detection of the transmission opportunities and an increase in the CR network performance.

3.3.4 Results

In the evaluations, we use a network topology where we consider a centralized PU network which operates in a licensed spectrum band with a bandwidth of W=6 MHz. This PU network consists of one PU and one primary base station. The primary base station has a PU transmission range of $250\ m$. The PU randomly communicates with the primary base station in this range. Moreover, we consider a CR network which operates within the PU transmission range in an opportunistic manner. This CR network has one CR base station and 20 CR users which are spread out within the PU transmission range.

The performance of the proposed model is also evaluated in terms of the CR user's achievable throughput. Figs. 30(a) and 30(b) represent the CR user's throughput as functions of the normalized effects of clustering, Φ_{1nor} and the normalized effects of correlation, Φ_{2nor}. In Figure 30(a), within $0 \leq \Phi_{1nor} \leq 0.45$, we observe an increase in the throughput from $4.8\ bps/Hz$ to $5.4\ bps/Hz$. The reason of this increase is expressed as

follows. As $0 \leq \Phi_{1nor} \leq 0.45$, the number of PU samples which fail the δ-test also increases, thereby raising the number of clusters. Since the PU activity fluctuations are more accurately captured using clusters, there is a reduction of P_f which is calculated. Therefore, the last term $(1 - P_f)$ increases which leads to an augmentation in throughput. However, within $0.45 \leq \Phi_{1nor} \leq 1$, the last term decreases due to the higher P_f, caused by the inaccurate PU activity detection, thereby degrading the throughput from $5.4\ bps/Hz$ to $4.1\ bps/Hz$. In the case of the Φ_{2nor}, we observe a continuous reduction in the CR user's throughput as shown in Figure 30(b). Since Φ_{2nor} and P_f are directly proportional, the last term decreases continuously while increasing Φ_{2nor} which results in throughput degradation. Although the throughput decreases with Φ_{2nor}, in the case of $\Phi_{2nor} = 0$, our proposed model provides a throughput of $5.2\ bps/Hz$, which is $26\ \%$ higher than the one provided by the Poisson model ($\Phi_{1nor} = 1$) which is $4.1\ bps/Hz$, as seen in Figure 30(b).

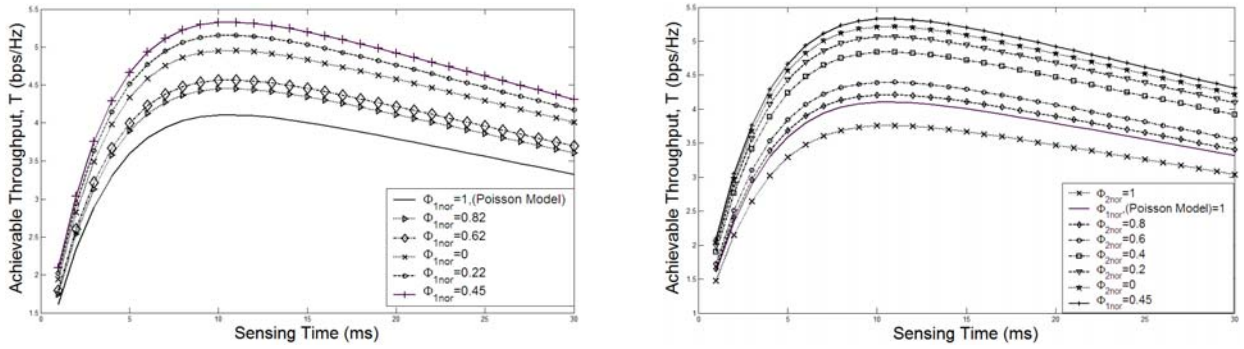

(a) (b)

Figure 30: Normalized Effect of (a) clustering (Φ_{1nor}) and (b) correlation (Φ_{2nor}) on achievable throughput T.

Overall, the key results are summarized in the Table 1, where the proposed model outperforms the Poisson model giving significant improvements in the normalized PU activity estimation error MSE, the false alarm probability P_f and CR user's throughput T.

Table 1: Key Results

	$Normalized\ MSE$	P_f	$T\ (bps/Hz)$
$Poisson\ Model$	0.65	0.67	4.1
$Proposed\ Model\ (0 \leq \Phi_{1nor} \leq 0.45)$	0.32	0.38	5.4
$Proposed\ Model\ (\Phi_{2nor} = 0)$	0.33	0.5	5.2
$Improvement(\%)\ (provided\ by\ \Phi_{1nor})$	50	43	31
$Improvement(\%)\ (provided\ by\ \Phi_{2nor})$	49	25	26

3.4 A QoS-Aware Framework for Available Spectrum Characterization and Decision

In CR networks, the choice of the spectrum bands, called *spectrum decision*, must be made carefully by considering the challenges in the spectrum availability over time, the short term fluctuations in the availability, and the heterogeneous Quality of Service (QoS) requirements of the cognitive radio users. Taking into account these challenges, the main contribution of this paper is to design a QoS-aware spectrum decision framework that achieves higher spectrum utilization and fairness in CR networks.

Previously, we developed an optimum spectrum decision framework is proposed by considering the basic QoS-specific CR user applications - real-time and best effort (BE) [26], where novel optimization schemes are defined for spectrum decision to maintain the specific QoS requirements such as capacity and delay for CR users. Furthermore, in recent studies, in [9], a spectrum allocation paradigm is proposed only for the devices with constrained communication resources, as seen in sensor and ad hoc networks. The trade-off between fairness and utilization is pointed out in [9] for basic CR user applications. The studies in [37], [39] give optimization solutions for overall spectrum utilization and fairness using collaboration of CR users with basic QoS classifications but without a specific spectrum characterization.

Overall, these aforementioned studies assume Poisson modeling to characterize the available spectrum and PU activities. However, the short-term fluctuations and spiky characteristics of the available spectrum should also be captured to achieve better spectrum utilization [7]. Moreover, recent studies consider some basic CR user applications without clear distinction of their traffic types. In order to analyze the effects of heterogeneous applications on the overall CR network fairness, we also need to consider different CR user types. With these motivations in mind, we extend our previous spectrum decision schemes, and propose a novel QoS-aware spectrum decision framework.

3.4.1 System Model

Our proposed framework, which is implemented in the BSs, has five modules as shown in Figure 31, which monitors the ongoing PU activities in the licensed spectrum band using *the PU Activity Module* consisting of two engines, i.e., *PU Activity Monitoring Engine* and *Available Spectrum Characterization Engine* where the PU activities are modeled by a special PU activity index as in [6]. Using the PU Activity Index for each spectrum band, the PU Activity Monitoring Engine models each spectrum band by a separate queue-server mechanism. Then, the Available Spectrum Characterization Engine analyzes each queue-server mechanism and defines *the Opportunity Index* Ψ for each spectrum band. The output of the Available Spectrum Characterization Engine is input to the Admission Control Module.

Our framework also characterizes the heterogeneous CR users according to their QoS requirements in *the QoS-aware Characterization Module of CR Users* by introducing a novel QoS parameter called *the Request Index*, κ. By using the opportunity index Ψ for all spectrum bands and the request index κ for all different CR user types as inputs, *the Admission Control Module*, stabilizes the QoS requirements of the CR users according to the available spectrum. More specifically, the Admission Control Module checks the QoS requirements of

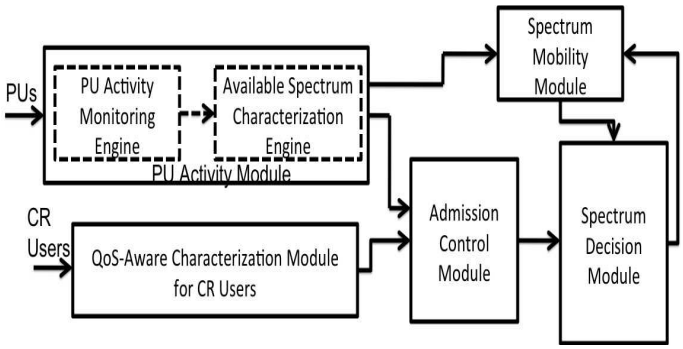

Figure 31: The Proposed Framework

the new CR users and accepts the new comers only if their QoS requirements do not cause any QoS degradation for existing CR users in the network. The output of the Admission Control Module is input to *the Spectrum Decision Module* which takes the admitted CR users as input and runs its decision algorithm to assign the most appropriate spectrum bands to all CR users. The appropriate spectrum band is chosen by considering an overall fairness among diverse QoS requirements of CR users. The Spectrum Decision Module is designed to provide higher spectrum utilization. The higher fairness and utilization are provided by a dynamic decision procedure.

Moreover, *the Spectrum Mobility Module* continuously monitors the available spectrum and updates the decisions of the Spectrum Decision module. More specifically, the Spectrum Mobility Module, has two inputs, the opportunity index Ψ defined in the PU Activity Module and the decisions taken in the Spectrum Decision Module. Using these two inputs, the Spectrum Mobility Module runs the mobility algorithm and checks for any dynamic changes in the available spectrum. If there is a change, it means that there are PUs appearing in the spectrum bands. Then, the Spectrum Mobility warns the Spectrum Decision Module to modify the decisions accordingly.

The following are the definitions of indices required in the proposed framework:

- *Primary User (PU) Activity Index:* This metric, $\Phi_m(t)$, is defined to parameterize the relation between the vector of the clustering parameters and the vector of the correlation parameters.

- *Opportunity Index:* The opportunity index, Ψ_m, is a new QoS metric which characterizes the available transmission opportunities that CR users can exploit in the m^{th} spectrum band. It can be expressed as the ratio between the spectrum availability of CR users and the maximum usage of PUs. This parameter shows the amount of available spectrum that CR users can exploit in the m^{th} spectrum band. The opportunity index is calculated in the Available Spectrum Characterization Engine of the PU Activity Module as shown in Figure 31.

- *Request Index:* The request index κ_n is a new QoS metric to characterize the heterogenous QoS requirements, throughput and delay, for *n* types of CR users. This metric can be expressed as the ratio between the spectrum request of CR users R_n and the maximum request of CR users R_{max}. The request index is calculated in the QoS-Aware Characterization Module for CR users as shown in Figure 31.

Table 2: Heterogeneous CR User Applications and their Queuing Disciplines

CR User Application	**CR User Type**	**Queuing Discipline**
E1/T1 type CBR	Type 1	$D/G/1$
Video-Conference	Type 2	$G/G/1$
VoIP	Type 3	$MMPP/G/1$
BE	Type 4	$M/G/1$

- *Assigned Spectrum Index:* The assigned spectrum index $\delta_n^{(m)}$ is a value to indicate how much of the m^{th} spectrum band is assigned to the CR users of type *n*. The value $\delta_n^{(m)}$ is bounded $0 \leq \delta_n^{(m)} \leq \Psi_m$. $\delta_n^{(m)}$ varies between 0 and the opportunity index value Ψ_m. This means that the spectrum band assigned to type n CR users in the m^{th} spectrum band can be equal to the transmission opportunities captured in the m^{th} band at the maximum.

3.4.2 QoS-Aware Characterization for CR Users

This module characterizes the heterogenous CR users according to their QoS requirements by defining a novel QoS parameter, *The Request Index* κ_n. In this module, the CR users are classified into four different types and each CR User type is modeled with a different queuing discipline. The different CR User types and their queuing disciplines are shown in Table 2. The output of the QoS-aware Characterization Module of CR Users, the request index κ_n, is input to the Admission Control Module.

3.4.3 Admission Control

The Admission Control Module, seen in Figure 31, is responsible for stabilizing the QoS requests of new CR users. The stabilization of QoS requirements is needed to achieve higher spectrum utilization and fairness. More specifically, when new CR users come, they should not affect the service quality of existing CR users in order not to degrade the fairness of the system. New CR users should also be checked how much of their QoS requirements can be satisfied according to the available spectrum bands in order to provide higher spectrum utilization. Therefore, new comers should be accepted to the system only if their QoS requirements do not make any degradation in the service quality of existing CR users.

The admission control module receives the QoS requirements of new CR users from the QoS-aware characterization module and the available spectrum information (i.e. the opportunity index Ψ) from the PU activity module. Then, the admission control module runs the *Prescreening Algorithm*.

The Prescreening Algorithm adjusts the QoS requirements of the new CR users considering the spectrum requests and available spectrum. New CR users are admitted to the system in a way that they don't cause any overload in the system resources.

3.4.4 Spectrum Decision

The spectrum decision module seen in Figure 31 selects the most appropriate spectrum bands for CR users. This module runs the Spectrum Decision Algorithm.

3.4.5 Spectrum Mobility

This module as shown in Figure 31 continuously monitors and checks all possible dynamic changes in the available spectrum. If there is any change, it means that there are PUs appearing in the spectrum bands. In these cases, the spectrum mobility module accordingly updates the results of the spectrum decision module by a warning as shown in Figure 31.

CR users can use the m^{th} spectrum band as long as no PU appears. Thus, the available portion of the m^{th} spectrum band is assigned to type n CR users when the opportunity index Ψ_m is greater than or equal to the assigned spectrum index $\delta_n^{(m)}$. Thus, the following inequality should be satisfied for CR transmission: $\Psi_m \geq \sum_{n=1}^{4} \delta_n^{(m)}$.

When PU appears in the m^{th} spectrum band, the opportunity index Ψ_m starts decreasing. This is because there will be less opportunities for CR users to exploit that spectrum band when PUs appear. Moreover, the moment when the opportunity index Ψ_m becomes smaller than the assigned spectrum index $\delta_n^{(m)}$ in the m^{th} spectrum band, the CR users should evacuate that band. In that moment, the PUs start occupying the spectrum band and CR users should not affect the PU transmissions. Accordingly we define the so-called *Mobility Condition*:

$$\Psi_m < \sum_{n=1}^{4} \delta_n^{(m)}, \qquad \forall\, m \in [1, 2, .., \iota]. \tag{88}$$

This condition holds when the available spectrum band becomes less than the assigned spectrum due to the PU appearance. Using Eq. (88), we design a spectrum mobility algorithm, which continuously monitors the condition, Eq. (88). The algorithm updates the decisions made by the spectrum decision module when the condition, holds, i.e., when PUs appear in the spectrum band.

3.4.6 Results

For simulations, we use a centralized CR network topology with one CR Base Station and 100 CR users. We assume 20 licensed spectrum bands ($\iota = 20$). Moreover, we consider that the CR users are randomly distributed over a network coverage of 250 m. The CR users are equipped with software defined radios (SDR) transceivers in order to select the appropriate spectrum band over a wide frequency range. There are 4 different types of CR users (n=4). The total number of CR users (100) is distributed among different CR User types.

To compare our framework in terms of spectrum utilization and fairness, we consider two cases (Case 1 and Case 2).

- *Case 1–traditional WFQ:* We implement a spectrum decision mechanism based on the traditional weighted fair queueing (WFQ) discipline.
- *Case 2–WFQ with PU avoidance:* We implement the same WFQ based spectrum decision mechanism with Case 1. Moreover, in this case, we also implement the dynamic PU avoidance provided by our spectrum mobility module.
- *Case 3–The proposed framework:* We implement our framework with all the modules.

The utilization factor U is the total amount of spectrum band capacity that is assigned to CR users and is given by

$$U = \sum_{m=1}^{\iota} \sum_{n=1}^{4} (\frac{\frac{1}{\Phi_m}}{\frac{1}{\Phi_m} + \tau}).\mu_m.\delta_n^{(m)}.c_m, \quad \forall\, m \in [1, 2, .., \iota] \tag{89}$$

In Figure 32(a), the utilization is maximized in all three cases when the number of Type-1 CR users (E1/T1) is greater than the other types (for x=40:25:25:10 values). This is due to the priority of Type-1 CR users being higher than the other traffic types. On the other hand, in Figure 32(a) we show that the utilization decreases when the number of CR users with less priorities increases. When the system has more CR users with less priorities, the available spectrum is decided by *the aggressive decision* part of the spectrum decision algorithm (Algorithm 2). Since the QoS requirements are not strictly considered in the aggressive decision, as a result the available spectrum utilization decreases.

In Figure 32(a), the utilization in Case 2 is higher than Case 1 because the CR users may utilize the available spectrum more efficiently using our spectrum mobility module which does not exist in Case 1. Moreover, as shown in Figure 32(a), the utilization of our proposed algorithm (Case 3) is higher than Cases 1 and 2. Case 3 has an admission control module in order to stabilize the QoS requirements of the new CR users. Besides, the admitted CR users are decided for available spectrum bands by three different decision procedures (perfect, smooth and aggressive). This leads to a dynamic spectrum decision mechanism for the new CR users since they can be assigned to more appropriate spectrum bands according to their QoS requirements.

Our framework is aimed to provide a feasible spectrum decision for all types of CR users. We define the fairness using the fairness index of [20] as:

$$F = \frac{\sum_{m=1}^{\iota} \left(\sum_{n=1}^{4} \delta_n^{(m)}\right)^2}{m \sum_{m=1}^{\iota} (\sum_{n=1}^{4} (\delta_n^{(m)})^2)}, \qquad \forall\, m \in [1, 2, .., \iota]. \tag{90}$$

The value of F fluctuates within 0 and 1 [20]. When F approaches 1, it indicates that the fairness among CR users increases.

As shown in Eq. (90), the fairness is related to the spectrum assigned to each CR User type ($\delta_n^{(m)}$). In Figure 32(b) we show the changes in the fairness dependent on different number of CR users ($\beta_n \quad \forall\, n \in [1, 2, 3, 4]$). We see an increase in the fairness while the number of less priority users increases for all three cases. More specifically, the fairness for Case 3 is less than 0.6 when there are more Type-1 CR users than

the other types (for x=40:25:25:10 values), whereas F is around 0.78 for the Case 3 when type-4 CR users are more than the others (for x=10:25:25:40 values). When there are more high priority CR users in the system, the available spectrum is mostly assigned to them. In order to satisfy the QoS requirements of high priority CR users, the low priority CR users must sacrifice their assigned spectrum.

In Figure 32(b), the fairness in Case 1 is higher than Case 2. In Case 2, the CR users are more dynamically assigned to the available spectrum compared to Case 1, according to the PU avoidance and without considering static weights. Moreover, our proposed framework achieves higher fairness than the other two cases as seen in Figure 32(b). This is because the CR users are not subject to an admission control mechanism in Case 1 and 2. Thus the CR users can degrade the QoS assignments of existing users in the system. Moreover, in Cases 1 and 2, the decision is based on a weighted fair queueing (WFQ) mechanism which does not consider the dynamic QoS requirements of CR users. On the other hand, our framework has a dynamic spectrum decision mechanism with three different decision procedures (perfect, smooth and aggressive) which causes a better fairness.

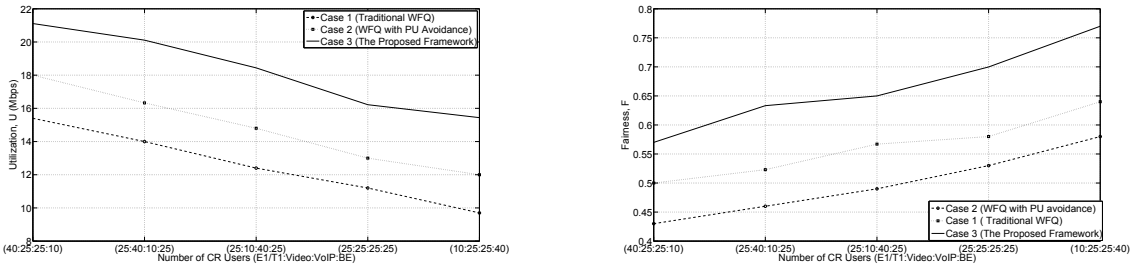

(a) (b)

Figure 32: (a) The utilization and (b) the fairness for different number of CR users.

3.5 Adaptive QoS-based Spectrum Sharing

In CR networks, the spectrum sharing function must consider the fluctuations in the spectrum bands due to the following reasons: CR users can transmit data only if the vacant (available) licensed spectrum bands are accurately detected. However, this detection process must account for possible errors caused by the physical channel conditions and the fluctuations of the available spectrum. These fluctuations are caused by dynamic primary user (PU) activities [1, 7]. Besides the determination of the available spectrum, the spectrum sharing mechanisms should also be aware of the heterogeneous QoS requirements of the CR users [1, 26]. In realistic scenarios, the QoS requirements of CR users can be classified into several heterogeneous application types, such as *Constant Bit Rate (CBR) traffic*, *video-conference*, *VoIP sessions and simple best effort (BE) communications*.

CR network operators compete for the spectrum in order to give better service to their CR users. This competition can be organized by a Spectrum Policy Server (SPS) [16, 38]. In this scheme, each operator announces its bandwidth request according to the service requirements of the corresponding CR users. Then, the SPS collects these requests and allocates to the operators the available spectrum accordingly. The main challenge in this procedure is to decide the proper strategy for the operators to maximize the spectrum usage.

In recent studies, there are some efforts to address the spectrum sharing problem in CR networks. In [24], a novel spectrum and power allocation framework is proposed for inter-cell spectrum sharing CR networks, achieving high fairness and network capacity but considering a basic QoS classification. In [16, 38] SPS-based systems are introduced for the coordination of spectrum demands in inter-network spectrum sharing. However, the bidding strategies employed in [16, 38] do not consider neither the short term PU activity fluctuations nor the heterogenous traffic types. In [32, 33, 42], the proposed spectrum sharing algorithms give solutions for only limited QoS requirements. In addition, the proposed spectrum sharing schemes in [32, 33, 42] are not adaptive to the dynamic changes in CR users' requests.

Overall, all these aforementioned studies do not account a detailed QoS classification of CR users in the spectrum sharing. However, the spectrum allocation and sharing should consider a clear and more detailed distinction in the heterogeneous service requirements of CR users [1, 11]. This is necessary to achieve high total throughput while maintaining the overall fairness among CR networks. Furthermore, the spectrum sharing schemes in [16, 32, 33, 38, 42] are not adaptive to the dynamic QoS requirements. However, dynamic QoS requests should also be integrated into the spectrum sharing mechanisms for more realistic results. Moreover, the SPS concept in [16, 38] should also be evaluated for environments with multiple operators to investigate the effect of the request mechanisms in spectrum allocation. Besides, none of these studies consider the PU activity fluctuations as well as the short term spiky characteristics of the PU traffic in their spectrum sharing mechanisms. Based on the drawbacks given above, we propose a novel adaptive QoS-based spectrum sharing scheme to coordinate dynamic spectrum demands. This scheme provides an adaptive approach according to bandwidth requests coming from the CR operators.

3.5.1 System Model

We consider a network topology with multiple CR operators, as shown in Fig.33(a). Each CR operator (Base Station, BS) is assumed to have an infrastructure-based CR network integrated in a licensed PU network. Each CR operator has access to multiple spectrum bands specified by the SPS and has associated CR users. The CR users are equipped with multiple software-defined radio (SDR) transceivers in order to transmit at a given spectrum band [26]. The monitored information is gathered by the operators to model the PU activity at each band. Moreover, the considered network environment has an SPS to coordinate the spectrum sharing among CR operators as seen in Fig.33(a). The operators communicate with the SPS and compete for the spectrum [16, 38]. Each operator announces its bandwidth request using the heterogeneous QoS requirements of the corresponding CR users. The SPS collects these requests and chooses the operators to use the available spectrum. The available spectrum bands are then shared by the CR users of the chosen operators.

The system we propose has three modules as shown in Fig.33(b). This system characterizes the heterogeneous CR users according to their QoS requirements in *The CR User QoS Classification Module* which is detailed in Section 3.5.2. This module uses the QoS parameter called *the QoS Index*, κ, developed using specific queueing disciplines for the employed traffic types [5].

The operators collect the bandwidth requests of the CR users and send the total amount requested to the

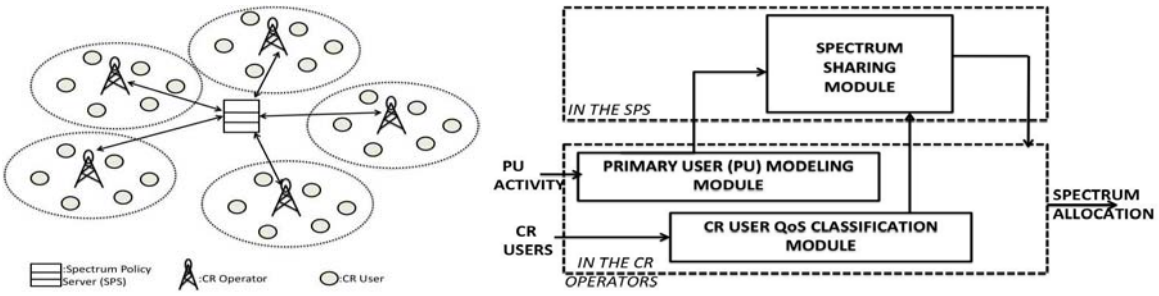

(a) (b)

Figure 33: (a) Network architecture and (b) the proposed system.

The Spectrum Sharing Module in the SPS. The SPS collects these accumulated bandwidth requests from the CR operators and allocates the available vacant spectrum accordingly. If the bandwidth assigned to a CR operator is less than its request, the spectrum sharing module allocates the vacant spectrum to the requesting CR users, based on the QoS types of them. Definitely, in this case, the allocated bandwidth to a CR user will be less than the requested one.

The spectrum sharing module is also fed by *The PU Modeling Module* in order to catch the vacant spectrum of the PU. This module models the PU activities by characterizing the spiky behavior and the short-term fluctuations of the PU traffic by employing the first-difference filter clustering and correlation scheme [7]. The details of the scheme is given in Section 3.5.2.

3.5.2 CR User QoS Classification

In this module, the QoS Index κ_n, is employed to characterize the heterogenous QoS requirements for the CR users [5]. In that work, CR users are grouped according to their QoS requests. κ_n, the QoS index for CR users of type-*n*, is the ratio between the spectrum request of CR users R_n and the available bandwidth R_a. κ_n is the request of CR users of type-*n* to use the available spectrum band, considering their QoS requirements [5].

$$\kappa_n = \frac{R_n}{R_a}, \qquad \forall\, n \in [1, 2, 3, 4]. \tag{91}$$

In this module, the CR users of four different types are modeled using appropriate different queuing disciplines. These four CR User types and the corresponding queuing disciplines are summarized as follows:

- *Type 1 CR Users—E1/T1 Type Applications*: Type 1 CR users are representing E1/T1 applications based on Constant Bit Rate (CBR) traffic. The traffic generated by these CR users has a deterministic behavior. They have the *highest* priority, i.e., they can occupy spectrum bands before all other CR user types. Type-1 CR users are modeled by a D/G/1 queueing system as in [19].
- *Type 2 CR Users—Video Conference Users*: Type 2 CR users are modeled by the G/G/1 queuing system [14]. They have the *second highest* priority, i.e., they can occupy spectrum band after serving Type 1 CR users and before Type 3 and 4 CR users.

- *Type 3 CR Users— Voice Over IP (VoIP) Users*: The VoIP traffic is modeled using a two-state Markov Modulated Poisson Process (*MMPP*) [13], where two states of MMPP are BUSY and IDLE periods of a VoIP call. The BUSY period is the talk duration of the VoIP call, and the IDLE period is the silent period. Consequently, the traffic of Type 3 CR users is modeled by a MMPP/G/1 queuing system [13]. They have the *third highest* priority, i.e., they can occupy spectrum band after other CR user types.

- *Type 4 CR Users— Best Effort (BE) Users*: Type 4 CR users can be modeled by using an M/G/1 queueing system. They have the *lowest* priority, i.e., they can occupy spectrum band after Type 1, 2 and 3 CR users.

3.5.3 Spectrum Sharing

The Spectrum Sharing Module, located in the SPS, is used to organize the bandwidth requests of the CR networks. Once the CR operators analyze the heterogeneous QoS requests of CR users and characterize requested bandwidths, they send them to the spectrum sharing module in the SPS. The SPS also receives the PU activity model from *the PU Modeling Module* in order to catch the vacant spectrum of the PU. Then, the spectrum sharing module assigns available spectrum of PUs to each CR operator. Consequently, CR operators allocate this available spectrum to the CR users. There are two situations that the spectrum sharing module can face, while allocating the available spectrum to the CR operators.

- If the total requested bandwidth of CR operators is higher than the assigned spectrum by the SPS, the CR operator allocates by the available spectrum band of the corresponding PU, according to a priority-based strategy. In this case, the bandwidth allocated to a CR user will be less than the requested one. Specifically, this strategy gives priority to each CR user type. CR user priorities are defined according to the QoS requirements of the corresponding applications. The priorities for the traffic types are defined as follows: Type-1 CR users have highest priority with $\epsilon_1 = 0.4$, Type-2 CR users have second highest priority with $\epsilon_2 = 0.3$, Type-3 CR users have the third-highest priority with $\epsilon_3 = 0.2$ and Type-4 CR users have the lowest priority with $\epsilon_4 = 0.1$. Using this strategy, the operators offer $\kappa_n^{(p)}$, which is calculated using the QoS indices κ_n as

$$\kappa_n^{(p)} = \epsilon_n.\kappa_n, \qquad \forall\, n \in [1, 2, 3, 4]. \tag{92}$$

- If the total requested bandwidth of CR operator is equal or less than the assigned spectrum by the SPS, SPS allocates the entire available spectrum to the operators' requests. Here, the available spectrum is shared proportionally among the CR operators according to their requests.

3.5.4 Results

We implement all the system modules and the algorithms in the MATLAB environment. We use an internetwork topology with 1 SPS, 20 CR operators and 200 CR users. We assume 20 licensed spectrum bands as in [26]. The PUs arrive with PU activity indices Φ of [7], which is summarized in Section 3.5.2. Moreover, we

consider that the CR users are randomly distributed and they are equipped with software defined radios (SDR) transceivers in order to select the appropriate spectrum band over a wide frequency range [26]. There are four different types of CR users *(n=4)* and the total number, 200, is distributed among different types. Specifically, we state that $\beta_1 + \beta_2 + \beta_3 + \beta_4 = 200$ where β_1 is the number of Type-1 CR users, β_2 is the number of Type-2 CR users, β_3 is the number of Type-3 CR users and β_4 is the number of Type-4 CR users . We assume that the channel is AWGN, and the noise power is selected as -115 dBm as in [26]. The results obtained for a confidence interval of 95% percentage, which are shown in the figures whenever they are not negligible.

The performance of the proposed system is compared based on total throughput and fairness. The performance is compared with those of two other CR network systems:

- CR Network System-1: In this system, there is an SPS in order to organize the spectrum sharing among CR operators. Here, the spectrum allocation among operators is more dependent to the total available spectrum than the individual bandwidth requirements. This system utilizes the Sum-Rate Scheduling maximization which is introduced in [38]. This scheme is aimed to maximize the total spectrum usage, by guaranteeing a minimum spectrum allocation of each CR operator. This approach is realized by allocating the fixed minimum spectrum to each CR operator.

- CR Network System-2: In this system, there is no SPS to organize the spectrum sharing among CR operators. Therefore, the spectrum allocation among operators is more dependent to the individual bandwidth requirements than the total available spectrum. It is the spectrum sharing mechanism of [33] where a minimum amount of available spectrum is assigned to the CR operators which is proportional with the individual bandwidth requests. This scheme aims maximizing the allocated available spectrum for individual operators, thereby increasing the overall fairness in the CR networks.

- CR Network System-3: It is the proposed system.

Consistency of the QoS Index: The consistency of the proposed QoS index , $\kappa_n \ \forall \ n \in [1, 2, 3, 4]$ is verified by simulation results for different number of channels as shown in Figure 34. It could be observed that, the analytical and the simulation results are very close to each other for all QoS indices.

Total Throughput: The total throughput *T* is the total spectrum band capacity that is assigned to CR operators. In Figure 35(a), the throughput is maximized in all three systems when the number of type-1 CR users (E1/T1) is greater than the other types (for x=100:40:40:20 values). This is due to the number of type-1 CR users in all three systems being significantly higher than the other traffic types. In the figure, we also see that the total throughput decreases when the number of CR users with less QoS requirements increases. When the system has more CR users with less QoS requirements, such as BE, the operators offer their bandwidth requests without strictly considering the QoS requirements of different user types, hence, the total available throughput decreases. The total available throughput in System 1 is higher than System 2 because the CR users may utilize the available spectrum since the scheduling mechanism in System 1 aims to maximize the throughput. Moreover, the total throughput of the proposed algorithm (System 3) is higher than Systems 1 and 2. System 3 has an adaptive request mechanism for operators in order for them to adjust their request strategies according

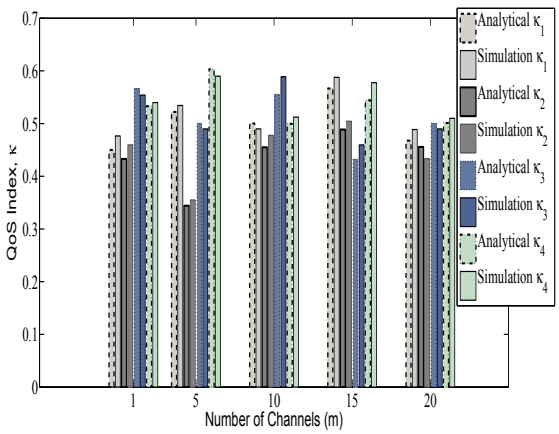

Figure 34: The Consistency of the QoS Index κ for Different Number of Channels

to the QoS requirements of the CR users. Besides, the spectrum sharing algorithm proposed employs a PU model which characterizes more accurately the spectrum holes in the spectrum bands, thereby increasing the total throughput compared to Systems 1 and 2.

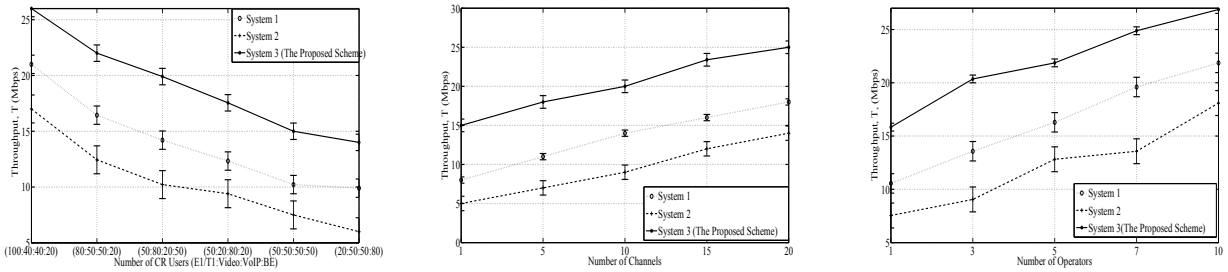

(a) (b) (c)

Figure 35: The Total Throughput for different Number of (a) CR Users, (b) channels, and (c) operators.

In Figure 35(b), the total throughput for different number of channels is shown. By increasing the number of channels, the available spectrum for CR users also increases. Thus, there are more available spectrum bands to utilize leading to an increase in the total throughput. Moreover, the proposed scheme achieves higher throughput than the other two systems because of the adaptive request mechanism of the operators considering the heterogeneous QoS requirements of users and the accurate PU modeling. In Figure 35(c), we show the total throughput for various number of operators. When the number of operators increases, more transmission opportunities are introduced. Moreover, the proposed scheme achieves the highest throughput than the other two systems because of the adaptive request mechanism of the operators considering the heterogeneous QoS classifications and the accurate PU modeling.

Fairness: The proposed system is aimed to provide a feasible spectrum sharing among the CR operators. We define the fairness among the CR operators in terms of allocated bandwidth, F, using the Jain's fairness index of [21]. F fluctuates within 0 and 1 [21]. When it approaches 1, it indicates that the fairness among CR

operators increases.

In Figure 36(a), we see an increase in the fairness while the number of CR users with less QoS requirements increases for all three Systems. When there are more CR users with less QoS requirements in the CR operators, the available spectrum is mostly assigned to these operators. In order to satisfy the high bandwidth requirements of CR users, the CR operators with low bandwidth requests must sacrifice their assigned spectrum, which may lead to an increase in fairness. Moreover, the fairness in System 2 is higher than System 1, because the sharing algorithm in System 2, assigns the available spectrum considering the individual QoS requirements, leading an increase in overall fairness. Moreover, the proposed framework achieves higher fairness than the other two Systems. This is because It provides an spectrum sharing mechanism with an adaptive request, achieving a dynamic spectrum sharing with the consideration the different QoS requirements of CR users. This mechanism is also enhanced by a more accurate PU modeling which is another factor of an higher fairness. Consequently, the proposed mechanism (System 3) causes a better fairness for CR users since the spectrum bands are allocated according to their dynamic QoS requirements.

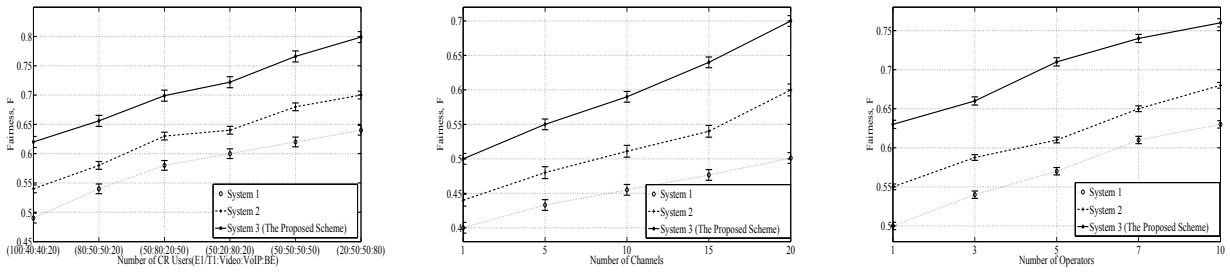

(a) (b) (c)

Figure 36: The Fairness for Different Number of (a) CR Users, (b) channels, and (c) operators.

In Figure 36(b), we show the variation of the fairness for different number of channels. The fairness for all three Systems increases with the number of channels because the CR operators are more likely to find available spectrum in the system. The scheme we propose (System 3) achieves higher fairness than the Systems 1 and 2 because System 1 and 2 do not account for the dynamic bandwidth requirements of CR operators whereas the proposed system provides an adaptive system for operators in order for them to share the spectrum considering the different user types. Figure 36(c) shows the variation of the fairness for different number of operators. As seen, The scheme we propose (System 3) achieves higher fairness than the Systems 1 and 2 when number of operators increases because of its adaptiveness towards heterogeneous service requirements of CR users.

4 RF/Analog IC System for Cognitive Radio Testbed

With the tremendous growth of wireless applications, many spectrum segments have been allocated to licensed spectrum users. These licensees have the privileged rights to use this authorized spectrum for commercial or public use. When the licensed spectrum band is carefully observed, however, some spectrum segments are found to be much less than fully utilized, depending on the time and location [12]. Therefore, researchers in

wireless technology have been urged to create a new wireless communication system to use the spectrum more efficiently than in the past [12]. For the success of cognitive radio (CR) systems improving the efficiency of spectrum usage, various spectrum processing techniques should be implemented for sensing and selecting the desired spectrum resources. To maximize the throughput of CR systems, those spectrum processing techniques should be highly flexible and reconfigurable to be adaptive, depending on the availability of spectrum resources. The most crucial requirements for spectrum sensing are the sensing sensitivity and sensing time to protect incumbent users and to improve data throughput. Lower sensitivity prevents a CR system from being adopted because of the danger of infringing upon incumbent users. A longer sensing time results in reduced throughput for the CR system and longer possible interference for primary users. In addition, low power consumption and simple implementation are desirable features from a CR system commercialization viewpoint [15].

As the CR concept is incorporated into emerging wireless standards, a reconfigurable testbed system is essential in validating proposed signal processing techniques and their hardware implementations. To support thorough testing of its own CR system and integrated circuit (IC) designs, a multi-standard, fully software (S/W) driven testbed system has been developed. This system has a capability of instant testing and evaluation of the algorithm levels of the communication system and of the RF/Analog ICs. Specifically, the spectrum sensing integrated circuit based on Multi-Resolution Spectrum Sensing (MRSS) algorithm was designed and fabricated in a $0.18\,\mu\mathrm{m}$ CMOS technology [34, 35].

4.1 Fully-integrated MRSS Receiver

Figure 37 shows a block diagram of the fully integrated MRSS receiver, which operates either as a spectrum sensing block or as a receiver front-end.

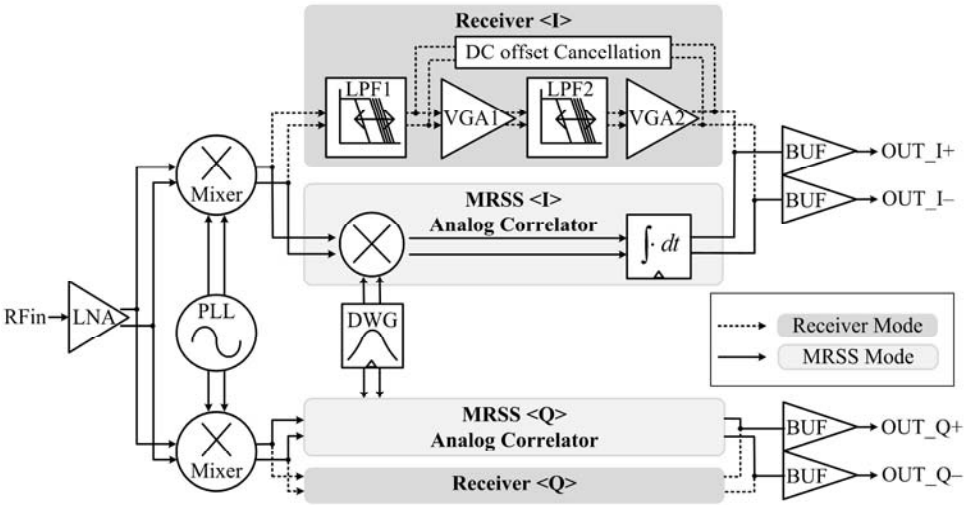

Figure 37: Block diagram of fully-integrated MRSS receiver.

The MRSS receiver is configured as a spectrum sensing energy detector. The down-converted baseband signal is correlated with a window generated from the DWG, yielding the filtered output within the window

bandwidth. The outputs in I and Q path are digitized by the external ADC, and the signal power is computed by $(OUT\_I2 + OUT\_Q2) \cdot 0.5$. In this mode, no analog filter is used in the RF signal path. The filtering effect comes from correlating the baseband received signal with a window. In this mode, all baseband filter blocks are disabled to save power.

4.2 Results

The MRSS receiver has been fabricated using $0.18\,\mu\mathrm{m}$ CMOS technology. The fabricated IC microphotograph is shown in Figure 38. The overall die occupies $4.8\,\mathrm{mm} - 2.4\,\mathrm{mm}$ and it consumes about $180\,\mathrm{mW}$ for both the receiver and MRSS modes with a $1.8\,\mathrm{V}$ supply voltage. The MRSS can detect any kind of complex modulated signals. Figure 3 compares the MRSS response with that of a spectrum analyzer. An OFDMA-modulated signal with $7\,\mathrm{MHz}$ bandwidth and $-35\,\mathrm{dBm}$ channel power centered at $609\,\mathrm{MHz}$ was combined with a $-50\,\mathrm{dBm}$ CW signal at $603\,\mathrm{MHz}$ and applied to the spectrum analyzer and the MRSS receiver, respectively. Figure 39 (a) is the output spectrum from the spectrum analyzer with resolution and video bandwidth of $200\,\mathrm{kHz}$. Figure 39 (b) shows the average of 100 independent MRSS measured results using a $100\,\mathrm{kHz}$ cos4 window, having a theoretical equivalent noise bandwidth of $194\,\mathrm{kHz}$. MRSS is detecting a signal power within its equivalent noise bandwidth, so an OFDMA signal with $-35\,\mathrm{dBm}$ of channel power and $7\,\mathrm{MHz}$ bandwidth is detected at about $-50\,\mathrm{dBm}$ power level, which is the same as in the spectrum analyzer. Therefore, it shows that MRSS can detect the RMS power of an arbitrary signal within its detection bandwidth, working like a simple spectrum analyzer.

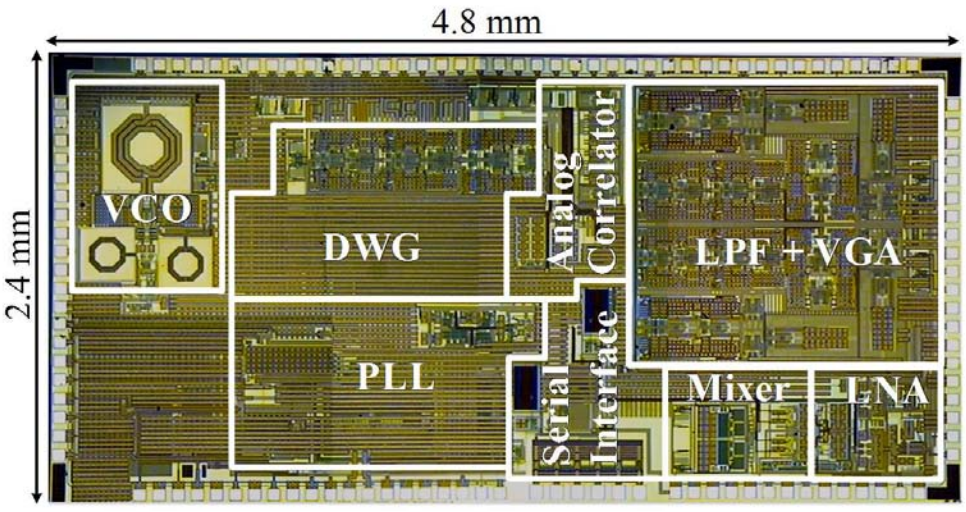

Figure 38: Die microphotograph.

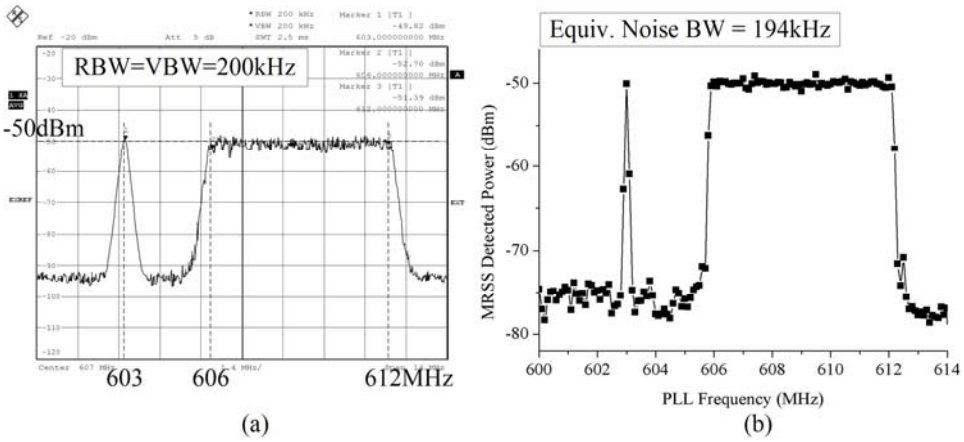

Figure 39: Comparison of spectrum analyzer and MRSS detections.

5 Publications Resulted from This Project

Journal Publications:

- I. F. Akyildiz, W. Y. Lee, M.C. Vuran, and S. Mohanty, "A Survey on Spectrum Management in Cognitive Radio Networks," *IEEE Communications Magazine*, vol. 46 , no. 4, pp. 40-48, Apr. 2008.
- B. Canberk, I. F. Akyildiz, and S. Oktug, "An Adaptive QoS-based Spectrum Sharing Scheme for CR Networks," submitted for journal publication, Dec. 2010.
- B. Canberk, I. F. Akyildiz, and S. Oktug, "Primary user activity modeling using first-difference filter clustering and correlation in cognitive radio networks," *IEEE/ACM Transactions on Networking*, vol. 19, no. 1, pp. 170-183, Feb. 2011.
- K. R. Chowdhury and I. F. Akyildiz, "Cognitive Wireless Mesh Networks for Dynamic Spectrum Access," *IEEE Journal of Selected Areas in Communications*, vol. 26, no. 1, pp. 168-181, Jan. 2008.
- G. Ganesan, Y. (G.) Li, B. Bing, and S. Li, "Spatiotemporal Sensing in Cognitive Radio Networks," *IEEE Journal on Selected Areas in Communications*, vol. 26, no. 1, pp. 5-12, Jan. 2008.
- W. Y. Lee and I. F. Akyildiz, "Optimal Spectrum Sensing Framework for Cognitive Radio Networks," IEEE Transactions on Wireless Communications, vol. 7, no. 10, pp. 3845-3857, Oct. 2008.
- W. Y. Lee and I. F. Akyildiz, "Dynamic Resource Allocation for Spectrum Sharing in Infrastructure-Based Cognitive Radio Networks," submitted for journal publication, Nov. 2009.
- W. Y. Lee and I. F. Akyildiz, "A Spectrum Decision Framework for Cognitive Radio Networks," *IEEE Transactions on Mobile Computing*, vol. 10, no. 2, pp. 161-174, Feb. 2011.
- W. Y. Lee and I. F. Akyildiz, "Spectrum-aware mobility management in cognitive radio cellular networks," to appear in *IEEE Transactions on Mobile Computing*, 2011.

- L. Li, X. Zhou, H. Xu, G. Y. Li, D. Wang, and A. C. K. Soong, "Simplified relay selection and power allocation in cooperative cognitive radio systems," *IEEE Transactions on Wireless Communications*, vol. 10, pp. 33-36, Jan. 2011.
- L. Li, X. Zhou, H. Xu, G. Y. Li, D. Wang, and A. C. K. Soong, "Energy-efficient transmission for protection of incumbent users," to appear in *IEEE Transactions on Broadcasting*, 2011.
- J. Ma, G. Zhao, and Y. (G.) Li, "Soft Combination and Detection for Cooperative Spectrum Sensing in Cognitive Radio Networks," IEEE Transactions on Wireless Communications, vol. 7, no. 11, pp. 4502-4507, Nov. 2008.
- J. Ma, G. Y. Li, and B. H. Juang, "Signal processing in cognitive radio," *Proceedings of the IEEE*, vol. 97, no. 5, pp. 805-823, May 2009.
- J. Ma, X. Zhou, and G. Y. Li, "Probability-based periodic spectrum sensing during secondary communication," *IEEE Transactions on Communications*, vol. 58, no. 4, pp. 1291-1301, Apr. 2010.
- J. Park, T. Song, J. Hur, S. M. Lee, J. Choi, K. Kim, K. Lim, C.-H. Lee, H. Kim, and J. Laskar, "A fully integrated UHF-band CMOS receiver with multi-resolution spectrum sensing (MRSS) functionality for IEEE 802.22 cognitive radio applications," *IEEE Journal of Solid-State Circuits*, vol. 44, no. 1, pp. 258-268, Jan. 2009.
- G. Zhao, J. Ma, G. Y. Li, T. Wu, Y. H. Kwon, A. Soong, and C. Yang, "Spatial spectrum holes for cognitive radio with relay-assisted directional transmission," *IEEE Transactions on Wireless Communications*, vol. 8, no. 10, pp. 5270-5279, Oct. 2009.
- G. Zhao, C. Yang, G. Y. Li, D. Li, and A. Soong, "Power and channel allocation for cooperative relay in cognitive radio networks," *IEEE Journal of Selected Topics in Signal Processing*, vol. 5, no. 1, pp. 151-159, Feb. 2011.
- X. Zhou, J. Ma, G. Y. Li, Y. H. Kwon, and A. Soong, "Probability-based optimization of inter-sensing duration and power control in cognitive radio," *IEEE Transactions on Wireless Communications*, vol. 8, no. 10, pp. 4922-4927, Oct. 2009.
- X. Zhou, J. Ma, G. Y. Li, Y. H. Kwon, and A. Soong, "Probability-based combination for cooperative spectrum sensing," *IEEE Transactions on Communications*, vol. 58, no. 2, pp. 463-466, Feb. 2010.
- X. Zhou, G. Y. Li, D. Li, D. Wang, and A. C. K. Soong, "Probabilistic resource allocation for opportunistic spectrum access," *IEEE Transactions on Wireless Communications*, vol. 9, no. 9, pp. 2870-2879, Sept. 2010.
- X. Zhou, G. Y. Li, and G. Sun, "Low-complexity spectral precoding for OFDM-based cognitive radio systems," submitted for journal publication, 2011.

Book Chapters:

- X. Zhou, G. Y. Li, D. Li, D. Wang, and A. C. K. Soong, "Bandwidth-efficient cooperative spectrum sensing," *Cognitive Radio for Wireless Cellular and Vehicular Networks*, H. Venkataraman and G.-M. Muntean, Eds., Boston, MA: Springer, to be published.

Conference Publications:

- S. Byun, K.-W. Kim, D.-H. Lee, J. Laskar, and C. S. Kim, "A self-calibrated LC quadrature VCO in a current-limited region," in *Proc. IEEE RFIC Symposium*, Jun. 2008, pp. 379-382
- B. Canberk, I. F. Akyildiz, and S. Oktug, "A QoS-Aware Framework for Available Spectrum Characterization and Decision in Cognitive Radio Networks," in *Proc. IEEE PIMRC*, Sept. 2010, pp. 1533-1538.
- W. Y. Lee, and I. F. Akyildiz, "Joint spectrum and power allocation for inter-cell spectrum sharing in cognitive radio networks," in *Proc. IEEE DySPAN*, Oct. 2008, pp. 1-12.
- S. M. Lee, T. Song, J. Park, K. Lim, and J. Laskar, "Analog pulse compressor for radar system," in *Proc. European Radar Conference (EuRAD)*, Oct. 2008, pp. 364-367.
- L. Li, X. Zhou, H. Xu, G. Y. Li, D. Wang, and A. C. K. Soong, "Energy-efficient transmission in cognitive radio networks," in *Proc. IEEE CCNC*, Jan. 2010, pp. 1-5.
- K. Lim, J. Park, J. Laskar, H. Kim, C. H. Lee, "Text on Multi-Resolution Spectrum Sensing," *IEEE 802.22 Doc. No. 22-07-0451-01-0001*, IEEE Standard Meeting, Big Island, Hawaii, Sept. 2007.
- J. Ma and Y. (G.) Li, "A Probability-based Spectrum Sensing Scheme for Cognitive Radio," in *Proc. IEEE ICC*, May 2008.
- J. Park, T. Song, J. Hur, S. M. Lee; J. Choi, K. Kim, J. Lee, K. Lim, C.-H. Lee, H. Kim, and J. Laskar, "A Fully-Integrated UHF Receiver with Multi-Resolution Spectrum-Sensing (MRSS) Functionality for IEEE 802.22 Cognitive-Radio Applications," in *Proc. IEEE ISSCC*, Feb. 2008, pp. 526-633.
- J. Park, K.-W. Kim, T. Song, S. M. Lee, J. Hur, K. Lim, and J. Laskar, "A Cross-layer Cognitive Radio Testbed for the Evaluation of Spectrum Sensing Receiver and Interference Analysis," *Proc. 3rd Int'l Conf. on Cognitive Radio Oriented Wireless Networks and Communications (CrownCom)*, May 2008, pp. 1-6.
- T. Song, S. M. Lee, J. Park, K. Lim, and J. Laskar "A Fully-integrated arbitrary waveform generator for analog matched filter," in *Proc. IEEE Asia-Pacific Microwave Conference (APMC)*, Dec. 2008.
- G. Zhao, J. Ma, G. Y. Li, A. C. K. Soong, and C. Yang, "Spatial spectrum holes in cognitive radio with relay transmission," in *Proc. IEEE VTC2009-Spring*, Apr. 2009, pp. 1-4.
- G. Zhao, C. Yang, G. Y. Li, D. Li, and A. C. K. Soong, "Channel allocation for cooperative relays in cognitive radio networks," in *Proc. IEEE ICASSP*, Mar. 2010, pp. 3258-3261.

- X. Zhou, G. Y. Li, Y. H. Kwon, A. C. K. Soong, and G. Zhao, "Probability-based transmit power control for dynamic spectrum access," in *Proc. IEEE DySPAN*, Oct. 2008, pp. 1-5.
- X. Zhou, G. Y. Li, Y. H. Kwon, and A. C. K. Soong, "Detection timing and channel selection for periodic spectrum sensing in cognitive radio," in *Proc. IEEE GLOBECOM*, Nov. 2008, pp. 1-5.
- X. Zhou, J. Ma, G. Y. Li, Y. H. Kwon, and A. C. K. Soong, "Probability-based combination for cooperative spectrum sensing in cognitive radio networks," *Proc. IEEE ICC*, Jun. 2009, pp.1-5.
- X. Zhou, G. Y. Li, D. Li, D. Wang, and A. C. K. Soong, "Bandwidth efficient combination for cooperative spectrum sensing in cognitive radio networks," in *Proc. IEEE ICASSP*, Mar. 2010, pp.3126-3129.
- X. Zhou, G. Y. Li, D. Li, D. Wang, and A. C. K. Soong, "Probability-based resource allocation in cognitive radio networks," in *Proc. IEEE GLOBECOM*, Nov. 2009, pp.1-6.
- X. Zhou, G. Y. Li, and G. Sun, "Low-complexity spectrum shaping for OFDM-based cognitive radios," in *Proc. IEEE WCNC*, Mar. 2011.
- X. Zhou, G. Y. Li, and G. Sun, "Multiuser spectral precoding for OFDM-based cognitive radios," to appear in *Proc. IEEE GLOBECOM*, Dec. 2011.

References

[1] I. F. Akyildiz, W.-Y. Lee, M. C. Vuran, and S. Mohanty, "NeXt generation / dynamic spectrum access / cognitive radio wireless networks: a survey," *Computer Networks Journal (Elsevier)*, vol. 50, pp. 2127–2159, Sept. 2006.

[2] I. Akyildiz, W.-Y. Lee, M. Vuran, and S. Mohanty, "A survey on spectrum management in cognitive radio networks," *IEEE Communications Magazine*, vol. 46, no. 4, pp. 40–48, Apr. 2008.

[3] C.-D. Chung, "Spectral precoding for rectangularly pulsed OFDM," *IEEE Transactions on Communications*, vol. 56, no. 9, pp. 1498–1510, Sept. 2008.

[4] B. Canberk, I. F. Akyildiz, and S. Oktug, "An adaptive QoS-based spectrum sharing scheme for CR networks," *submitted for publication*, Jun. 2010.

[5] ——, "A QoS-aware framework for available spectrum characterization and decision in cognitive radio networks," in *Proc. of IEEE PIMRC*, Sept. 2010.

[6] B. Canberk and S. Oktug, "On The Self Similarity Behavior of VoIP Traffic under IEEE 802.16d WiMAX Environment," in *Proc. of 23rd International Symposium on Computer and Information Sciences (ISCIS)*, Oct. 2008.

[7] B. Canberk, I. F. Akyildiz, and S. Oktug, "Primary User Activity Modeling Using First-Difference Filter Clustering and Correlation in Cognitive Radio Networks," *IEEE/ACM Transactions on Networking*, vol. 19, no. 1, pp. 170–183, Feb. 2011.

[8] L. Cao and H. Zheng, "Distributed spectrum allocation via local bargaining," in *Proc. of IEEE SECON*, Sept. 2005, pp. 475–486.

[9] ——, "Distributed rule-regulated spectrum sharing," *IEEE Journal on Selected Areas in Communications*, vol. 26, no. 1, pp. 130–145, Jan. 2008.

[10] C.-T. Chou, N. Sai Shankar, H. Kim, and K. Shin, "What and how much to gain by spectrum agility?" *IEEE Journal on Selected Areas in Communications*, vol. 25, no. 3, pp. 576–588, Apr. 2007.

[11] R. Etkin, A. Parekh, and D. Tse, "Spectrum Sharing for Unlicensed Bands," *IEEE Journal on Selected Areas in Communications*, vol. 25, no. 3, pp. 517–528, Apr. 2007.

[12] S. Haykin, "Cognitive radio: Brain-empowered wireless communications," *IEEE Journal on Selected Areas in Communications*, vol. 23, no. 2, pp. 201–220, Feb. 2005.

[13] H. Heffes and D. Lucantoni, "A Markov Modulated Characterization of Packetized Voice and Data Traffic and Related Statistical Multiplexer Performance," *IEEE Journal on Selected Areas in Communications*, vol. 4, no. 6, pp. 856–868, Sept. 1986.

[14] D. Heyman, A. Tabatabai, and T. Lakshman, "Statistical Analysis and Simulation Study of Video Teleconference traffic in ATM Networks," *IEEE Transactions on Circuits and Systems for Video Technology*, vol. 2, no. 1, pp. 49–59, Mar. 1992.

[15] *Functional requirements for the 802.22 WRAN standard*, IEEE Std. [Online]. Available: http://www.ieee802.org/22/Meeting_documents/2006_Nov/22050007480000_RAN_Requirements.doc

[16] O. Ileri, D. Samardzija, and N. Mandayam, "Demand Responsive Pricing and Competitive Spectrum Allocation Via Spectrum Server," in *Proc. of IEEE DySPAN*, Nov. 2005, pp. 194–202.

[17] J. van de Beek, "Sculpting the multicarrier spectrum: a novel projection precoder," *IEEE Communications Letters*, vol. 13, no. 12, pp. 881–883, Dec. 2009.

[18] J. van de Beek and F. Berggren, "EVM-constrained OFDM precoding for reduction of out-of-band emission," in *Proc. of IEEE VTC2009-Fall*, Sept. 2009.

[19] L. Kleinrock, *Queueing Systems, Volume 2: Computer Applications*. Wiley and Sons, 1976.

[20] L. B. Le and E. Hossain, "Resource allocation for spectrum underlay in cognitive radio networks," *IEEE Transactions on Wireless Communications*, vol. 7, no. 12, pp. 5306–5315, Dec. 2008.

[21] ——, "Resource Allocation for Spectrum Underlay in Cognitive Radio Networks," *IEEE Transactions on Wireless Communications*, vol. 7, no. 12, pp. 5306–5315, Dec. 2008.

[22] W.-Y. Lee and I. F. Akyildiz, "Dynamic resource allocation for spectrum sharing in infrastructure-based cognitive radio networks," *submitted for publication*, 2009.

[23] ——, "Spectrum-aware mobility management in cognitive radio cellular networks," *to appear in IEEE Transactions on Mobile Computing*, 2011.

[24] ——, "Joint spectrum and power allocation for inter-cell spectrum sharing in cognitive radio networks," in *Proc. of IEEE DySPAN*, Oct. 2008, pp. 1–12.

[25] ——, "Optimal spectrum sensing framework for cognitive radio networks," *IEEE Transactions on Wireless Communications*, vol. 7, pp. 3845–3857, Oct. 2008.

[26] ——, "A Spectrum Decision Framework for Cognitive Radio Networks," *IEEE Transactions on Mobile Computing*, vol. 10, no. 2, pp. 161–174, Feb. 2011.

[27] L. Li, X. Zhou, H. Xu, G. Y. Li, D. Wang, and A. C. K. Soong, "Energy-efficient transmission for protection of incumbent users," *to appear in IEEE Transactions on Broadcasting*, 2011.

[28] ——, "Simplified relay selection and power allocation in cooperative cognitive radio systems," *IEEE Trans. on Wireless Communications*, vol. 10, no. 1, pp. 33–36, Jan. 2011.

[29] L. Li, X. Zhou, H. Xu, G. Li, D. Wang, and A. Soong, "Energy-efficient transmission in cognitive radio networks," in *Proc. IEEE CCNC*, Jan. 2010, pp. 1–5.

[30] J. Ma, G. Y. Li, and B. H. Juang, "Signal processing in cognitive radio," *Proceedings of the IEEE*, vol. 97, no. 5, pp. 805–823, May 2009.

[31] J. Ma, X. Zhou, and G. Y. Li, "Probability-based periodic spectrum sensing during secondary communication," *IEEE Transactions on Communications*, vol. 58, no. 4, pp. 1291–1301, Apr. 2010.

[32] M. Ma and D. H. Tsang, "Impact of Channel Heterogeneity on Spectrum Sharing in Cognitive Radio Networks," in *Proc. of IEEE ICC*, May 2008.

[33] L. Musavian and S. Aissa, "Quality-of-Service Based Power Allocation in Spectrum-Sharing Channels," in *Proc. of IEEE GLOBECOM*, Dec. 2008.

[34] J. Park, T. Song, J. Hur, S. M. Lee, J. Choi, K. Kim, J. Lee, K. Lim, C.-H. Lee, H. Kim, and J. Laskar, "A fully-integrated UHF receiver with multi-resolution spectrum-sensing (MRSS) functionality for IEEE 802.22 cognitive-radio applications," in *Proc. of IEEE ISSCC*, Feb. 2008, pp. 526–633.

[35] J. Park, T. Song, J. Hur, S. M. Lee, J. Choi, K. Kim, K. Lim, C.-H. Lee, H. Kim, and J. Laskar, "A fully integrated uhf-band cmos receiver with multi-resolution spectrum sensing (mrss) functionality for ieee 802.22 cognitive radio applications," *IEEE Journal of Solid-State Circuits*, vol. 44, no. 1, pp. 258–268, Jan. 2009.

[36] V. Paxson and S. Floyd, "Wide area traffic: the failure of poisson modeling," *IEEE/ACM Transactions on Networking*, vol. 3, no. 3, pp. 226–244, Jun. 1995.

[37] C. Peng, H. Zheng, and B. Y. Zhao, "Utilization and fairness in spectrum assignment for opportunistic spectrum access," *ACM Mobile Networks and Applications (MONET)*, vol. 11, no. 4, pp. 555–576, Aug. 2006.

[38] C. Raman, R. Yates, and N. Mandayam, "Scheduling Variable Rate Links Via A Spectrum Server," in *Proc. of IEEE DySPAN*, Nov. 2005, pp. 110–118.

[39] P. Svedman, S. Wilson, and B. Ottersten, "A QoS-aware proportional fair scheduler for opportunistic OFDM," in *Proc. of IEEE VTC2004-Fall*, Sept. 2004, pp. 558–562.

[40] W. Wang and M. Zhao, "Joint effects of radio channels and node mobility on link dynamics in wireless networks," in *Proc. of IEEE INFOCOM*, Apr. 2008, pp. 933–941.

[41] T. Weiss and F. Jondral, "Spectrum pooling: an innovative strategy for the enhancement of spectrum efficiency," *IEEE Communications Magazine*, vol. 42, no. 3, pp. 8–14, Mar. 2004.

[42] Y. Wu and D. H. Tsang, "Distributed Power Allocation Algorithm for Spectrum Sharing Cognitive Radio Networks with QoS Guarantee," in *Proc. of IEEE INFOCOM*, Apr. 2009.

[43] W. Yu and R. Lui, "Dual methods for nonconvex spectrum optimization of multicarrier systems," *IEEE Transactions on Communications*, vol. 54, no. 7, pp. 1310–1322, Jul. 2006.

[44] G. Zhao, J. Ma, G. Li, T. Wu, Y. Kwon, A. C. K. Soong, and C. Yang, "Spatial spectrum holes for cognitive radio with relay-assisted directional transmission," *IEEE Transactions on Wireless Communications*, vol. 8, no. 10, pp. 5270–5279, Oct. 2009.

[45] G. Zhao, C. Yang, G. Y. Li, D. Li, and A. Soong, "Power and channel allocation for cooperative relay in cognitive radio networks," *IEEE Journal of Selected Topics in Signal Processing*, vol. 5, no. 1, pp. 151–159, Feb. 2011.

[46] G. Zhao, J. Ma, G. Li, A. C. K. Soong, and C. Yang, "Spatial spectrum holes in cognitive radio with relay transmission," in *Proc. IEEE VTC2009-Spring*, Apr. 2009, pp. 1–4.

[47] G. Zhao, C. Yang, G. Y. Li, D. Li, and A. C. K. Soong, "Channel allocation for cooperative relays in cognitive radio networks," in *Proc. IEEE ICASSP*, Mar. 2010, pp. 3258–3261.

[48] X. Zhou, G. Y. Li, D. Li, D. Wang, and A. C. K. Soong, "Bandwidth-efficient reporting for cooperative spectrum sensing," in *Proc. IEEE ICASSP*, Mar. 2010.

[49] ——, "Probabilistic resource allocation for opportunistic spectrum access," *IEEE Transactions on Wireless Communications*, vol. 9, no. 9, pp. 2870–2879, Sep. 2010.

[50] ——, *Bandwidth-efficient cooperative spectrum sensing in Cognitive Radio for Wireless Cellular and Vehicular Networks*. Boston, MA: Springer, 2011.

[51] X. Zhou, G. Y. Li, and G. Sun, "Low-complexity spectral precoding for OFDM-based cognitive radio systems," *submitted for publication*, 2011.

[52] ——, "Low-complexity spectrum shaping for OFDM-based cognitive radios," in *Proc. IEEE WCNC*, Mar. 2011.

[53] ——, "Multiuser spectral precoding for ofdm-based cognitive radios," *to appear in Proc. of IEEE GLOBECOM*, Dec. 2011.

[54] X. Zhou, J. Ma, G. Y. Li, Y. H. Kwon, and A. C. K. Soong, "Probability-based combination for cooperative spectrum sensing in cognitive radio networks," in *Proc. of IEEE ICC*, Jun. 2009, pp. 1–5.

[55] ——, "Probability-based combination for cooperative spectrum sensing," *IEEE Transactions on Communications*, vol. 58, no. 2, pp. 463–466, Feb. 2010.

[56] X. Zhou, G. Li, D. Li, D. Wang, and A. C. K. Soong, "Probability-based resource allocation in cognitive radio networks," in *Proc. IEEE GLOBECOM*, Nov. 2009, pp. 1–6.

[57] X. Zhou, Y. Li, Y. H. Kwon, and A. Soong, "Detection timing and channel selection for periodic spectrum sensing in cognitive radio," in *Proc. IEEE GLOBECOM*, Nov. 2008.

[58] X. Zhou, J. Ma, G. Li, Y. H. Kwon, and A. Soong, "Probability-based optimization of inter-sensing duration and power control in cognitive radio," *IEEE Transactions on Wireless Communications*, vol. 8, no. 10, pp. 4922–4927, Oct. 2009.

[59] X. Zhou, J. Ma, Y. Li, Y. H. Kwon, A. Soong, and G. Zhao, "Probability-based transmit power control for dynamic spectrum access," in *Proc. of IEEE DySPAN*, Oct. 2008, pp. 1–5.